FIBER CHARACTERIZATION
BY IMPULSE RESPONSE MEASUREMENTS

By

Saeid O. Belkasim

A thesis submitted to the Faculty of Graduate Studies and Research

in partial fulfillment of the requirements for the degree of

Master of Engineering

Departement of Electrical Engineering

Montreal, Quebec

August, 1985

ABSTRACT

The fiber parameters i.e. attenuation, numerical aperture, impulse response, and frequency response were measured for different samples of graded-index fibers. A Tektronix Digital Sampling Oscilloscope was used to store and digitize the waveforms. The oscilloscope was interfaced with an PDP-11/23 Computer System, in which the impulse responses were computed using two methods: the FFT and the moment method. The oscilloscope was also programmed to plot the numerical aperture of the fiber and to compute and plot the impulse response using the moment method. The advantages of the moment over the FFT method are discussed and the former is proposed as being appropriate for industrial fiber characterization applications.

RESUME

Les paramètres des fibres tels que, l'atténuation, l'ouverture numérique, la réponse en fréquence ont été mesurés pour différentes fibres à gradient d'indice. Un oscilloscope à échantillonage digital Tektronix a été utilisé pour mettre en mémoire et codifier en numérique les signaux. Cet oscilloscope communiquait avec un ordinateur PDP-11/23, utilisé pour calculer la réponse impulsionnelle et la réponse en fréquence par deux méthodes différentes: la methode par TFR et la méthode des moments. Cet oscilloscope a été programmé pour afficher l'ouverture numérique de la fibre, et aussi pour calculer et afficher la réponse impulsionnelle avec la méthode des moments.

Les advantages de la méthode des moments sur celle par TFR sont discutés, et la première est proposé comme étant convenable pour la caractérisation industrielle des fibres.

ACKNOWLEDGEMENT

I would like to express my deep gratitude to Prof. G. L. Yip my supervisor for his guidance, support, and helpful remarks throughout the course of this work.

I am also very grateful to Mr A. Puc and Mr F. Ferri for their great help and cooperation. I wish also to thank the technicians of both the mechanical and the electrical workshops especially Mr J. Foldvari, and Mr R. Quik. Finally, I would like to thank all my fellow graduate students and my colleagues, M. Bélanger, R. Osborne, and J. Albert for their help and support.

TABLE OF CONTENTS

LIST OF FIGURES

LIST OF TABLES

CHAPTER 1

INTRODUCTION

The announcement of an optical fiber with a low attenuation of 20 dB/km in 1970 by Corning Glass Work has transformed communication engineers' dream of optical communication into a practical reality. Optical fiber waveguides now make possible a communication link, which is of low cost, high bandwidth, very low loss, immune to external electromagnetic interference, and hence secure. For these and several other advantages such as light weight, plentiful supply of glass etc.[1.1,1.2,1.3], optical fiber systems have the potential of becoming one of the dominant systems of terrestrial communication.

Optical fiber waveguides consist mainly of two cylindrical layers. These two layers are made of pure silica or plastic with slightly different refractive indices. The inner layer is called the core and the surrounding layer is called the cladding. The refractive index of the core is slightly higher than that of the cladding. The cross-section of an optical fiber waveguide is shown in Fig.1.1.

The propagation of light along a waveguide can be described by a set of guided electromagnetic waves usually referred to as modes. Each guided mode yields a pattern of electric and magnetic field lines that are repeated along the fiber at intervals equivalent to the wavelength[1.4].

Optical fiber waveguides can be classified into two categories: step-index fibers and graded-index fibers. In step-index fibers, the core has a constant refractive index, while in graded-index fibers the refractaive index of the core varies quadratically as a function of the core radius.

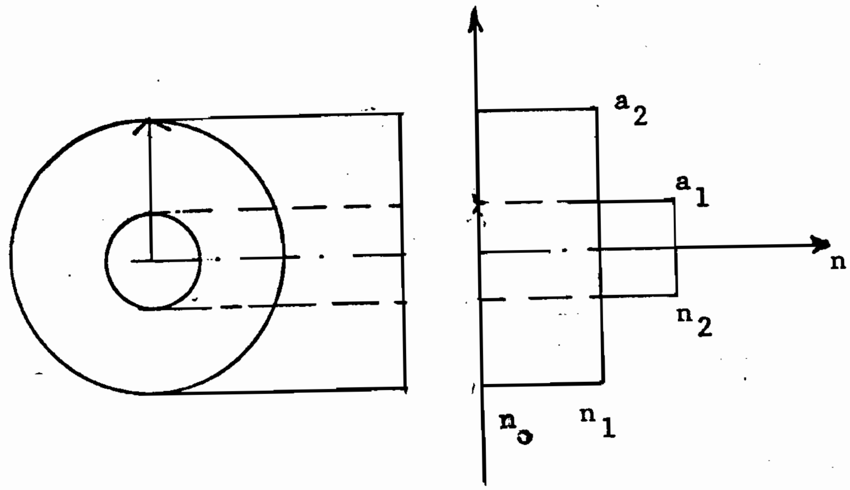

Fig. 1.1 Cross-section of step-index optical fiber waveguide

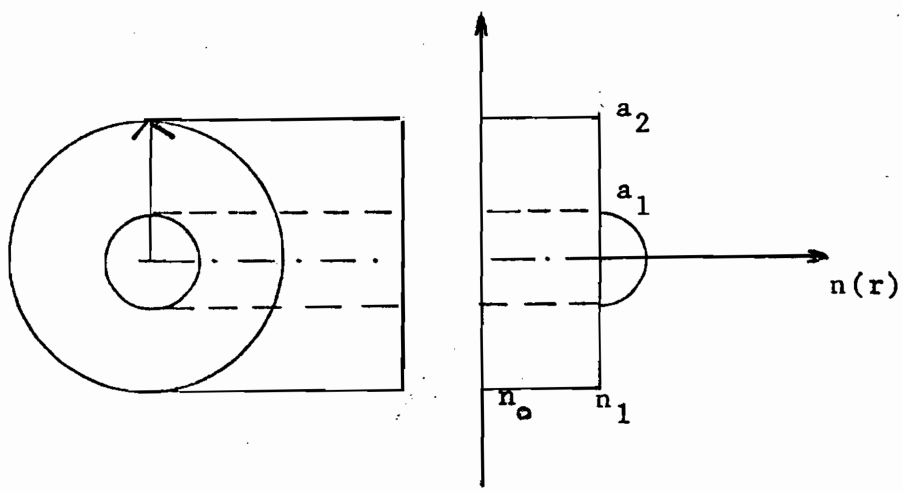

Fig. 1.2 Cross-section of graded-index optical fiber waveguide

The core refractive index in graded-index fibers starts from the maximum at the core center and decreases gradually until it reaches its minimum at the core cladding interface, as shown in Fig.1.2.

The step-and graded-index fibers can also be single-moded and multi-moded. Single-mode fibers support the propagation of one mode only, while multimode fibers permit the propagation of many modes.

Single-mode operation is possible by properly reducing the radius of the core so that it permits single-mode operation only. Single-mode propagation depends critically on the ratio of the refractive indices of the core and the cladding (n_1/n_2). The larger this ratio, the smaller the core radius a required. This ratio is usually kept close to unity to achieve the largest core radius possible[1.5] for light coupling purposes. The typical core radius for single-mode fibers is usually less than 4 μm and for multimode fibers is between 15 μm and 200 μm[1.6].

The propagation of light in optical fibers can be achieved by either launching a continuous beam of light or in the form of discrete light pulses into the core. As light pulses travel through the fiber, they become increasingly distorted. The main feature of this pulse distortion takes the form of what is known as the pulse dispersion or pulse broadening, where the pulse, after travelling through the fiber, appears to have a larger pulse width than the original one. Pulse dispersion can limit the bandwidth and the information capacity of optical fibers.

The pulse dispersion can be divided into two parts: intermodal pulse dispersion and intramodal pulse dispersion. The intermodal pulse dispersion is due to the differences in the group velocities of the various modes. In multi-mode step-index fibers, higher-order modes (represented by rays which enter the fiber at larger angles than the lower-order modes which travel parallel or close to the central axis of the fiber) have to travel a larger distance than the lower-order modes. Consequently, this leads to different arrival times for the various modes. As a result, the width of the pulse will be broadened as it travels through the fiber. The intermodal pulse dispersion in multimode graded-index fibers is much smaller than that in multimode step-index fibers. The reason for this is that in multi-mode graded-index fibers the change in the core refractive index compensates for the change in the group velocity of the various modes. Because the group velocity is inversly proprtional to the refractive index, rays which propagate near the center of the core i.e. lower-order modes travel with slower group velocity than the rays which propagate near the core-cladding interface i.e. higher-order modes. This compensation will eventually reduce the differnce in arrival time and hence the pulse broadening. The intermodal pulse dispersion is predominant in multimode fibers and vanishes in single-mode fibers.

The intramodal pulse dispersion, which can be divided into material dispersion and waveguide dispersion, is predominant in single-mode fibers. The cause of the material dispersion is the variation of the refractive index as a function of the source wavelength. The waveguide dispersion arises from the fact that the propagation constant of each mode is a function of the ratio of the core radius to the source wavelength (a/λ)[1.7,1.8].

To achieve an efficient launching of optical power into the fiber, the numerical aperture or the largest acceptance angle should be determined. A direct method to determine the numerical aperture is to measure it. Several other measurements can be made to characterize the fiber. The attenuation, bandwidth, frequency response and impulse response measurements are among them. Of these, the most important one is, perhaps, the impulse response. Its importance comes from the fact that by measuring the impulse response several other parameters like the bandwidth, pulse dispersion and attenuation[1.9,1.10] can be determined.

In previous measurements[1.10], a picture of the output and the input pulses were recorded using a polaroid camera. These pictures were sampled by simply dividing each picture into several vertical stripes. In this process, the number of vertical lines which intersect with the pulse indicates the number of sampling points. After this process is completed, a discrete signal can be constructed from these sampling points, which are fed into a computer to perform the numerical computations.

The previous method is difficult to perform, slow, inaccurate and susceptible to human errors. Due to these disadvantages, it is necessary to use a digital sampling oscilloscope which makes the process much easier and more efficient. The 7854 Tektronix Digital Sampling Oscilloscope was used in the measurements reported here. This oscilloscope samples, digitizes and stores the signal using a built-in microprocessor. The oscilloscope can also be interfaced with a computer. In our particular measurements, the oscilloscope was interfaced with a PDP-11/23 computer system, where numerical computations were caried out. Using the advantage of speed, accuracy and efficiency provided by this system, comprehensive on-the-spot study of the impulse response is possible. This allows immediate corrections and adjustments in cases where errors are evident such as caused by misalignment or variations in launching conditions for each set of experiments.

The most reliable method to compute the impulse response of the fiber is through the convolution approach using the fast Fourier transform (FFT). In the work presented here, we introduced a much simpler method which is called the moment method. This method is based on approximating the impulse response of the fiber by a Gaussian pulse. With the help of the moment method, the impulse response of the fiber can even be computed on the microprocessor of the Tektornix 7854 Digital Oscilloscope. The FFT would require the availability of a computer to perform the same computations. This makes the moment method more suitable for portable measurement systems and industrial applications.

The second chapter of this report gives some definitions and brief description of the various methods for measuring the attenuation, numerical aperture, impulse response and frequency response. In the third and fourth chapters, the measurements of the attenuation and numerical aperture of multi-mode graded-index fibers are described. The results are presented, discussed and compared with the manufacturer's data. In the fifth chapter, derivations of the FFT and the moment methods are presented. These derivations are important for understanding how these two different methods have been used to obtain the impulse and frequency responses of the test fiber. The sixth chapter which is the main chapter of this report describes the impulse response measurement of optical fibers at two wavelengths 900 nm and 1300 nm. The accuracy of the moment method was tested against the results obtained from the FFT. Results of the pulse dispersion, bandwidth, and attenuation are presented and compared with the manufacturer's data for each fiber. In the last chapter, a brief conclusion about the measurement is given and a few suggestions for the improvement of this work are discussed.

CHAPTER 2

CHARACTERIZATIONS OF OPTICAL FIBERS

Recent advances in optical fiber research have made fiber characterizations and measurements very important. Accordingly, novel measurement techniques and theoretical methods for processing measured data are needed.

The full characterization of optical fibers should involve a study of the mode coupling and distribution of modal power at the launching point and at subsequent points along the fiber. Such a comprehensive study is likely to be both time consuming and difficult to perform.

There are several main properties which would give the necessary information needed to characterize the fiber. Three of them are fiber attenuation, fiber numerical aperture or light gathering ability, and bandwidth or impulse response and frequency response.

2.1 Attenuation Measurement:

Attenuation is an important parameter for characterizing a fiber. Its importance comes from the fact that when a fiber is used in a communication link, it plays an important role in determining the maximum distance allowed between the succcessive repeaters.

The attenuation factor is defined as follows[2.1]:

$$\alpha = [10/(z_2 - z_1)]\log[P(z_1)/P(z_2)] \text{ ------------- } (2.1)$$

where α is the attenuation factor expressed in dB/unit length, $P(z_1)$ is the optical power at a distance z_1 and $P(z_2)$ is the optical power at a distance

z_2. The distance z_1 is usually taken to be one meter and z_2 is the whole length of the fiber.

One of the principal characteristics of optical fibers is the variation of attenuation as a function of the wavelength, as shown in Fig.2.1.

In the early 1970's, the fibers made then exhibited a local minimum attenuation at the 800-900 nm wavelength band[2.2]. Although there was another local minimum near the 1300 nm wavelength, optical sources and photodetectors were available only for the 800 to 900 nm. In the late 1970's fiber manufacturers were eventually able to fabricate fibers with low losses in the 1100 to 1600-nm region by reducing the concentration of hydroxyl and metallic ion impurities in the fiber material. The development since has been mainly directed to the 1300 nm wavelength since pure silica fibers have a minimum signal distortion at this wavelength.

When an optical signal has traveled a certain distance along a fiber, it will reach a point where attenuation and distortion are such that a repeater is needed to amplify and reshape that signal. This repeater consists of a receiver and a transmitter. The receiver detects and converts the incoming optical signals into electrical signals which are amplified, reshaped, and then sent to the transmitter. The transmitter converts the reshaped electrical signals into optical signals and launches them back into the optical fiber.

The relation between the attenuation and the maximum distance between the successive repeaters is given by[2.3]:

$$D = (10/\alpha)\log[P_t/P_r] \qquad (2.2)$$

where D is the distance between the successive repeaters, α is the fiber attenuation in dB/km, P_t is the mean transmitted power and P_r is the mean received power. Fig.2.2 shows how the attenuation and the system loss tolerance limit (which depends on the type of the photodetector used in the receiver) affect the maximum fiber length[2.4].

There are different techniques to measure the attenuation of the fiber, e.g. differential technique, insertion-loss technique, back-scattering technique, lateral-scattering technique, and pulse-reflection technique[2.5] etc. The differential technique or the cutback method is one of the most commonly used methods to measure the attenuation of fiber. A schematic diagram of the measurement set-up is shown in Fig.2.3. The main advantage of the cutback method is that it is simple and easy to implement. In this method, the output power is measured from the output end of the whole length of the fiber. The reference power is taken as the output measured from one meter of fiber cut from the input end of the fiber, leaving the launching conditions fixed. The cutback method is considered destructive particularly when high accuracy measurement is required, where the meaurement has to be repeated several times for each fiber. This process results in wasting a few meters of the fiber under test.

In the insertion loss method, usually a fixed source fiber assembly is connected to the fiber under test. By knowing the assembly loss, the output power from the fixed source fiber assembly, and the loss of the connector, the loss inserted by the fiber then can be obtained by simple measurement of the output power. The advantage of this method is that it is a non-destructive method. Its main disadvantage is that its accuracy is poor.

The back-scattering method, sometimes called the optical time domain reflectometry method[2.6,2.7,2.8], is a non-destructive method. It is based upon sending a narrow pulse through one end of the fiber and receiving the echoes, scattered by the fiber, at the same end. The power echoed by scattering is recorded at several time intervals and used to plot a least square fit. The resulting curve usually takes the exponential form and the attenuation coefficient will be given by[2.1]

$$\alpha = [\log(P(t_2)/P(t_1)]n/[c(t_2-t_1)] \qquad \text{---------} \ (2.3)$$

where $P(t_1)$ is the reflected power at time t_1, $P(t_2)$ is the reflected power at time t_2, c is the speed of light and n is the fiber refractive index.

A similar technique is the lateral-scattering technique, where the power is gathered laterally around the fiber at different sections.

In the pulse-reflection method, a laser pulse is launched into the fiber. A mirror, mounted on the other end of the fiber, is used to reflect the laser pulse. The reflected signal can be taken from a short section of the fiber. The main reason for using this method is that no measuring set-up is needed at the far end of the fiber. This is sometimes useful in the field measurements. The main disadvantage is that this method is very sensitive to the alignment of the reflecting mirror.

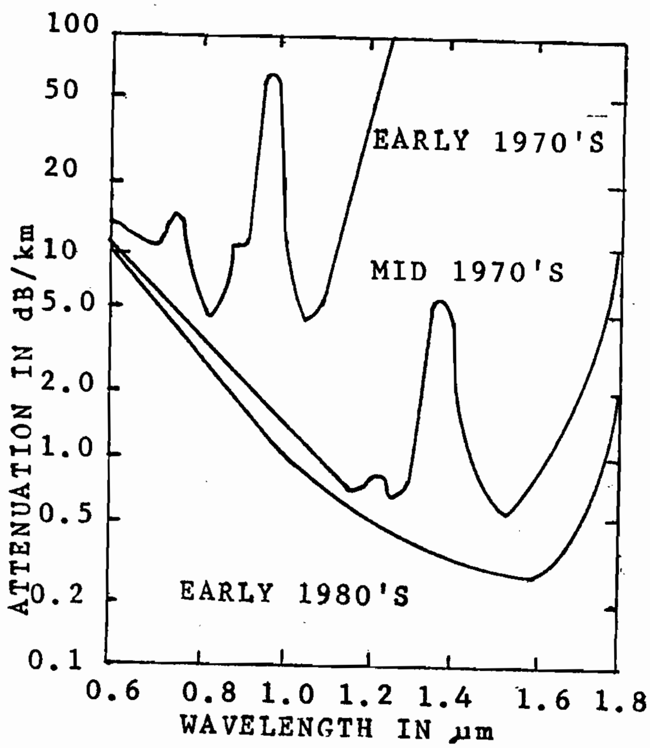

Fig. 2.1 Attenuation versus wavelength

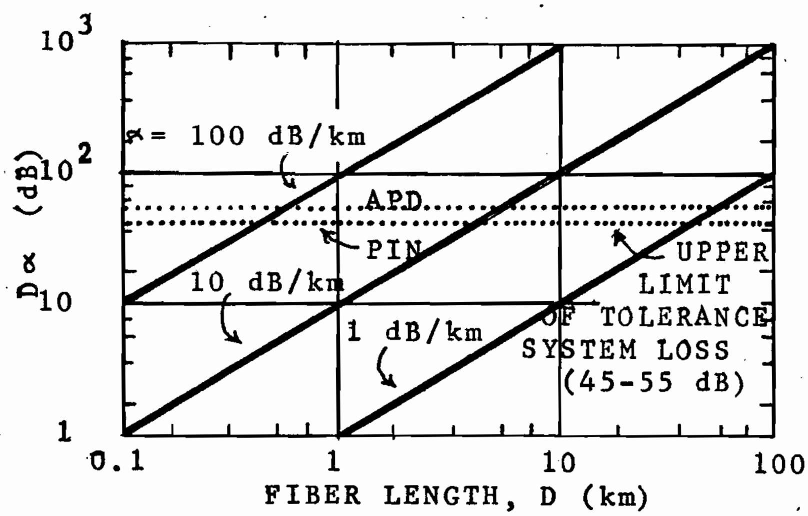

Fig. 2.2 Product of fiber length and attenuation

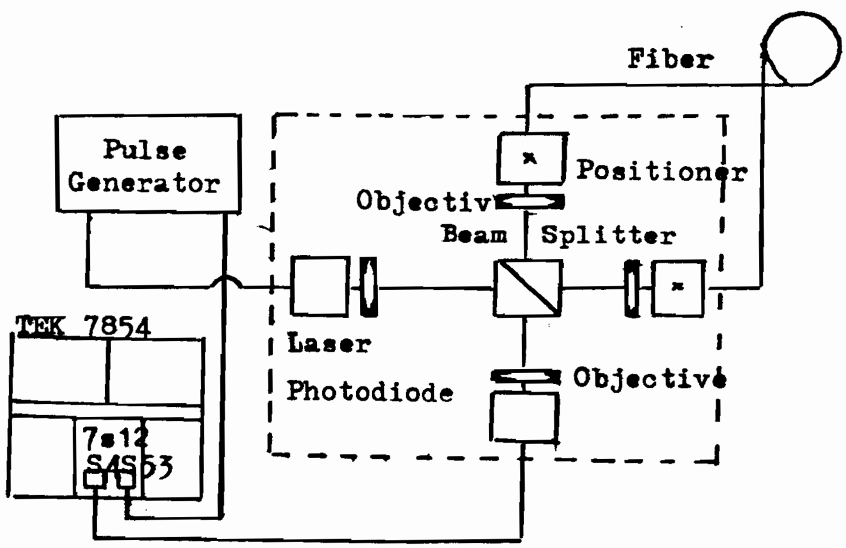

Fig. 2.3 Experimental set-up for the attenuation measurement

2.2 Numerical Aperture Measurements:

In most cases the numerical aperture of the fiber is defined[2.9] as:

$$NA = \sin \psi \quad \text{-------------} \quad (2.4)$$

where NA is the numerical aperture and ψ is the the largest angle which an incident ray can make with the axis of the fiber as shown in Fig.2.4.

There are several techniques[2.10] for measuring the numerical aperture and they generally come under two main categories:

1- The fiber acceptance angle technique.

2- The fiber radiation angle technique.

In the first method, the output power P_0 is scanned as a function of the angle θ_0 which the detector makes with the central axis of the output fiber. In the second method, the output power is measured as a function of the launching angle θ_1. Fig.2.4 shows the numerical aperture measurement using both techniques.

There are some angle dependent losses[2.10,2.11,2.12,2.13] which arise from the deflection due to the lens surface or the non-uniformity of the photodetector response over the numerical aperture range of the fiber. Spherical aberration might also affect the measurement. The presence of spherical aberration can be checked by optimizing the launch numerical aperture to give the maximum launch power. Optimizing the launch numerical aperture can be achieved by changing the launch numerical aperture from fully open to the closed position.

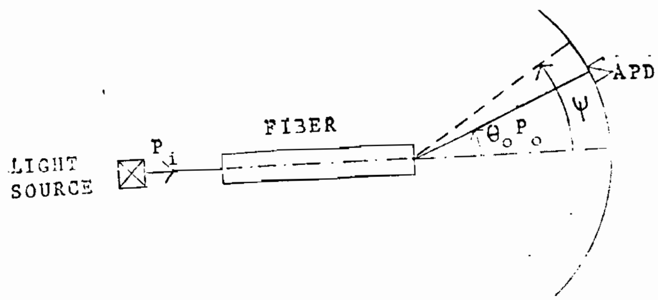

(a)

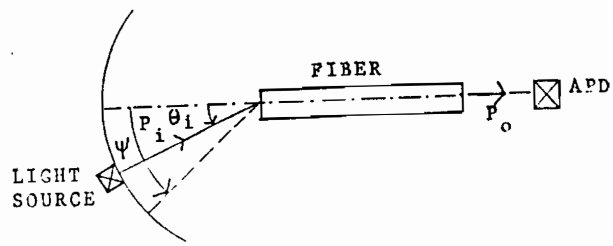

(b)

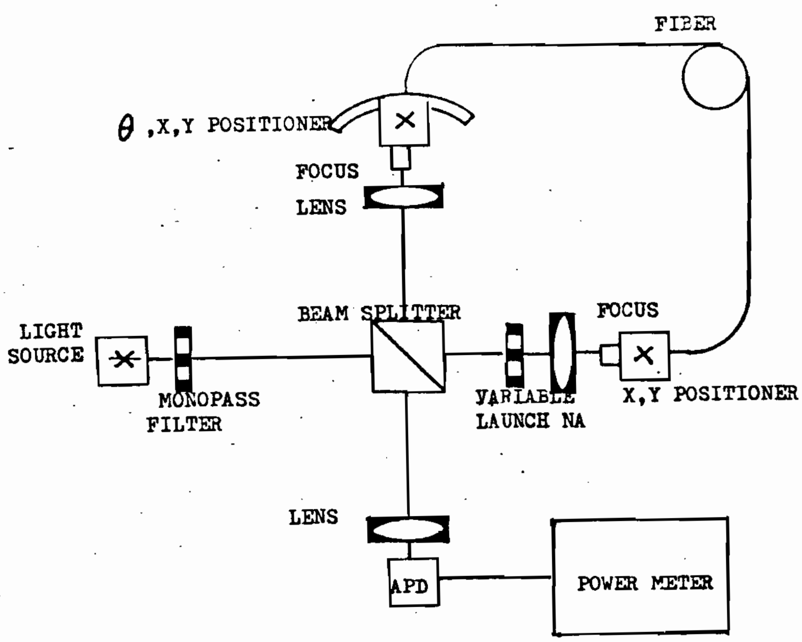

(c)

Fig. 2.4 a: Radiation angle technique
b: Acceptance angle technique
c: Experimental set-up for the numerical aperture measurement

2.3 Impulse and Frequency Response Measurements:

The impulse response function h(t) can be defined using the convolution integral as follows[2.14]:

$$r(t) = \int_{-\infty}^{\infty} s(t)h(t-\tau)d\tau$$

$$= s(t)*h(t) \qquad \text{------------------} \quad (2.4)$$

where r(t) is the output signal which is equal to the convolution of the impulse response h(t) with the input signal s(t). In the ideal case when the input pulse resembles an impulse or its width approaches zero, its impulse response approaches unity.

The frequency response can be obtained from:

$$R(f) = S(f)H(f) \qquad \text{--------------------} \quad (2.5)$$

Equation (2.5) transforms equation (2.4) from convolution in time domain into simple multiplication in frequency domain, which is easier to compute. H(f) is called the frequency response, S(f) and R(f) are the input and output after being transformed into the frequency domain.

There are two main techniques used to measure the impulse and frequency response:

1- The time domain technique.

2- The frequency domain technique.

The first technique is to measure the output pulse after it propagates through the fiber, measure the input pulse, and store the two. The two stored data are then deconvoluted together using numerical methods[2.1,2.12,2.13]. With the help of a computer, the impulse response and the frequency response can be obtained. A measurement set-up for performing the measurement is shown in Fig.2.5.

In the second technique[2.1,2.12,2.15,2.16,2.17] the measurement is made in the frequency domain. The laser signal is sinusoidally modulated and launched into the fiber. The output and the input are detected using two avalanche photodetectors. The two signals are then fed to a tuned spectrum analyser which records the two signals. A simple division of the two signals is then sufficient to obtain the frequency response of the fiber over a certain frequency sweep range. A set-up for performing the measurement in the frequency domain is shown in Fig.2.6.

The first method is easier to implement, but it has some errors associated with the numerical deconvolution, measuring and storing the data. Although the second method is difficult to implement and more expensive, it provides a better accuracy than the first method. In this report, the first method was used to measure the impulse response due to its simplicity over the second method.

When measuring the impulse response of the fiber one has to deal with short duration, fast rise-time laser pulses. These short pulses cannot be viewed on a normal oscilloscope because they are within the range of accuracy of the electronic components of the oscilloscope. On the other hand, these pulses can be viewed on a sampling oscilloscope. To view a pulse on a sampling osilloscope, it has to be repetitive. This pulse is sampled at several points along the time domain and a replica of the original signal is displayed on the oscilloscope using these sampling points.

As stated in chapter 1[2.18], the previous measurement techniques in our laboratory were rather clumsy. By using the 7854 Tektronix Digital Processing Oscilloscope interfaced with a PDP-11/23 computer system, we have adopted the state-of-art technique in fiber measurements.

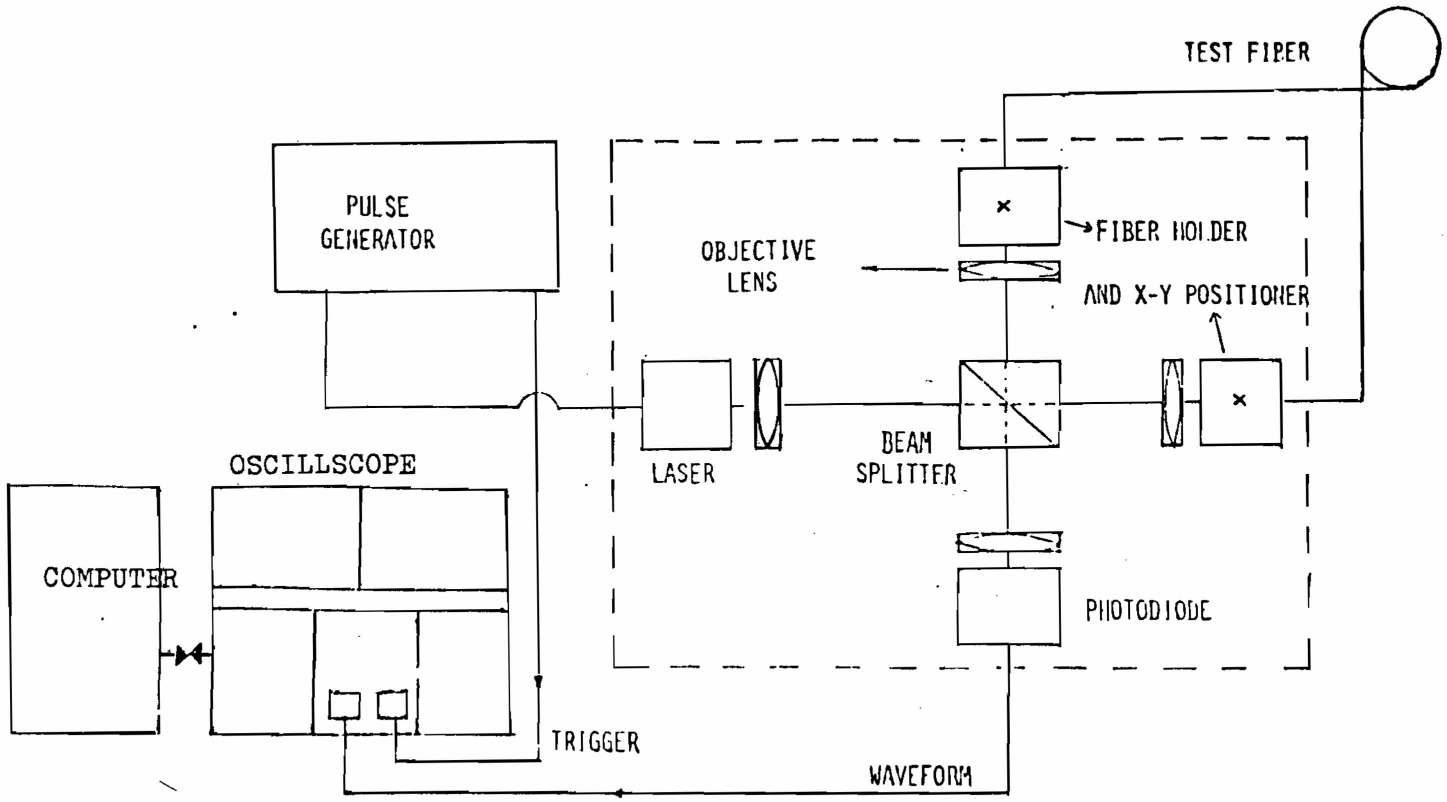

Fig. 2.5 Experimental set-up for measuring the impulse response of the fiber

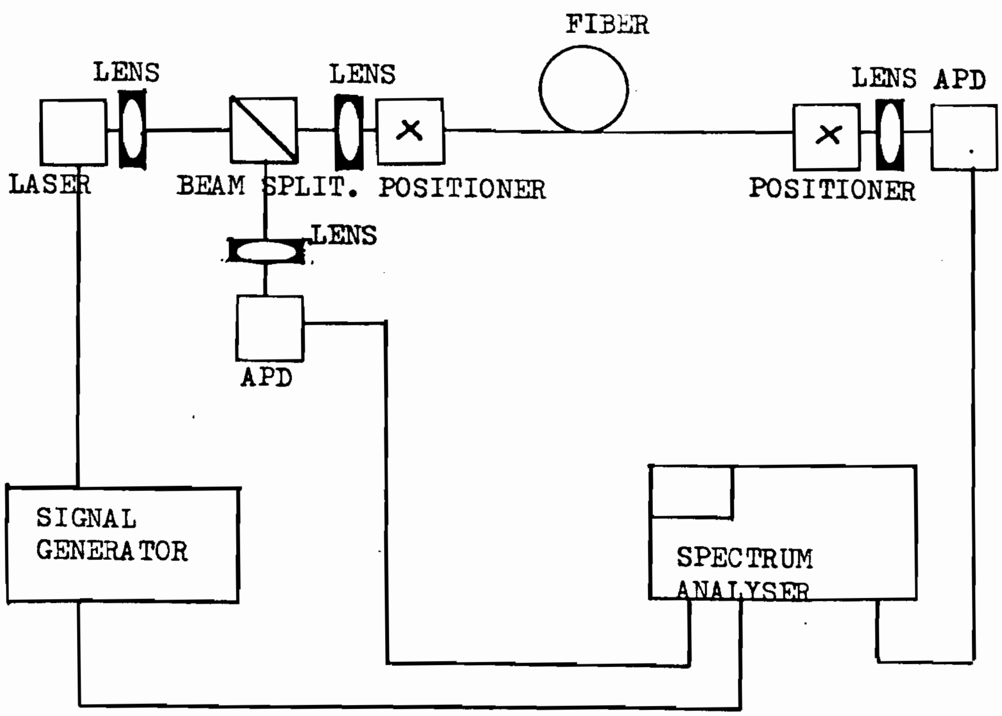

Fig. 2.6 Experimental set-up for the frequency response measurement

CHAPTER 3

THE ATTENUATION IN GRADED INDEX FIBERS

3.1 Factors Contributing to Fiber Attenuation.

Attenuation in fibers is one of the main factors which determine the characteristics of each particular kind of fiber. The attenuation of a graded index fiber can be derived using the ray optics approach[3.1,3.2,3.3,3.4]. The main difficulty encountered when trying to determine the attenuation factor α is that it requires a knowledge of the index profile. In most cases the index profile can be approximated, which makes this method inaccurate. The other alternatives are either measuring the index profile or measuring the attenuation directly, which is simpler.

The attenuation measurement for multimode fibers has more problems than single mode fibers due to the fact that each mode propagates with a different attenuation constant. As these modes propagate in the fiber, the high-loss modes vanish near the input end of the fiber and the relative power content[3.5,3.6,3.7] for each remaining mode does not change. The attenuation coefficient then becomes the same for all the remaining modes.

The main factors which contribute to the power attenuation are:

(a) The excitation of leaky rays

(b) Imperfections in the waveguide

(c) Intrinsic material absorption loss

(d) The bending losses

3.1.a Attenuation Due to The Excitation of Leaky Rays:

There are three main classifications of rays in optical fibers: refracted rays, tunnelling rays, and bound rays[3.5,3.6,3.7,3.8,3.9,3.10]. The first two are called leaky rays. The refracted rays can be neglected because they leave the fiber at a distance close to the source. The bound rays usually do not encounter any power attenuation. From the previous discussion, it is clear that the main source of the power attenuation is the tunnelling rays.

3.1.b Attenuation Due to Imperfection

There are two main causes of the power loss due to imperfection[3.6,3.10]. The first one is the irregularity in the fiber dimensions, and the second cause is the deviation from the ideal refractive index profile. Such an irregularity could cause radiation loss and redistribution of the power among the bound rays. The refractive index variation also causes what is known as Rayleigh-type scattering[3.11].

3.1.c Attenuation Due to Absorption

There are two absorption coefficients[3.6,3.10]. One is due to the core and the other one is due to the cladding. The one in the cladding has a larger effect because it affects both the leaky rays and the bound rays.

In the graph shown in Fig.3.2, the absorption losses and the Rayleigh scattering loss are plotted as a function of the wavelength. The Rayleigh scattering loss decreases at higher wavelengths[3.11,3.12]. The ultraviolet absorption loss which appears below 1200 nm wavelength is due to the excitation of the electrons of the oxygen ions by ultraviolet photons. The infrared absorption loss which appears above 1300 nm wavelength is caused by molecular vibrations. There are three absorption loss peaks due to the vibration of the hydroxyl ion (OH^-), appearing at 950, 1250 and 1300 nm wavelengths.

3.1.d Attenuation Due to Bending

When a waveguide is bent, there will be no bound rays remaining. The only remaining rays are tunnelling rays and refracted rays[3.10]. Bending will cause the power to be lost through radiation. Fig.3.1 shows the tunnelling, bound and refracted rays as they propagate in the fiber.

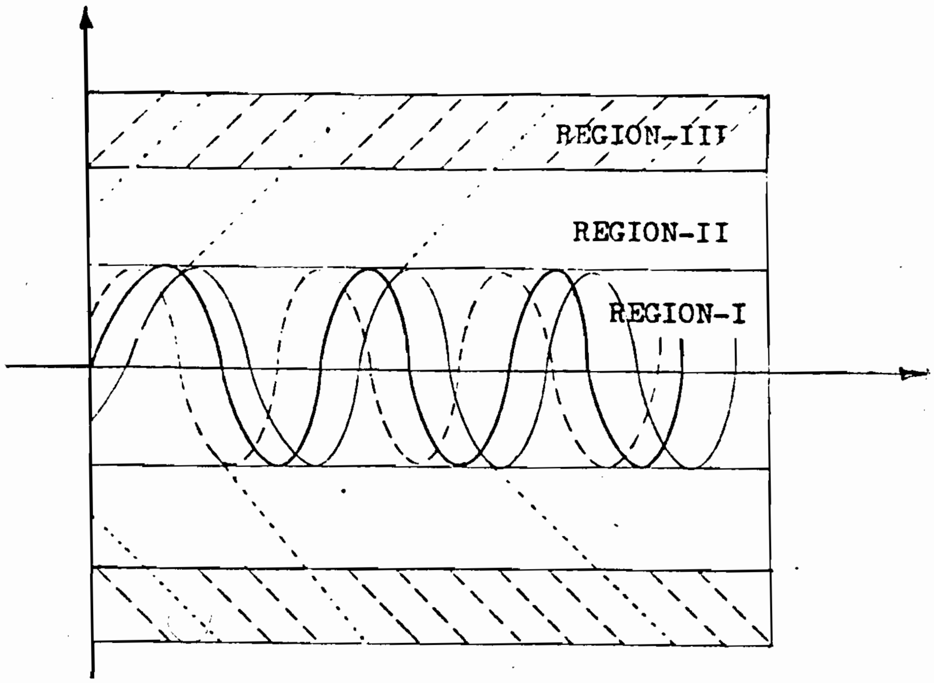

Fig. 3.1 Classification of rays in graded-index fiber
Region I contains tunnelling and bound rays
Region II contains refracted rays only
Region III contains refracted and tunnelling rays

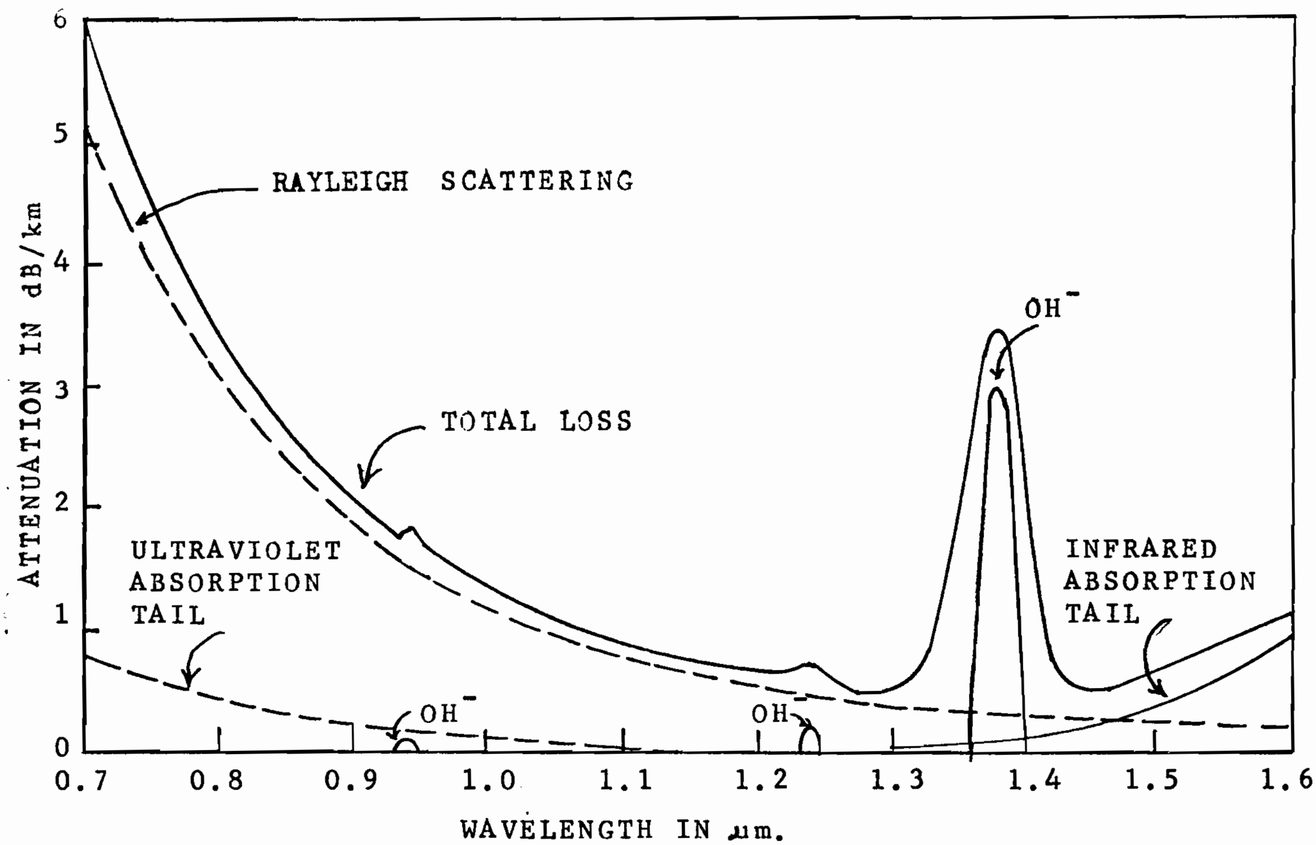

Fig. 3.2 The attenuation losses as a function of the wavelength

3.2 Attenuation Measurements

Attenuation was measured using the Photon Kinetic FOA-1000 Universal Fiber Optics Analyser[3.13], which provides a complete optical fiber characterization system, built in one unit. The system is built in such a way that the input and output optical paths cross each other. One path runs from the light source to the input end of the fiber. The other runs from the output end of the fiber to the detector. The two paths intersect at a common point. At the common intersection point, a beam splitter is inserted. The beam splitter would split the beam between the two paths, and it can be switched on and off, depending on the kind of measurement to be made. Fig.3.3 shows the layout of the Universal Fiber Optics Analyser A more detailed description is given in section 4.3.

3.2.1 Attenuation Measurement Using a Halogen Lamp

The attenuation measurement using the Universal Fiber Analyser can be made using two sources, i.e. the halogen lamp, and the laser source. The light from the halogen lamp is reflected towards the beam splitter using a mirror as shown in Fig.3.4. A momopass filter is used to filter out the unwanted wavelengths.

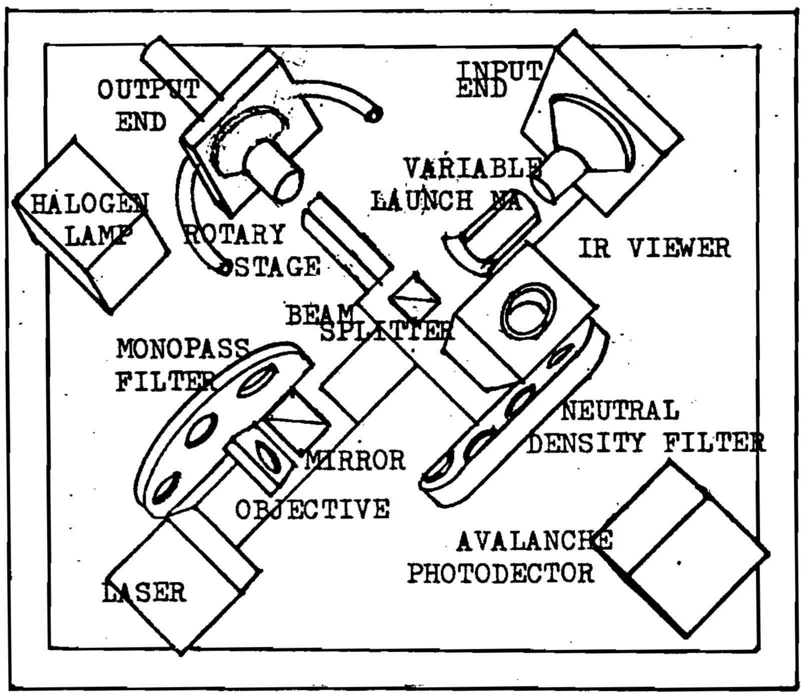

Fig. 3.3 Layout of the Universal Fiber Optics Analyser

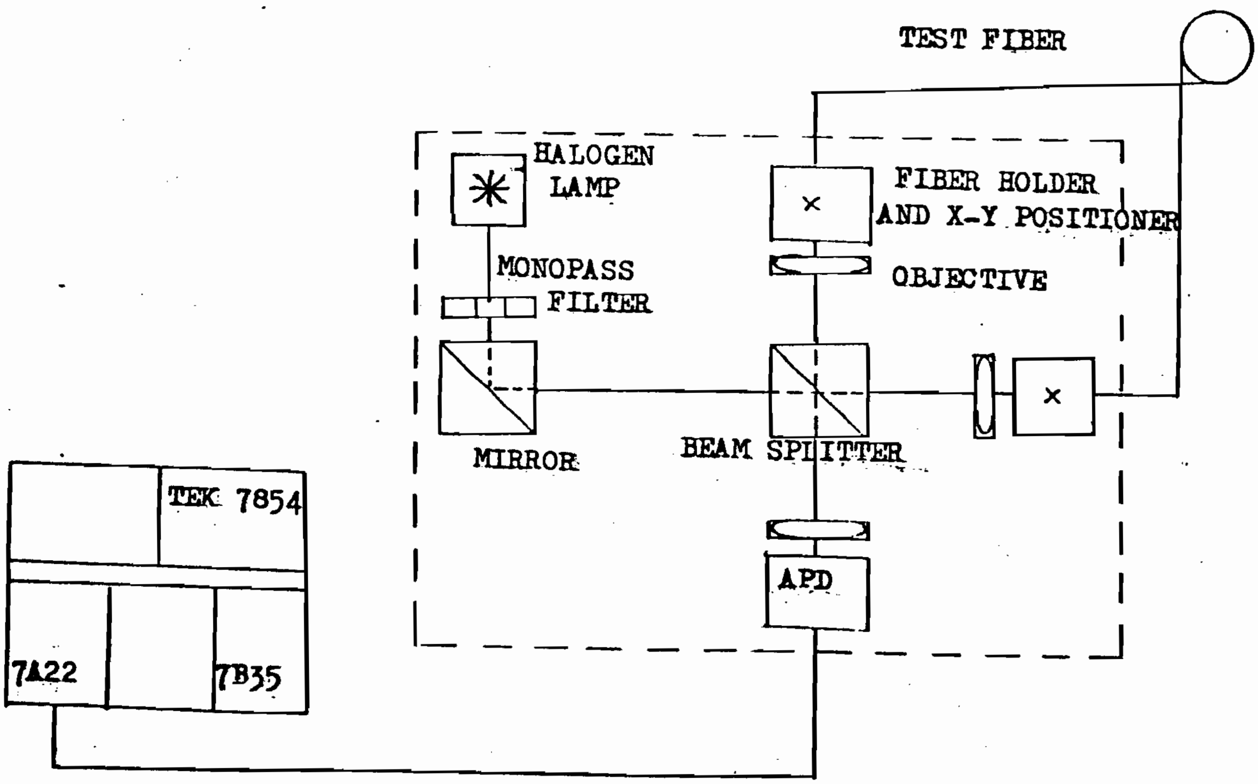

Fig. 3.4 Attenuation measurement using a halogen lamp

3.2.1.a System Preparation[3.13]:

The Universal Fiber Optics Analyser is prepared for attenuation measurements using the halogen lamp as below:

a- For warming up, the halogen lamp has to be turned on for at least five minutes before making any measurements.

b- The output signal from the photo-detector should be connected to the vertical amplifier of the oscilloscope (7A22 or 7A24 can be used). A semi-rigid coaxial cable with SMA connector should be used to connect the signal between the detector and the vertical amplifier.

c- For viewing the input signal, the cross-path beam splitter should be switched into the optical path.

d- The neutral density filter should be open or in zero position.

e- The IR viewer should be switched into the optical path or in the view position, and its beam splitter should point toward the output fiber, in order to view it.

f- Looking into the IR viewer, the brightest image can be obtained by adjusting the input fiber x and y positions. Switch the cross-path beam splitter out of the optical path (the lower postion).

g- Adjustment of the input fiber focus can be achieved by adjusting the outer ring of the input stage. This should be done until the maximum image can be seen. The x, y and z should be adjusted to give the brigtest image on the IR viewer.

h- The output fiber focus should be adjusted for smallest possible image.

i- For aligning the beam on the surface of the beam splitter the IR viewer should point towards the detector.

j- Again the smallest spot should be seen on the IR viewer and can be achieved by adjusting the output fiber focus and also x and y positions.

k- By the time the previous steps are carried out, signal should be seen on the oscilloscope screen. In that case the IR viewer should be lifted out of the optical path (from VIEW to THRU position). Adjustments can be made for a maximum signal on the scope.

3.2.1.b Measurements and Results

After winding the fiber on a larger diameter drum (15 inches), several meaurements were made. The wavelengths at which the attenuation was measured were 650, 750, 800, 850, 900, 950, 1050 nm. Several fibers of a graded-index type were considered for the attenuation measurements. In order to have a good smooth end surface, the fiber was cut using a special fiber cutter. After cutting, the end face was observed under the microscope for smoothness. The fiber then was installed in the fiber holders, and the output was measured and recorded. The fiber input end was kept fixed with the same launching conditions, while the output end was removed from the fiber holder and one meter was cut from the fiber input end. Light travelling through this one-meter of fiber suffers negligible attenuation compared to a one-kilometer one. Hence, a one-meter fiber can be considered as a reference in comparison with a longer one. The output power was measured from the reference fiber. The attenuation was calculated from the ratio of the output power from the longer fiber to that from the reference fiber. A comparison was made between the results obtained with the Photon Kinetics detector and a separate optical power meter. Incident power to the photodetector was measured in terms of the vertical deflection of the trace on the oscilloscope calibrated in volts. The data for the power in the Tables were taken from the oscilloscope readings.

3.2.1.c List of The Equipment

Photon Kinetics universal fiber optics analyser.

United Detector optical power meter 21A.

Tektronix oscilloscope 7854.

Tektronix vertical plug-in unit 7A22 or 7A24.

Tektronix horizontal plug-in unit 7B35.

wavelength	intensity for 1196 meter P_1 in mv	intensity for 1 meter P_2 in mv	attenuation $\sigma=10\log(P_1/P_2)$
650 nm	56	450	7.56 db/km
750 nm	170	500	3.91 db/km
800 nm	150	400	3.56 db/km
850 nm	160	390	3.23 db/km
900 nm	130	290	2.91 db/km
950 nm	90	200	2.9 db/km

Table 3.1 Attenuation for fiber (code 6/1046 A)

wavelength	intensity for 1194 meter P_1 in mv	intensity for 1 meter P_2 in mv	attenuation $\sigma=10\log(P_1/P_2)$
650 nm	55	500	8.02 db/km
750 nm	150	550	4.7 db/km
800 nm	130	450	4.5 db/km
850 nm	140	430	4.08 db/km
900 nm	120	350	3.9 db/km
950 nm	80	250	4.1 db/km
1050 nm	30	80	3.56 db/km

Table 3.2 Attenuation for fiber (code 6/1064 B)

wavelength	intensity for 1165 meter P_1 in mv	intensity for 1 meter P_2 in mv	attenuation $\alpha = 10\log(P_1/P_2)$
650 nm	40	400	8.36 db/km
750 nm	135	420	4.2 db/km
800 nm	125	380	4.1 db/km
850 nm	125	350	3.8 db/km
900 nm	110	275	3.4 db/km
950 nm	20	180	8.1 db/km
1050 nm	25	60	3.2 db/km

Table 3.3 Attenuation for fiber (code 8/780 A)

wavelength	intensity for 2871 meter P_1 in mv	intensity for 1 meter P_2 in mv	attenuation $\alpha = 10\log(P_1/P_2)$
650 nm	5	425	6.72 db/km
750 nm	20	500	4.86 db/km
800 nm	25	400	4.2 db/km
850 nm	42	400	3.4 db/km
900 nm	40	320	3.1 db/km
950 nm	30	250	3.2 db/km
1050 nm	18	750	2.2 db/km

Table 3.4 Attenuation for fiber (code 9/548 A)

wavelength	intensity for 2260 meter P_1 in mv	intensity for 1 meter P_2 in mv	attenuation $\sigma = 10\log(P_1/P_2)$
650 nm	6	400	8 db/km
750 nm	42	450	4.5 db/km
800 nm	55	360	3.6 db/km
850 nm	70	340	3.0 db/km
900 nm	60	290	3.0 db/km
950 nm	60	200	6.7 db/km
1050 nm	23	70	2.1 db/km

Table 3.5 Attenuation for fiber (code 9/574 B)

wavelength	intensity for 2260 meter P_1 in μw	intensity for 1 meter P_2 in μw	attenuation $\sigma = 10\log(P_1/P_2)$
650 nm	0.013	0.070	3.2 db
750 nm	0.014	0.080	2.5 db
800 nm	0.015	0.074	3.0 db
850 nm	0.017	0.085	3.1 db
900 nm	0.017	0.085	3.1 db
950 nm	0.013	0.086	3.6 db
1050 nm	0.018	0.058	2.2 db

Table 3.6 Attenuation measurement using the United Detector power meter. for fiber (code 9/574 B)

wavelength in nano meter	attenuation using the universal analyser		attenuation using the power meter	
650	8	db/km	3.2	db/km
750	4.5	db/km	2.5	db/km
800	3.6	db/km	3.0	db/km
850	3.0	db/km	3.1	db/km
900	3.0	db/km	3.1	db/km
950	6.7	db/km	3.6	db/km
1050	2.1	db/km	2.2	db/km

Table 3.7 Comparison between the measurement using the power meter and the Universal Fiber Optics Analyser for fiber (code 9/574B)

Fiber code	Manufacturer value in db/km	measured value in db/km (using universal analyser)
6/1064B	2.9	3.9
8/780A	3.0	3.4
9/548A	3.1	3.1
9/574B	3.4	3.0

Table 3.8 Comparison between manufacturer's data and measured data for the attenuation at 900 nano meter wavelength.

3.2.2 Attenuation Measurement Using a Laser Source

The previous measurements were made using a halogen lamp as the light source. In the present method, the light source was the laser diode of the universal fiber optics analyser, which operates at a wavelength of 904 nm .

In this method, the input pulse was measured through a 3-db beam splitter. The input pulse was averaged and stored using the Tektronix 7854 digital oscilloscope. The beam splitter then was moved out of the optical path, and the output pulse coming from the fiber was also averaged and stored on the oscilloscope. The energy in each case was obtained using the area command of the waveform calculator of the Tektronix digital oscilloscope. Refer to Fig.3.5.

3.2.2.a System Preparation

The Universal Fiber Optics Analyser was also used to measure the attenuation as was previously described in the case of the halogen lamp. The system can also be prepared as before except for the first two steps which will be described as below:

a- Connect the HP 8013B Pulse Generator to the trigger input of the laser (triggering signal at 500 mv, 25 khz). Swich on the laser for warming up for at least 7 minutes.

b- The output signal from the avalanchephotodetector (APD) should be connected to the sampling head of the oscilloscope S4, and the delayed triggering signal coming from the pulse generator is connected to S53 on the scope. The rest of the steps are similar to the ones in section 3.2.1.a from c to k.

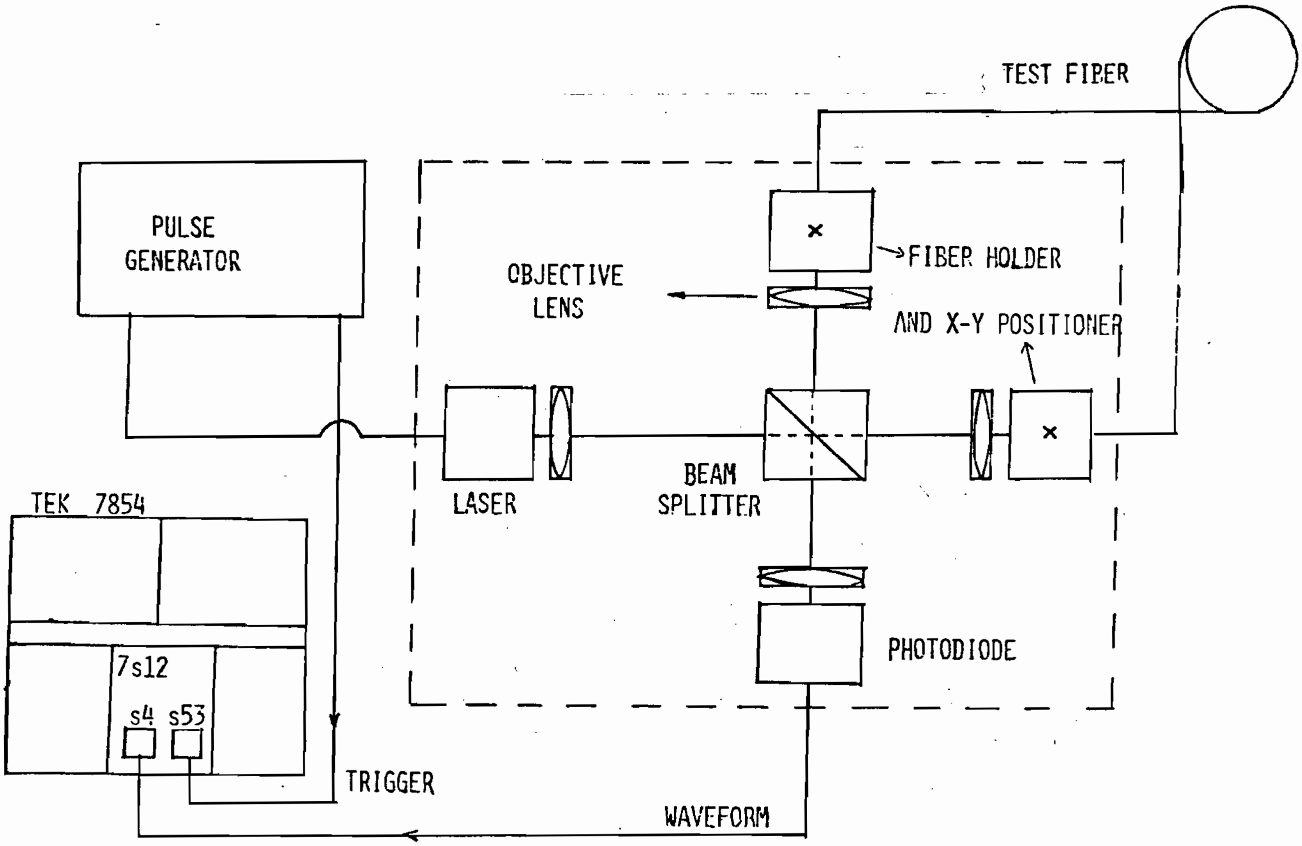

Fig.3.5 Set-up for the attenuation measurement using a laser source

3.2.2.b Measurements and Results:

The measurements in this case were done using the same equipment which was used in the previous mesurements except that the light in this case was provided by a laser diode. The light source has the following specifications: A pulsed laser with a peak wavelength of 904 nm. Two laser pulses are provided by the source: a short pulse (from a Q-switched laser: Model 25C) of 500 psec. pulse width, and a long pulse (Model 725C) of pulse width around 25 nano second. The input trigger level of this source is 400 millivolts. The pulse repetition rate is 20 kilo pulse/sec or less. The output power is about 1 W. A silicon avalanche photodetector (Model 35C), with a spectral response of 400 nm to 1100 nm and a rise time of about 150 pico second, is used.

The attenuation was calculated as follows:

The attenuation = 10log(2"Energy output from the beam splitter"/"Energy output from the fiber")

fiber code	fiber length in km	Energy output from the fiber in pw	Energy reflected from the beam splitter in pw	Attenuation in db/km
10/477B	1.21	14.1	12.3	1.997
9/574B	2.253	8.7	13.14	2.131
8/780	1.16	11.64	12.2	2.69
6/1064B	1.196	13.03	14.42	2.885

Table 3.9 Attenuation results using the laser as a light source

fiber code	Manufact.data attenuation in db/km	Exp. data attenuation in db/km	Difference in db	Error%
10/477B	2.2	1.997	0.203	9.22%
9/574B	3.4	2.131	1.269	37%
8/780	2.96	2.69	0.198	9.12%
6/1064B	2.85	2.885	0.035	1.228%

Table 3.10 Comparison with the manufacturer's data.

3.3 Discussion and Conclusion:

Table 3.8 shows the comparison between the measured attenuation using a halogen lamp and the data supplied by the manufcturer of the fiber under test. The results show a reasonable agreement. There is a small discrepancy between the two. This discrepancy is due to the influence of stray light and other sources of outside interference. This interference would cause the attenuation to vary slightly. Also, care should be taken when cutting the fiber. The surface of the cut should be straight and flat. Otherwise, reflection might occur leading to higher attenuation.

In Table 3.7, the attenuation values were in agreement for the data points 850 nano meter and 900 nano meter. For the other wavelengths the attenuation was higher for the measurements made using the photodetector of the universal fiber optics analyser. The reason for this is possibly due to the nonlinear spectral response of the silicon photodetector of the fiber analyser. Unlike the universal analyser, the united photodetector has a flat response over most of the spectral range.

Comparing the measurements using a halogen lamp with the measurements using a laser source, the ones using a laser source were more reliable. This is due to the fact that the stray light noise and outside interference have much less effect on the laser. Refer to Tables 3.9, 3.10.

The discrepency for fiber 9/574B in Table 3.10 is possibly due to the roughness of the end face of that fiber. The reason for not including fiber 10/477B in Table 3.8 and fiber 9/548A in Table 3.10 is that these two fibers broke in the middle during the measurement process.

Observing the measurements listed in Tables 3.1 to 3.6, it is clear that the attenuation decreases as the wavelength increases. This is possibly due to scattering losses which are high at the lower wavelenghs, as is domenstrated by Fig.3.2.

CHAPTER 4

THE NUMERICAL APERTURE OF GRADED-INDEX FIBERS

The numerical aperture or the radiation angle is a very important parameter in characterizing the fiber. A knowledge of this parameter is necessary in the design of a fiber system, particularly in the coupling between the source and the input fiber end, and also the detector and the output fiber end. The launching efficiency depends greatly on this parameter[4.1].

4.1 Definition of The Numerical Aperture of Fibers:

The classical definition of the numerical aperture of the fiber[4.2] states that the numerical aperture is the sine of the largest angle which an incident ray makes with the normal to the surface of the fiber end, as shown in Fig.4.1.

The numerical aperture of the step-index fiber according to classical definition is:

$$NA = \sin \phi \qquad \text{---------------} \quad (4.1)$$

where NA is the numerical aperture and ϕ is the largest angle that an incident ray can make with the axis of the fiber as shown in Fig.4.1.

Equation (4.1) leads to the popular definition of the numerical aperture,

$$(NA)_0 = [(n_1)^2 - (n_2)^2]^{1/2} \qquad \text{--------------} \quad (4.2)$$

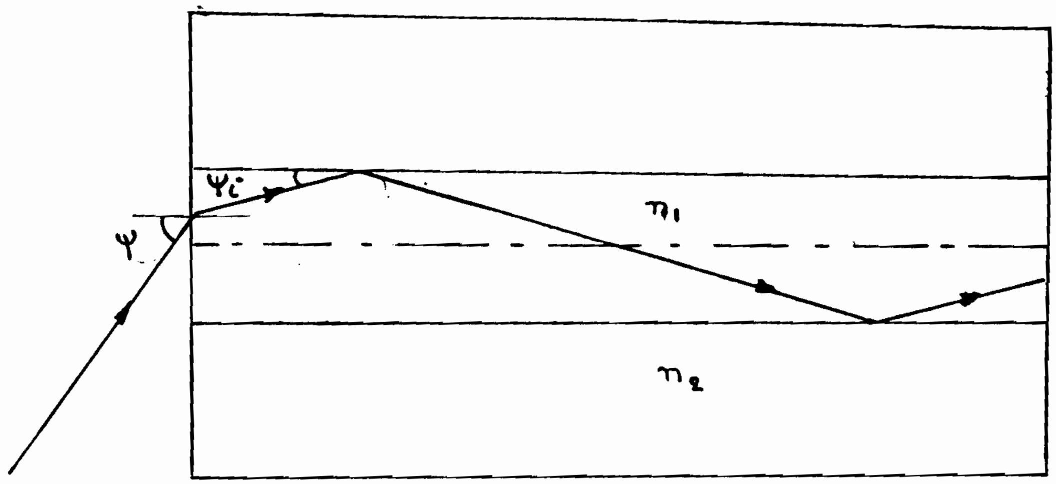

Fig. 4.1 The acceptance angle of a fiber

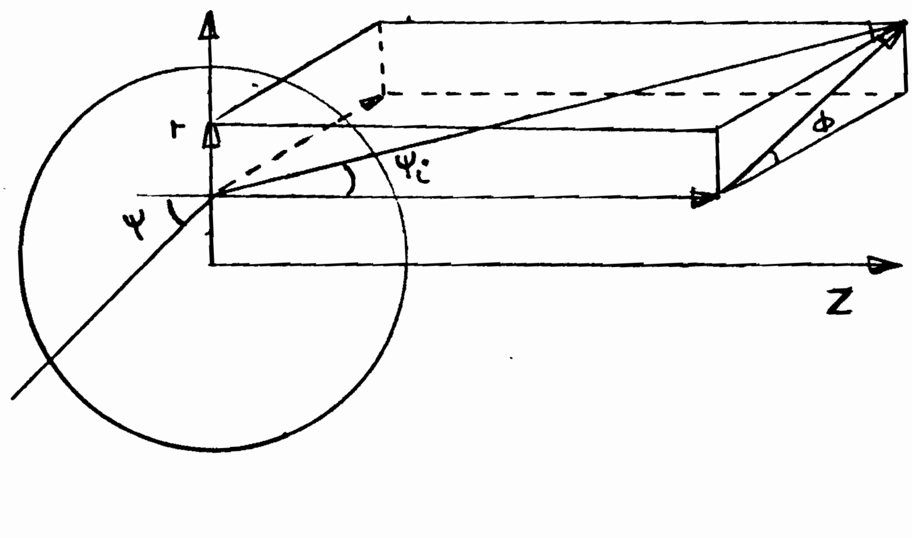

Fig. 4.2 The azimuthal and radial components of an optical ray

where $(NA)_0$ is the numerical aperture according to the popular definition, n_1 and n_2 are the refractive indices at r = 0 and r = a respectively

In general, the popular definition given by equation (4.2) is not an adequate measure of the light gathering ability[4.2] because it does not take into consideration the skew rays which cannot be ignored in some situations.

A more complete definition is given by[4.1]

$$NA = (NA)_0[1 - (r/a)^q]^{1/2} / [1 - (r/a)^2 \cos^2\phi]^{1/2} \text{-------} \quad (4.3)$$

where r and ϕ are the radial and azimuthal components of the ray in a cylindrical coordinate system, q is the profile parameter and a is the core radius (q = 2 for parabolic index fibers and q = ∞ for step index fibers), as shown in Fig.4.2.

The definition given by equation (4.2) can still be considered adequate for graded-index fibers. The reason is that, in graded-index fibers, all rays including skew rays have an acceptance angle which is not greater than the acceptance angle given by equation (4.2). The meridional rays usually determine the largest acceptance angle in a graded-index fiber. The reason for this is that the acceptance angle of meridional rays is greater than that of skew rays[4.3]. To clarify this point, the ratio of the numerical aperture $NA/(NA)_0$ given by equation (4.3) is plotted in Fig.4.3 as a function of (r/a) for several values of q and ϕ. As is apparent from the graph in Fig.4.3, the popular definition given by (4.2) is in agreement with the one given by (4.3) in the case of step-index fiber (q = ∞) only when skew rays are not present ($\phi = \pi/2$). This means that the popular definition is not adequate to define light gathering ability when skew rays are present.

In the case when the fiber is parabolic (q = 2), the numerical aperture given by equation (4.3) is always less than the one given by the popular definition in (4.2).

In conclusion, a ray is accepted into a fiber depending on its incident angle ϕ and the radius r by which it impinges on the fiber. Keeping r small by properly adjusting and focusing the launched light beam, the classical definition given by (4.1) can be used to define the numerical aperture.

In this particular measurement, the classical definition was used because of the lack of the proper equipment and the difficulty of measuring the refractive index of the fiber. The measurement of the refractive index of the fiber would be required if one were to measure the numerical aperture of the fiber using the definition provided by equation (4.3).

4.2 The Numerical Aperture Measurements

AS it has been shown earlier the numerical aperture is defined as the sine of the maximum acceptance angle. In practice it is difficult to measure the maximum acceptance angle as the angle at which the intensity curve, shown in Fig.4.4, intersects with the x-axis. The definition of the maximum angle depends on the accuracy of the equipment, and the conditions under which the measurements are performed. Normally, the maximum acceptance angle is defined as the angle at which the intensity drops from its maximum value to the 10% value[4.4]. In previously reported measurements[4.1] the maximum acceptance angle was considered to be at the point where the intensity curve reaches 5% of its maximum value.

The measurements used here are the far-field ones, rather than the near field ones. The difference between the two is that the near-field measurements determine the fiber characteristics in the plane of the output end of the fiber. On the other hand, the far-field ones are synonymous with the Fraunhofer diffraction. The distance at which the measurements can be considered as far field measurements is defined as follows[4.1]:

$$L = (2a)/\lambda \qquad \text{------------} \qquad (4.4)$$

as shown in Fig.4.5, where λ is the wavelength and a is the core radius. For practical reasons, the far-field measurements are usually made at a distance ten times the distance L.

The numerical aperture measurements were all made using the Universal Fiber Optics Analyser. The fibers which were used throughout the measurements have a 50 μm core diameter. To be sure that the input light cone covered the whole core-surface area, an overfilled launch numerical aperture was considered throughout all the measurements. The overfilled launch numerical aperture for graded index fiber usually leads to more accurate results[4.5], because it ensures that all modes are launched into the fiber. An overfilled launch numerical aperture is the numerical aperture which is large enough to cover the whole core-surface area. In these particular measurements a .3-launch numerical aperture was used.

To determine the angle 2ψ from Tables 4.1-4.6 between the two 10% light intensity points as shown in Fig. 4.4, a smooth curve was drawn to fit the data points for each set of measurements. It should be noted that the angle readings for the two 10% intensity points may not be necessarily the same. The value of ψ in the bottom row of Tables 4.1-4.6 was taken to be half of $2\psi = |\psi_1|+|\psi_2|$.

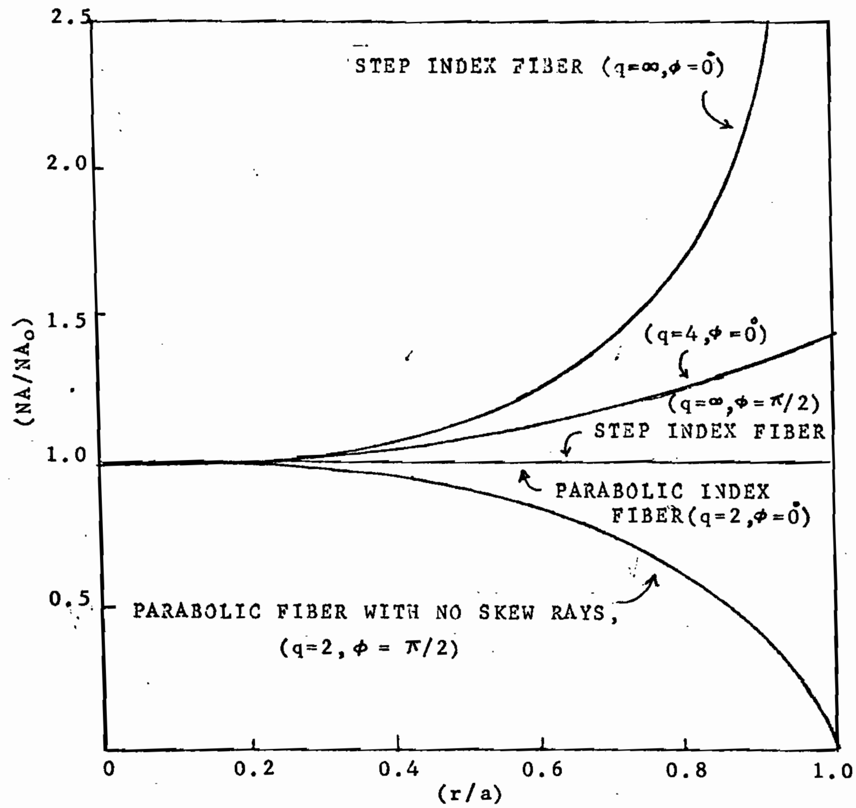

Fig. 4.3 (NA/NA_0) versus (r/a)

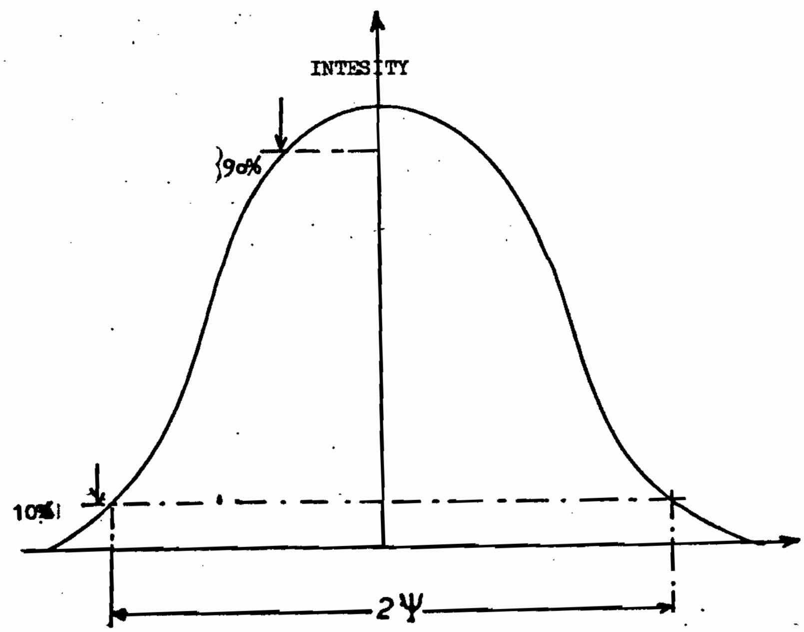

Fig. 4.4 Obtaining the NA angle by plotting the intensity versus the fiber angle

4.3 The Universal Fiber Optics Analyser

4.3.1 Overview

The Photon Kinetics FOA-1000 Universal Fiber Optics Analyser[4.6] consists of optical components mounted on optical rails. Light passes through two main optical paths. One path runs from the light source to the input end of the fiber. The second path goes from the output end of the fiber to the photo-detctor, as shown in Fig.4.6. A beam splitter is placed at the crossover point. With the help of this beam splitter, it is possible to view both the output and the input end of the fiber simultaneously. The output fiber was mounted on a rotary stage, which allows the fiber end to be rotated about the main axis. The Universal Analyser converts the angular rotation to an electric voltage, which can be easily read using a normal voltmeter. There are two light sources: a halogen lamp and a laser source. A neutral density filter wheel is provided to maintain the dynamic range of the optical signal to be within the linear range of the detector . An IR viewer is used for the alignment of the input and the output ends of the fiber under test. A launch numerical aperture wheel is provided to restrict the angle of the light cone before it enters the fiber.

4.3.2 The Main Parts of The Universal Fiber Optics Analyser.

Referring to Fig.4.6, the numerals denote the following components :

(1) Halogen lamp source

(2) Monopass filter

(3) Emitter mirror

(4) Cross-path beam splitter

(5) Launch numerical aperture

(6) Input objective

(7) Input fiber end

(8) Input fiber holder

(9) Output fiber holder

(10) Output rotary stage

(11) Output fiber end

(12) Output objective

(13) Neutral density filter

(14) IR viewer

(15) Detector objective

(16) Detector

(17) Laser source objective

(18) Laser source

4.3.3 The IR Viewer

The IR viewer is an equipment through which the output and the input end of the fiber can be seen (when light is transmitted through it). The IR viewer consists of a single stage image connector tube and an objective lens. The tube has a photocathode and a phosphorus screen. The function of the objective lens is to focus the image of the light source (coming from the output or the input end of the fiber) on to the photocathode. A visual green light appears on the phosphorus screen as a result of the conversion of the source light by the photocathode. Due to this conversion of images, no laser emission can reach the viewer's eye.

The spectral response of the viewer is between 400 nm and 1300 nm . It reaches its maximum sensitivity between 700 nm and 900 nm and, drops to below 20% of its maximum sensitivity below 400 nm and above 1100 nm.

4.3.4 The Detector

The detector used in the Universal Fiber Optics Analyser is an avalanche photodiode (PD-1000). It has a high multiplication rate. It has a rise time of 150 pico second and a cutoff frequency of 2 GHZ. The spectral response of this detector lies between 500 nm and 900 nm. The active area of the diode is 0.03 mm^2. The multiplication rate at a wavelength of 800 nm is 30 at a bias voltage of about 90% of the breakdown voltage. The signal to noise ratio is proportional to the multiplication factor of the diode.

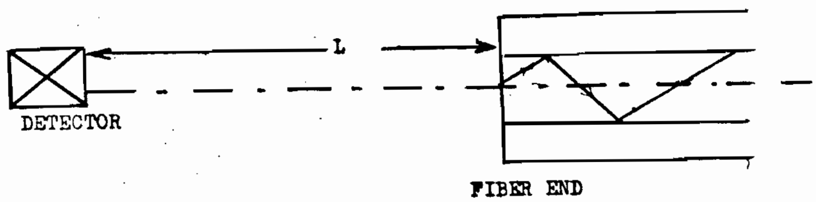

Fig. 4.5 The far-field measurements

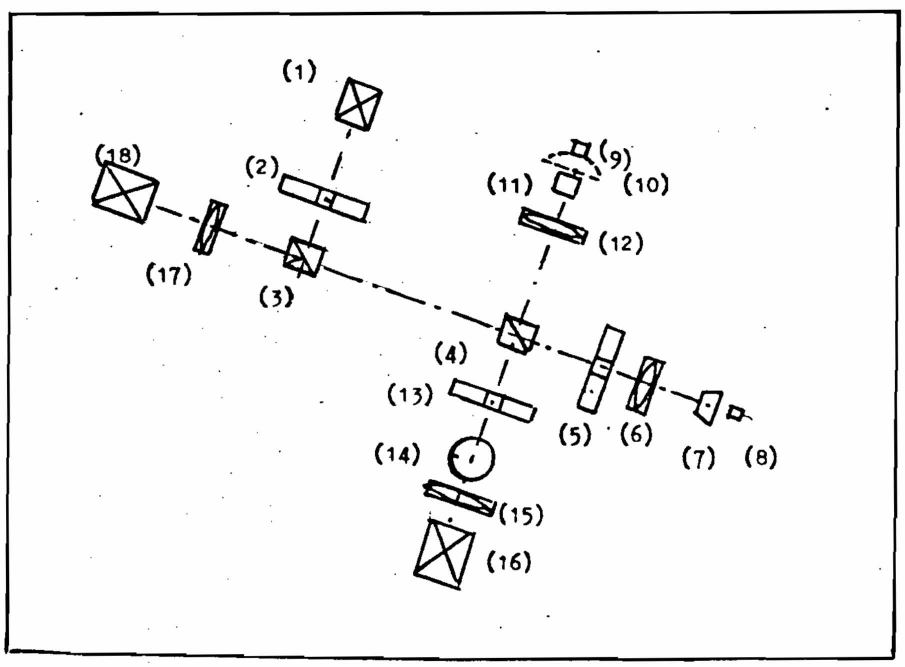

Fig. 4.6 Universal fiber optics analyser

4.4 Set-Up for The Numerical Aperture Measurements

The set-up for the numerical aperture measurements is shown in Fig.4.7. The Universal Fiber Optics Analyser was used throughout these measurements. The light sources in this analyser are the halogen lamp and the laser diode. When the halogen lamp is used, the light passes from the source to the reflector mirror through a monopass filter. The monopass filter gives output light at the wavelengths from 650 nm to 1050 nm. The launch numerical aperture of the Universal Analyser was adjusted to 0.3 NA to make sure it covered the whole core. The emerging light from the output end of the fiber can be swung on the rotary stage between -30 degrees and +30 degrees. The rotation is converted to an electrical signal by the Universal Analyser and can be read, using a normal voltmeter. On the scale of the voltmeter, each 10 millivolts represent 1 degree of rotation. The output can be viewed on the IR viewer, which should be focussed and adjusted for the maximum possible intensity. When these steps are completed, the IR viewer can be removed from the optical path in order to allow the light to pass on to the detector. The output from the detector can be measured using a voltmeter or an oscilloscope. The output power from the detector is recorded each time the rotary stage is moved.

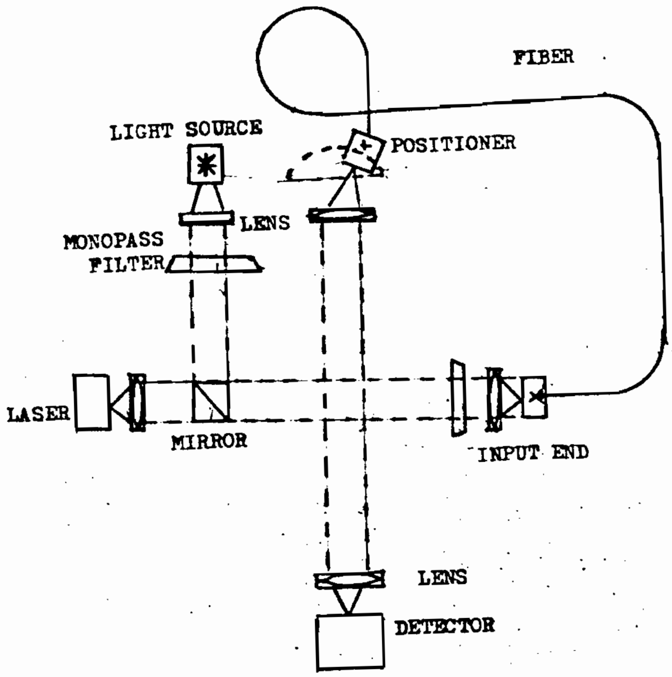

Fig. 4.7 Numerical aperture measurement set-up

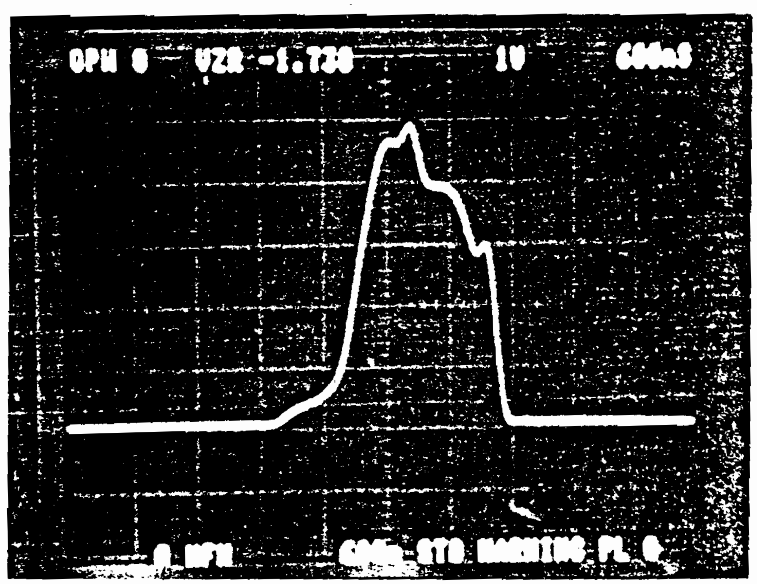

Fig. 4.8 Plotting the numerical aperture for the fiber code: 10/477b, using the 7854 Tecktronix Oscilloscope. Each division in the horizontal scale represents 6 degrees.

Angle	Energy in 10^{-2} watts for the wavelengths					
	650 nm	750 nm	850 nm	900 nm	950 nm	1050
-20.2	.040	.048	.19	.006	.003	.0004
-16.9	.435	.608	.250	.078	.044	.002
-13.9	1.664	2.31	1.103	.372	.211	.014
-11.3	3.423	4.666	2.403	.828	.476	.036
- 7.5	6.151	8.009	4.41	1.613	.883	.076
- 5.4	7.236	9.242	5.244	1.96	1.188	.090
- .2	7.84	9.673	5.954	2.341	1.3	.102
+ 6.3	3.349	4.709	2.439	.864	.518	.04
+10.2	.828	1.145	.562	.202	.115	.008
+12.8	.168	.26	.122	.048	.025	.001
+14.7	.048	.048	.044	.017	.008	.0004
ψ	12.5°	12.75°	12.3°	12.15°	12.25°	12.0°
NA	0.216	0.22	0.213	0.210	0.212	0.207

Table 4.1 Numerical aperture data points for the fiber (code 3/1233A)

Angle	Relative energy in pico watts
-17.7	3.59
-14.5	9.543
-10.6	29.58
- 6.6	45.4
- .5	65.48
+ 3.7	54.83
+ 7.9	15.46
+10.0	7.02
+12.0	4.7
ψ	13.12°
NA	0.2269

Table 4.2 Data points for the numerical aperture of the fiber (code 3/1233A) using laser light.

Angle	Power in 10^{-2} watts for the wavelengths 650 nm	750 nm	850 nm	950 nm	1050 nm
-17.1	.09	.16	.09	.01	
-16.3	.25	.49	.25	.09	
_14.9	.81	1.21	1.0	.16	.01
-12.4	3.61	4.41	2.56	.49	.04
- 8.6	10.24	16.81	6.76	1.44	.16
- 7.8	12.25	20.25	9.0	1.8	.20
- 3.0	16.81	29.16	12.25	2.25	.25
- .4	23.04	32.49	17.64	3.61	.36
+ 3.6	16.0	33.64	12.96	2.56	.25
+ 6.9	7.84	17.64	5.29	1.43	.16
+ 9.8	1.21	2.89	.64	.25	.01
+10.7	.36	.81	.36	.16	
+12.1	.09	.25	.04	.04	
ψ	11.1°	11°	11.15°	11.2°	11.1°
NA	0.192	0.190	0.193	0.194	0.192

Table 4.3 Data points for the numerical aperture of the fiber (code 9/574B)

Angle	Power in pico watts
- 18.8	2.5
- 16.1	4.9
- 11.5	16.81
- 3.9	45.16
- .0	54.97
+ .9	57.18
+ 5.4	15.87
+ 8.1	4.9
+ 10.7	2.33
ψ	11.5°
NA	0.199

Table 4.4 The numerical aperture data for the laser source for the fiber (code 9/574B)

Angle	Power in 10^{-2} watts					
	650 nm	750 nm	850 nm	900 nm	950 nm	1050 nm
-23.1	.17	.21	.12	2.35	.04	
-20.6	3.4	3.64	.98	3.49	.067	
-18.6	12.81	16.0	14.82	11.15	.828	.0676
-12.9	32.6	36.6	28.9	24.7	13.0	2.13
- 9.9	37.4	39.06	30.22	24.7	19.8	4.0
- 6.2	39.4	41.0	34.0	28.0	24.0	6.3
0.0	39.7	42.25	35.64	29.59	26.11	7.8
+ 7.9	21.25	17.14	29.37	9.92	10.3	.518
+ 9.9	9.8	12.11	9.92	3.76	2.56	.109
+12.1	.96	.81	.28	1.0	.39	.07
+13.4	.22	.25	.10	.78	.04	
ψ	15.1°	15.0°	15.0°	15.3°	13.75°	12.25°
NA	0.26	0.258	0.258	0.263	0.237	0.212

Table 4.5 Data points for the fiber (code 10/477B)

Angle	Power in picowatt
-20.0	16.11
-18.5	22.94
-14.6	63.03
-11.8	92.1
- 9.1	97.3
- 6.7	102.0
- 1.6	119.17
- 1.0	138.2
+ .7	109.3
+ 2.3	63.84
+ 8.1	12.96
ψ	14.5°
NA	0.25

Table 4.6 Data points for the numerical aperture of the fiber (code 10/477B), using the laser source

Fiber code	Numerical aperture for the following wavelengths				
	650 nm	750 nm	850 nm	950 nm	1050 nm
3/1233A	0.21	0.22	0.21	0.21	0.20
9/574B	0.19	0.19	0.193	0.194	0.19
10/477B	0.26	0.258	0.258	0.237	0.21

Table 4.7 Numerical aperture results using different wavelengths

Fiber code	NA for laser	NA for Halogen Lamp	Manufacturer data
3/1233A	0.22	0.21	0.20
9/574B	0.20	0.19	0.19
10/477B	0.25	0.26	0.17

Table 4.8 Comparison between a light source at 900 nm wavelength

4.5 Conclusion and Discussion

In Table 4.7, the numerical aperture of three different fibers are shown. The numerical apertures of these fibers were measured for 5 different wavelengths. By looking at this table, it is clear that there is no significant change in numerical aperture with respect to the wavelength and the numerical aperture is constant over most of the spectral range. Table 4.8 shows a comparison between the measured data for the numerical aperture of different fibers, and the data supplied by the manufacturer of these fibers. The first two values are in agreement with the manufacturer's data, while both the measured data using a laser and a halogen lamp for the third fiber are higher.

The measurement using the laser source is considered more reliable. The reason is that the stray light might affect the accuracy of the measurement in the case where the halogen lamp was used as the light source.

The National Bureau of Standards[4.1] suggests that the largest measured angle is to be taken when the output intensity, for the numerical aperture measurement, drops to the 5% level of its maximum value. For the measurements presented here, the 10% level was considered instead of the 5% level. This is because the 5% level fell outside the range of the accuracy of the measurement set-up.

It is clear that the NA values for the 1050 nm wavelength were smaller than the values for 850 nm wavelength. This is due to the fact that the former wavelength falls within the non-linear range of the APD detector.

Generally, the numerical aperture does not change significantly with the wavelength as shown in Tables 4.1 to 4.6.

CHAPTER 5

THE FREQUENCY AND IMPULSE RESPONSE

In this chapter, the frequency and impulse response will be described using two methods. The first one will be the Fast Fourier Transform (FFT), and the second one the Moment Method.

5.1 The Impulse and Frequency Response Using FFT

In this section, the Fast Fourier Transform will be developed from the Discrete Fourier Transform. Also, a method using the FFT to obtain the impulse and frequency response, from a set of discrete data points, will be described.

5.1.1 The Discrete Fourier Transform

It is known that the Fourier Transform and the Inverse Fourier Transform have the following forms[5.1a]:

$$X(f) = \int_{-\infty}^{+\infty} x(t)\, e^{-j2\pi ft}\, dt \qquad \text{--------- (5.1a)}$$

and

$$x(t) = \int_{-\infty}^{+\infty} X(f)\, e^{+j2\pi ft}\, df \qquad \text{--------- (5.1b)}$$

These two equations can be written in a discrete form to give

$$X(f) = T \sum_{k=0}^{N-1} x(t_k)\, e^{-j2\pi ft} \qquad \text{---------- (5.2a)}$$

$$x(t_k) = \Delta f \sum_{n=0}^{N-1} X(f)\, e^{j(2\pi/N)nk} \qquad \text{---------- (5.2b)}$$

where $\Delta f = 1/NT$, and T is the sampling interval in the time domain.

$k = 0,1,2,.....N-1, \quad$ and $n = 0,1,2,.......N-1.$

Let $x_k = T\, x(t_k)$ and $X_n = X(j2\pi f)$

Hence,

$$X_n = \sum_{k=0}^{N-1} x_k \, e^{-j(2\pi/N)nk} \quad \text{-------------- (5.3a)}$$

$$x_k = (1/N)\sum_{n=0}^{N-1} X_n \, e^{j(2\pi/N)nk} \quad \text{-------------- (5.3b)}$$

And let $W_N = e^{-j2\pi/N}$

Hence,

$$X_n = \sum_{k=0}^{N-1} x_k \, W_N^{nk} \quad \text{-------------- (5.3c)}$$

where x_k is a sampled point of $x(t)$ at $t=kT$.

In order to express this as a Fast Fourier Transform, some adjustments have to be made.

Using $W_N = e^{-j2\pi/N}$, $(W_N^2) = e^{-j2\pi/(N/2)}$, and $U = N/2$, we can write

$$X_n = \sum_{k=0}^{U-1} x_{2k} W_N^{2nk} + \sum_{k=0}^{U-1} x_{2k+1} W_N^{n(2k+1)} \quad \text{-------------- (5.4a)}$$

Writting $a_k = x_{2k}$ and $b_k = x_{2k+1}$, equation (5.4a) becomes

$$X_n = \sum_{k=0}^{U-1} a_k \, W_U^{nk} + W_N^n \sum_{k=0}^{U-1} b_k \, W_U^{nk}$$

$$= A_n + W_N^n B_n \quad \text{------------------ (5.4b)}$$

$n= 0,1,2,.............N-1$

where $$A_n = \sum_{k=0}^{U-1} a_k W_U^{nk}$$ ------------ (5.4c)

for the even points.

and, $$B_n = \sum_{k=0}^{U-1} b_k W_U^{nk}$$ ----------------- (5.4d)

for the odd points.

Using the properties[5.1b]

$$A_n = A_{U+n} \text{ and } B_n = B_{U+n}$$ ------------------- (5.5a)

for $n= 0,1,2,\ldots\ldots\ldots\ldots\ldots(U-1)$

Since

$$W_N^{U+n} = (W_N^U)(W_N^n)$$

$$= (e^{-j2\pi/N})^U (W_N^n) = -W_N^n$$ ----- (5.5b)

Hence

$$X_{U+n} = A_n - W_N^n B_n \text{ for } n=0,1,2\ldots\ldots(U-1)$$ -----(5.6)

Repeating the above process once more, we let

$$c_k = a_{2k} = x_{4k}$$ ----------- (5.7a)

$$d_k = a_{2k+1} = x_{4k+2}$$ ----------- (5.7b)

$$e_k = b_{2k} = x_{4k+1}$$ ----------- (5.7c)

$$f_k = b_{2k+1} = x_{4k+3}$$ ----------- (5.7d)

for $k=0,1,2,\ldots\ldots(N/4)-1$

Hence, from (5.3c), (5.4c), (5.4d), and putting V = N/4, we can obtain

$$A_n = C_n + W_N^{2n} D_n \qquad \text{------------- (5.8a)}$$

$$B_{V+n} = E_n + W_N^{2n} F_n \qquad \text{------------- (5.8b)}$$

$$A_{V+n} = C_n - W_N^{2n} D_n \qquad \text{------------- (5.8c)}$$

$$B_{V+n} = E_n - W_N^{2n} F_n \qquad \text{------------- (5.8d)}$$

for n=0,1,2,........,(V-1)

where

$$C_n = \sum_{k=0}^{V-1} c_k W_V^{nk} \qquad \text{------------- (5.9a)}$$

$$D_n = \sum_{k=0}^{V-1} d_k W_V^{nk} \qquad \text{------------- (5.9b)}$$

$$E_n = \sum_{k=0}^{V-1} e_k W_V^{nk} \qquad \text{------------- (5.9c)}$$

$$F_n = \sum_{k=0}^{V-1} f_k W_V^{nk} \qquad \text{------------- (5.9d)}$$

In order to visualize these properties let equation (5.4c) be written for N=4

$$A_n = \sum_{k=0}^{1} a_k W_2^{nk} \qquad \text{------------ (5.10)}$$

i.e.

$$A_0 = a_0 W_2^0 + a_1 W_2^0 = x_0 W_2^0 + x_2 W_2^0$$

$$A_1 = a_0 W_2^0 + a_1 W_2^1 = x_0 W_2^0 + x_2 W_2^1$$

$$A_2 = a_0 W_2^0 + a_1 W_2^2 = x_0 W_2^0 + x_2 W_2^2$$

$$B_0 = b_0 W_2^0 + b_1 W_2^0 = x_1 W_2^0 + x_3 W_2^0 \quad \text{-- (5.11)}$$

$$B_1 = b_0 W_2^0 + b_1 W_2^1 = x_1 W_2^0 + x_3 W_2^1$$

$$B_2 = b_0 W_2^0 + b_1 W_2^2 = x_1 W_2^0 + x_3 W_2^2$$

Hence, using (5.4b), we get

$$X_0 = A_0 + W_4^0 B_0$$

$$X_1 = A_1 + W_4^1 B_1$$

$$X_2 = A_2 + W_4^2 B_2 \quad \text{------ (5.12)}$$

$$X_3 = A_3 + W_4^3 B_3$$

and using (5.5b) we get

$$W_4^2 = - W_4^0 \quad , \quad W_4^3 = - W_4^1 \quad \text{------ (5.13)}$$

Hence, writing $X(n) = X_n$

$$X(0) = A_0 + W_4^0 B_0$$

$$X(1) = A_1 + W_4^1 B_1$$

$$X(2) = A_0 - W_4^0 B_0 \qquad \text{---- (5.14)}$$

$$X(3) = A_1 - W_4^1 B_1$$

Let $W^n = W_N^n$ and $x_0(n) = x_n$

Hence, from (5.14) and using (5.11),

$$X(0) = x_0(0) W_2^0 + x_0(2) W_2^0 + W_4^0 [x_0(1) W_2^0 + x_0(3) W_2^0]$$

$$X(1) = x_0(0) W_2^0 + x_0(2) W_2^1 + W_4^1 [x_0(1) W_2^0 + x_0(3) W_2^1]$$

$$X(2) = x_0(0) W_2^0 + x_0(2) W_2^0 - W_4^0 [x_0(1) W_2^0 + x_0(3) W_2^0] \quad \text{-- (5.15)}$$

$$X(3) = x_0(0) W_2^0 + x_0(2) W_2^1 - W_4^1 [x_0(1) W_2^0 + x_0(3) W_2^1]$$

Since $W_2^1 = W^2 = - W^0$, where $W = W_N = e^{-j2\pi/N}$,

$$X(0) = x_0(0) + x_0(2) W^0 + W^0 [x_0(1) + x_0(3) W^0]$$

$$X(1) = x_0(0) - x_0(2) W^0 + W^1 [x_0(1) - x_0(3) W^0]$$

$$\text{---(5.16)}$$

$$X(2) = x_0(0) + x_0(2) W^0 - W^0 [x_0(1) + x_0(3) W^0]$$

$$X(3) = x_0(0) - x_0(2) W^0 - W^1 [x_0(1) - x_0(3) W^0]$$

Before getting into the details of the Fast Fourier Transform it is worthwhile to check the number of multiplications and additions needed to compute the Discrete Fourier Transform. From equation (5.3c), which is used to compute the DFT for N sample points, the number of complex multiplications is NxN and the number of complex additions is N(N-1).

5.1.2 The Fast Fourier Transform

It is possible to reduce the computational steps in the DFT by a factorization of the matrix such as in (5.16). This leads to the FFT[5.2].

Using (5.3a) and writing $X(n) = X_n$, and $x_0(n) = x_n$

$$X(n) = \sum_{k=0}^{N-1} x_0(k)\, e^{-j(2\pi/N)nk} \qquad \text{----- (5.17)}$$

$$\begin{aligned}
X(0) &= x_0(0)\, W^0 + x_0(1)\, W^0 + \dots\dots\dots + x_0(N-1)\, W^0 \\
X(1) &= x_0(0)\, W^0 + x_0(1)\, W^1 + \dots\dots\dots + x_0(N-1) W^{N-1} \\
X(2) &= x_0(0)\, W^0 + x_0(1)\, W^2 + \dots\dots\dots + x_0(N-1)^{2(N-1)} \\
&\dots\dots\dots\dots\dots\dots\dots\dots\dots\dots \\
&\dots\dots\dots\dots\dots\dots\dots\dots\dots\dots \\
X(N-1) &= x_0(0)\, W^0 + x_0(1)\, W^{N-1} + \dots\dots\dots + x_0(N-1)^{(N-1)^2}
\end{aligned} \qquad \text{----(5.18)}$$

or

$$\begin{vmatrix} X(0) \\ X(1) \\ X(2) \\ X(3) \\ .. \\ X(N-1) \end{vmatrix} = \begin{vmatrix} W^0 & W^0 & W^0 & \dots & W^0 \\ W^0 & W^1 & W^2 & \dots & W^{N-1} \\ W^0 & W^2 & W^4 & \dots & W^{2(N-1)} \\ . & . & . & \dots & . \\ . & . & . & \dots & . \\ W^0 & W^{N-1} & W^{2(N-1)} & & W^{(N-1)^2} \end{vmatrix} \begin{vmatrix} x_0(0) \\ x_0(1) \\ x_0(2) \\ . \quad . \\ . \quad . \\ x_0(N-1) \end{vmatrix} \qquad \text{----- (5.19)}$$

Equation (5.19) can be rewritten for N=4, as follows,

$$\begin{vmatrix} X(0) \\ X(1) \\ X(2) \\ X(3) \end{vmatrix} = \begin{vmatrix} W^0 & W^0 & W^0 & W^0 \\ W^0 & W^1 & W^2 & W^3 \\ W^0 & W^2 & W^4 & W^6 \\ W^0 & W^3 & W^6 & W^9 \end{vmatrix} \begin{vmatrix} x_0(0) \\ x_0(1) \\ x_0(2) \\ x_0(3) \end{vmatrix} \quad \text{------(5.20)}$$

Writing $W^{nk} = e^{-j2\pi nk/N}$

$$W^0 = 1 = W^4 , \quad W^6 = W^{-j2\pi 6/4} = W^{-j2\pi 2/4} \cdot W^{-j2\pi 2/4} \cdot W^{-j2\pi 2/4}$$

$$W^{nk} = W^{(nk \text{ MOD } N)} = W^{(\text{Remainder of the division of nk by N})}$$

$$W^{(6 \text{ MOD } 4)} = W^2$$

Equation (5.20) can be written as

$$\begin{vmatrix} X(0) \\ X(1) \\ X(2) \\ X(3) \end{vmatrix} = \begin{vmatrix} 1 & 1 & 1 & 1 \\ 1 & W^1 & W^2 & W^3 \\ 1 & W^2 & W^0 & W^2 \\ 1 & W^3 & W^2 & W^1 \end{vmatrix} \begin{vmatrix} x_0(0) \\ x_0(1) \\ x_0(2) \\ x_0(3) \end{vmatrix} \quad \text{---------- (5.21)}$$

Using the previous properties and interchanging the second and third rows , the last matrix can be expanded as

$$\begin{vmatrix} X(0) \\ X(2) \\ X(1) \\ X(3) \end{vmatrix} = \begin{vmatrix} 1 & W^0 & 0 & 0 \\ 1 & W^2 & 0 & 0 \\ 0 & 0 & 1 & W^1 \\ 0 & 0 & 1 & W^3 \end{vmatrix} \begin{vmatrix} 1 & 0 & W^0 & 0 \\ 0 & 1 & 0 & W^0 \\ 1 & 0 & W^2 & 0 \\ 0 & 1 & 0 & W^2 \end{vmatrix} \begin{vmatrix} x_0(0) \\ x_0(1) \\ x_0(2) \\ x_0(3) \end{vmatrix} \quad \text{---(5.22)}$$

Equation (5.22) can be written as

$$\begin{vmatrix} X(0) \\ X(2) \\ X(1) \\ X(3) \end{vmatrix} = \begin{vmatrix} 1 & W^0 & 0 & 0 \\ 1 & W^2 & 0 & 0 \\ 0 & 0 & 1 & W^1 \\ 0 & 0 & 1 & W^3 \end{vmatrix} \begin{vmatrix} x_1(0) \\ x_1(1) \\ x_1(2) \\ x_1(3) \end{vmatrix} \text{---------------}(5.23a)$$

and

$$\begin{vmatrix} x_1(0) \\ x_1(1) \\ x_1(2) \\ x_1(3) \end{vmatrix} = \begin{vmatrix} 1 & 0 & W^0 & 0 \\ 0 & 1 & 0 & W^0 \\ 1 & 0 & W^2 & 0 \\ 0 & 1 & 0 & W^2 \end{vmatrix} \begin{vmatrix} x_0(0) \\ x_0(1) \\ x_0(2) \\ x_0(3) \end{vmatrix} \text{--------}\ (5.23b)$$

Expanding equation (5.23b), and using $W^2 = -W^0 = -1$ we get

$$\begin{aligned} x_1(0) &= x_0(0) + x_0(2)W^0 \\ x_1(1) &= x_0(1) + x_0(3)W^0 \\ x_1(2) &= x_0(0) - x_0(2)W^0 \qquad \text{-------}\ (5.23c) \\ x_1(3) &= x_0(1) - x_0(3)W^0 \end{aligned}$$

And also from (5.23a) we get

$$\begin{aligned} X(0) &= x_1(0) + x_1(1)W^0 \\ X(1) &= x_1(2) + x_1(3)W^1 \\ X(2) &= x_1(0) - x_1(1)W^0 \qquad \text{--------}\ (5.23d) \\ X(3) &= x_1(2) - x_1(3)W^1 \end{aligned}$$

Note in the previous set of equations, in (5.23c), $x_1(2)$ and $x_1(3)$ can be computed by simply subtracting the two corresponding terms for $x_1(0)$ and $x_1(1)$. In (5.23d), X(2) can be obtained by subtracting $x_1(0)$ and $w^o x_1(2)$, and X(3) by subtracting $x_1(2)$ and W $x_1(3)$ respectively. From this, it is clear that the FFT would reduce the number of multiplications for each matrix by one half. In (5.23c), $x_1(0)$ and $x_1(2)$ as well as $x_1(1)$ and $x_1(3)$ are examples of the so-called "dual node pair" in the sense that they are formed from the same pair of data points in a previous data array.

Equations (5.23a) and (5.23b) give

$$
\left.
\begin{aligned}
X(0) &= x_0(0) + x_0(2)\,W^0 + W^0[x_0(1) + x_0(3)\,W^0\,] \\
X(1) &= x_0(0) - x_0(2)\,W^0 + W^1[x_0(1) - x_0(3)\,W^0\,] \\
X(2) &= x_0(0) + x_0(2)\,W^0 + W^2[x_0(1) + x_0(3)\,W^0\,] \\
X(3) &= x_0(0) - x_0(2)\,W^0 + W^3[x_0(1) - x_0(3)\,W^0\,]
\end{aligned}
\right\} \text{------}(5.24)
$$

or

$$
\left.
\begin{aligned}
X(0) &= x_0(0) + x_0(2)\,W^0 + W^0[x_0(1) + x_0(3)\,W^0\,] \\
X(1) &= x_0(0) - x_0(2)\,W^0 + W^1[x_0(1) - x_0(3)\,W^0\,] \\
X(2) &= x_0(0) + x_0(2)\,W^0 - W^0[x_0(1) + x_0(3)\,W^0\,] \\
X(3) &= x_0(0) - x_0(2)\,W^0 - W^1[x_0(1) - x_0(3)\,W^0\,]
\end{aligned}
\right\} \text{--------}(5.25)
$$

Equation 5.25 is exactly the same as 5.16 , which was previously derived from the DFT algorithm.

From the previous factorization, it should be noted that, for $N= 2^{IR}$, the FFT algorithm factorizes the N by N matrix into IR - matrices. Each matrix has N by N elements, and each requires only (N/2) multiplications. From this, we get the total multiplication for the FFT to be equal to (N/2)IR. The big advantage of the FFT can be seen when we compare this to the discrete Fourier Transform, (DFT) which requires N^2 multiplications. There is one minor difficulty in the computation of the FFT and that is the interchange of x(1)-row with x(2)-row. This interchange has one property, i.e. when expressing x(1) in binary form as x(01) and x(2) as x(10), x(1) and x(2) can be interchanged by bit-reversing the binary argument, i.e. 01 becomes 10 and 10 becomes 01 etc.

For example the previous samples can be written as

$x(0) = x(00)$			$x(00) = x(0)$
$x(1) = x(01)$	and if the binary bits		$x(10) = x(2)$
$x(2) = x(10)$	are reversed we get	-->	$x(01) = x(1)$
$x(3) = x(11)$			$x(11) = x(3)$

5.1.3 Programming The FFT

Equation (5.18) can be written for a dual node pair in the following form

$$x_L(i) = x_{L-1}(i) + W^p x_{L-1}[i + (N/2^L)]$$
$$\text{---------} \quad (5.26)$$
$$x_L[i + (N/2^L)] = x_{L-1}(i) - W^p x_{L-1}[i + (N/2^L)]$$

where L is the array number or the current computation step and L-1 is the previous computaion step.

$W^n = W^p$, $n = 0, 1, 2, \ldots\ldots, N-1$, $i = 0, 1, 2, \ldots\ldots\ldots, N-1$ and i indicates the node to be computed. From equation (5.26), it should be noted that, if the first N/2 dual nodes are computed, there is then no need to compute the next N/2 dual nodes. In general, the first $N/(2^L)$ are computed and the next $N/(2^L)$ are skipped until i reaches N-1.

It was noted earlier this computation has the bit reversal property. If L is the array number and given $N = 2^{IR}$ then p is the power of W and p = bit reversal of (IR - L).

A flow chart can be constructed to program the FFT[5.1, 5.2]. The inverse FFT can be computed from FFT as shown in the flow chart by letting KODE = -1, or in other words by changing the sign of the sine function.

5.1.4 FFT Flow Chart

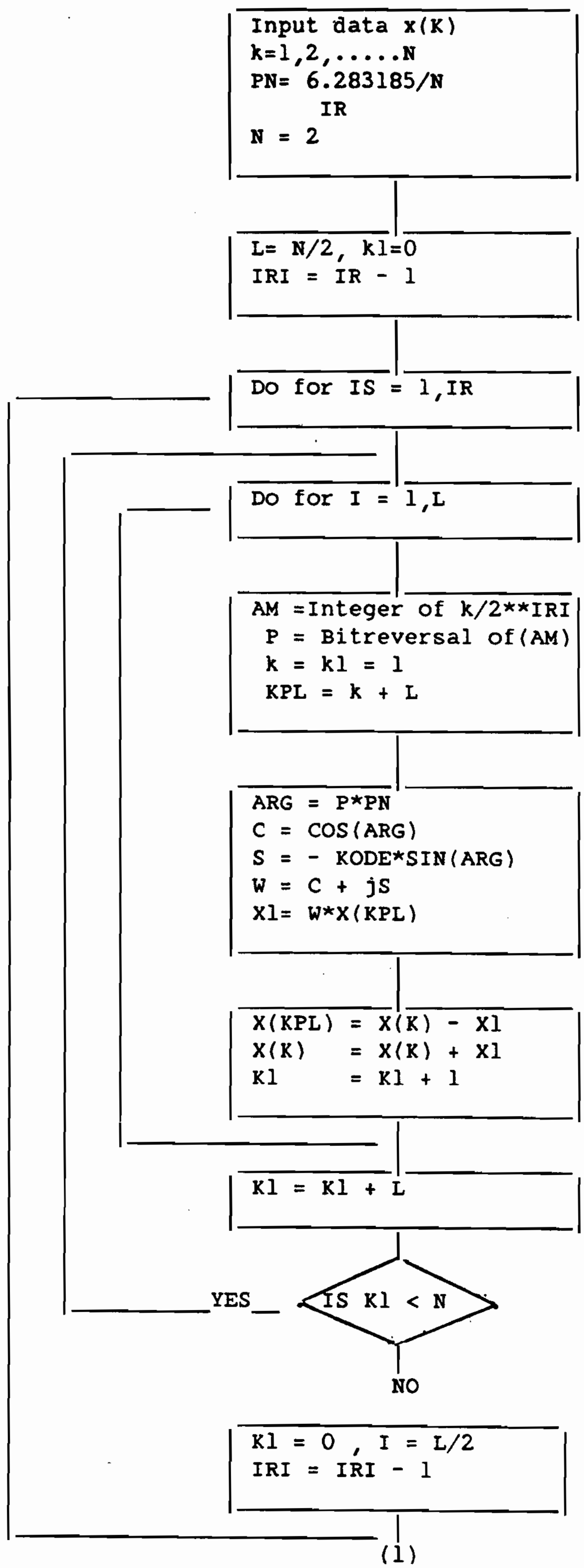

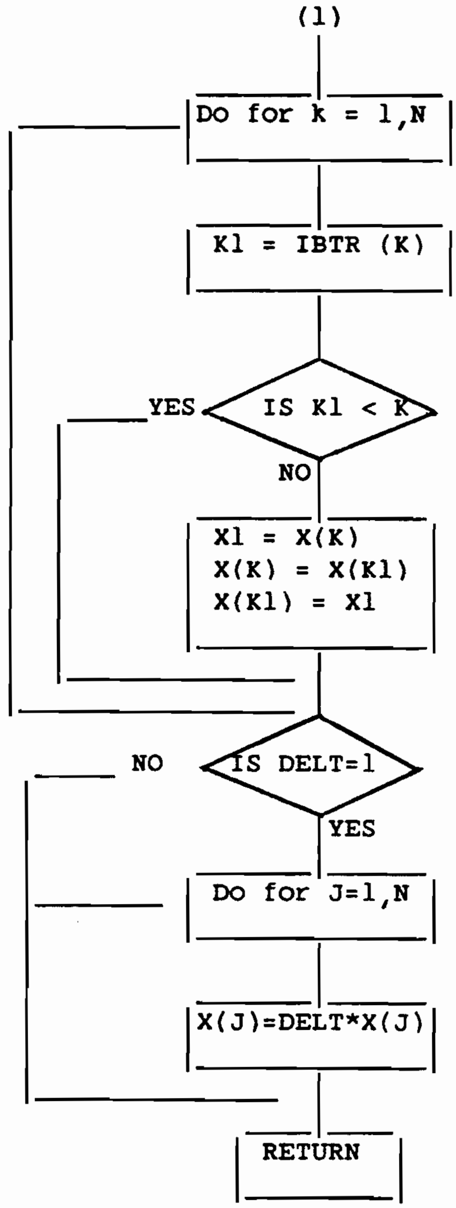

The Main FFT Subroutine

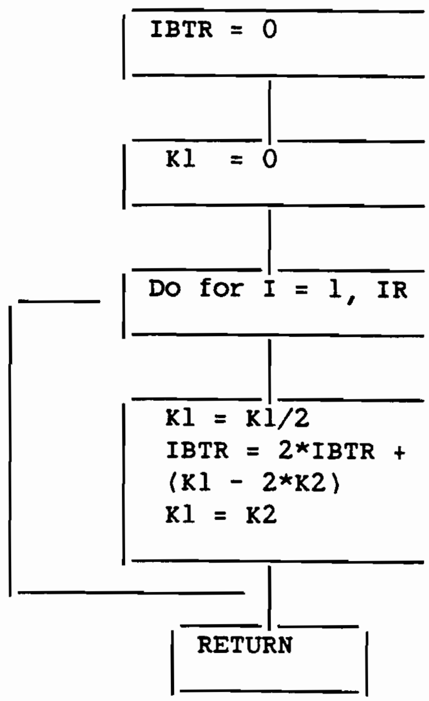

IBTR the bit reversal function

5.1.5 FFT Computing Efficiency

It is known that for a real signal $x(k)$,

$$Im[x(k)] = 0 \quad \text{for } k=1,2,3......N \qquad ----- (5.27)$$

and such functions[5.3] possess a spectrum which exhibits complex conjugate symmetry:

$$X(n) = X^*(N-n) \quad \text{for } n=1,2,3,......(U-1) \qquad ----- (5.28)$$

where $X(n)$ is the Fourier Transform of $x(k)$, and $U = N/2$. For FFT of N real points, 2N storage points are needed, i.e. the real and the imaginary. Half of this storage location could be regarded as redundant. Furthermore, computing time would be wasted in evaluating the negative half of the frequency spectrum. A method, which eliminates these sources of inefficiency in processing real data, will be examined here.

Using the symmetry property:

$$X(n) = X_{even}(n) + X_{odd}(n) \quad ,n=1,2,3,.....(U-1) \qquad ----- (5.29)$$

where $X_{even}(n) = [X(n)+X(N-n)]/2 \qquad ----- (5.30)$

and $X_{odd}(n) = -X_{odd}(N-n)$

$=[X(n)-X(N-n)]/2 \quad ,n=1,2,3,....(U-1) \qquad ---- (5.31)$

and $X_{even}(0) = X(0)$

$X_{even}(U) = X(U)$

$--------------- (5.32)$

$X_{odd}(0) = 0$

$X_{odd}(U) = 0$

For two real signals $y_s(k)$ and $y_r(k)$, the Fourier Transforms are $Y_s(n)$ and $Y_r(n)$, where, $x(k) = y_s(k) + jy_r(k)$ for N points. The midpoint U will be chosen as N/2.

Hence,

$$\mathrm{Real}\ [Y_s(n)] = \mathrm{Real}[\ X(n) + X(N-n)]/2$$

$$\mathrm{Imag}\ [Y_s(n)] = \mathrm{Imag}[\ X(n) - X(N-n)]/2$$

$$\mathrm{Real}\ [Y_r(n)] = \mathrm{Imag}[\ X(n) + X(N-n)]/2 \qquad \text{----}\ (5.33)$$

$$\mathrm{Imag}\ [Y_r(n)] = \mathrm{Real}[\ X(N-n) - X(n)]/2$$

$$n = 1,2,3,\ \ldots\ldots\ldots\ (U-1)$$

$$\mathrm{Real}[Y_s(0)] = \mathrm{Real}[X(0)]$$

$$\mathrm{Real}[Y_r(0)] = \mathrm{Imag}[X(0)]$$

$$\mathrm{Real}[Y_s(U)] = \mathrm{Real}[X(U)]$$

$$\mathrm{Real}[Y_r(U)] = \mathrm{Imag}[X(U)] \qquad \text{------}\ (5.34)$$

$$\mathrm{Imag}[Y_s(0)] = \mathrm{Real}[Y_s(U)]$$

$$\mathrm{Imag}[Y_r(0)] = \mathrm{Real}[Y_r(U)]$$

From equations 5.33 and 5.34, it is clear that the Fourier Transform of the two signals $y_s(K)$ and $y_r(k)$ can be computed by calling the FFT routine once, for the combined signal $x(k)$, instead of calling it twice (once for each signal).

5.1.6 The Impulse and Frequency Response

The frequency response can be evaluated using the discrete convolution in the frequency domain of both the input and the output signals

$$H(f) = Y_r(f)/Y_s(f) \qquad \text{-------} \quad (5.35)$$

where $Y_r(f)$ is the spectrum of the output signal and $Y_s(f)$ is that of the input signal and H(f) is the frequency response of the system. The input signal $y_s(t)$ can be transformed to $Y_s(f)$ using the FFT algorithm as was previously shown. The impulse response can be obtained using the inverse FFT of H(f).

The convolution of $y_s(t)$ with the impulse response h(t) can be expressed by the following summation

$$y_r(kT) = \sum_{n=0}^{N-1} y_s(nT)\ h[(k-n)T] \qquad \text{-------} \quad (5.36)$$

$$= y_s(kT)*h(kT)$$

where $y_s(nT)$ and h((k-n)T) are two periodic functions each with a period NT.

If the number of samples for y (kT) = N_1 and for h(kT) = N_2, then the period must be chosen such that[5.4,5.5]

$$N = N_1 + N_2 - 1 \qquad \text{---------} \quad (5.37)$$

This comes from the fact that the convolution of a function represented by N_1 samples and another one by N_2 samples, is a function represented by (N_1 + N_2 - 1) samples.

5.1.7 The Impulse and Frequency Response Flowchart:

Read $y_r(I)$, $y_s(I)$

for I = 1, N

$X(I) = y_s(I) + jy_r(I)$

for I = 1, N

Call FFT[X(I)]

Do for J = 1, N/2

$\mathrm{Real}(Y_s(J)) = \mathrm{Real}[X(J)+X(N-J)]/2$

$\mathrm{Imag}(Y_s(J)) = \mathrm{Imag}[X(J)-X(N-J)]/2$

$\mathrm{Real}(Y_r(J)) = \mathrm{Imag}[X(J)+X(N-J)]/2$

$\mathrm{Imag}(Y_r(J)) = \mathrm{Real}[X(N-J)-X(J)]/2$

Do for I= 1,N/2

$H(I) = Y_r(I)/Y_s(I)$

Call IFFT [H(I)]

Call plot[H(I)]

STOP

5.2 The Impulse and Frequency Response Using The Moment Method

5.2.1 The Impulse Response

In this section an alternative method will be described. This method is based upon using the moments of both the input and output function to get the impulse response. The moments of a function h(t) is defined as[5.6,5.7]

$$M_n = \int_{-\infty}^{+\infty} t^n \, [h(t)/\text{area}]dt \qquad \text{-------------------(5.38a)}$$

$$n = 0,1,2,.........N$$

where $$\text{area} = \int_{-\infty}^{+\infty} h(t)\, dt$$

$$M_1 = \int_{-\infty}^{+\infty} t\, [h(t)/\text{area}]\, dt$$

and $$M_2 = \sigma^2 = \int_{-\infty}^{+\infty} t^2 \, [\, h(t)/\text{area}\,]dt$$

where σ is the standard deviation or the dispersion of h(t). Equation (5.38) can be rewritten as the following

$$M_n = \int_{-\infty}^{+\infty} t^n \; f(t)\; dt \qquad \text{--------- (5.38b)}$$

where $f(t) = h(t) / \text{area}$

Since most of the signals we are dealing with are Gaussian or near Gaussian, the function f(t) can be approximated by a Gaussian function in the following form,

$$f(t) = 1/[\sigma \sqrt{(2\pi)}\ ]\ e^{-t^2/2\sigma^2} \qquad \text{---------- (5.39)}$$

and its error can be expressed as

$$\epsilon(t) = f(t) - 1/[\sigma\sqrt{(2\pi)}]\, e^{-t^2/2\sigma^2} \quad \text{--------} \ (5.40)$$

It is more convenient to define the error function in terms of orthogonal polynomials such as Hermite polynomials.

$$\text{Hence}, \quad \epsilon(t) = 1/[\sigma\sqrt{(2\pi)}]\, e^{-t^2/2\sigma^2} \sum_{k=0}^{\infty} C_k H_k(t/\sigma) \quad \text{----}(5.41)$$

where $H_k(t/\sigma)$ is the Hermite polynomial and C_k is a constant.

$$\text{and} \qquad H_k(t/\sigma) = (-1)^k\, e^{t^2/2\sigma^2} (d^k/dt^k)\, e^{-t^2/2\sigma^2}$$

$$= (t/\sigma)^k - \binom{k}{2}(t/\sigma)^{k-2} + 1.3\binom{k}{4}(t/\sigma)^{k-4} - 1.3.5\binom{k}{6}(t/\sigma)^{k-6} + \text{-----}$$

$$\text{------}(5.42)$$

Using equation (5.41) and (5.40) and taking the moments on both sides to get

$$\sum_{k=0}^{\infty} \int_{-\infty}^{+\infty} t^n\, [1/\sigma\sqrt{(2\pi)}]\, e^{-t^2/2\sigma^2}\, C_k \left[(t/\sigma)^k - \binom{k}{2}(t/\sigma)^{k-2} + 1.3\binom{k}{4}(t/\sigma)^{k-4} \right.$$

$$\left. - 1.3.5\binom{k}{6}(t/\sigma)^{k-6} + \text{---------} \right] dt$$

$$= \int_{-\infty}^{+\infty} t^n\, f(t)\, dt - \int_{-\infty}^{+\infty} t^n/\sigma\sqrt{(2\pi)}\, e^{-t^2/2\sigma^2}\, dt \quad \text{---------} \ (5.43)$$

The right hand side of equation (5.43) becomes

$$\int_{-\infty}^{+\infty} t^n\, f(t)\, dt - \int_{-\infty}^{+\infty} t^n/\sigma\sqrt{(2\pi)}\, e^{-t^2/2\sigma^2}\, dt$$

$$= M_n - A_n/(\sigma^{-n}) \quad \text{-----------} \ (5.44)$$

where $\quad A_n = 1.3.5 \ \ldots\ldots\ldots\ldots \ (n-1) \qquad$ for n = even,

and $\quad A_n = 0 \qquad$ for n = odd.

and the left hand side of (5.43) becomes

$$\sum_{k=0}^{\infty} (\sigma^{n}) C_k \left(A_{n+k} - \binom{k}{2} A_{n+k-2} + 1.3 \binom{k}{4} A_{n+k-4} - 1.3.5 \binom{k}{6} A_{n+k-6}\right.$$

$$= M_n - (\sigma^{n}) A_n \quad \text{-----------------} \ (5.45)$$

$$A_m = 0 \qquad \text{for } m \text{ odd.}$$

The constants C_k can be determined from equation (5.45) for k=0 to k=6 , n=0,1,2,3,4,5,and 6, using

$$A_{2m} = (2m-1)(2m-3)(2m-5)\ldots\ldots. \ 5.3.1$$

$$= (2m-1) A_{2m-2}$$

The C_k's are found to be

$C_0 = M_0 - 1 = 0$

$C_1 = M_1 / \sigma = 0$ if the function is even.

$C_2 = (M_2 / \sigma^2 - 1)/2 = 0$

$C_3 = [M_3 / (\sigma^3 \, 3!)] - (1/2)C_1$

$C_4 = [M_4/(\sigma^4 \, 4!)] - 3/4!$

$C_5 = [M_5 / (\sigma^5 \, 5!)] - (1/2)C_3 - (1/2.4)C_1$

$C_6 = [M_6 / (\sigma^6 \, 6!)] - (A_6 / 6!) - (1/2)C_4$

Using these C_k's we get

$$h(t) = A_h/(\sigma\sqrt{(2\pi)})\, e^{-t^2/2\sigma^2} [1 + C_1H_1 + C_2H_2 + C_3H_3 + C_4H_4 + C_5H_5 + C_6H_6]$$

$$\text{---------------}(5.46)$$

where $A_h = M_0$ = area

$$H_1 = (t/\sigma)$$

$$H_2 = (t/\sigma)^2 - 1$$

$$H_3 = (t/\sigma)^3 - 3(t/\sigma)$$

$$H_4 = (t/\sigma)^4 - 6(t/\sigma)^2 + 3$$

$$H_5 = (t/\sigma)^5 - 10(t/\sigma)^3 + 15(t/\sigma)$$

$$H_6 = (t/\sigma)^6 - 15(t/\sigma)^4 + 45(t/\sigma)^2 - 15$$

The moments of h(t) can be evaluated as it will be shown later on, and hence h(t) can be determined in terms of t.

In order to write the formula of h(t) in higher orders, a simpler and general formula for obtaining the constants C_k shall be derived.

Let C_5 and C_6 be rewritten as the following

$$C_5 = [(M_5/\sigma^5) - A_5]/5! - (1/2)C_3 - 1/(2.4)\,C_1 \quad \text{-------}\ (5.47)$$

$$C_6 = [(M_6/\sigma^6) - A_6]/6! - (1/2)C_4 \quad \text{-------}\ (5.48)$$

Using n=7 , equation (5.45) , $A_{12} = 9.11.A_8$, and $A_{10} = 9A_8$ we get

$$C_7 = [(M_7/\sigma^7) - A_7]/7! - (1/2)C_5 - (1/2.4)C_3 - (1/2.4.6)C_1 \quad \text{-------}\ (5.49)$$

Comparing equations (5.49) , (5.48), and (5.47), the equation for C_8 can be found as follows

$$C_8 = [(M_8/\sigma^8) - A_8]/8! - (1/2)C_6 - (1/2.4)C_4 \quad \text{------}\ (5.50)$$

and,

$$C_9 = [(M_9/\sigma^9) - A_9]/9! - (1/2)C_7 - (1/2.4)C_5 - (1/2.4.6)C_3 - (1/2.4.6.8)C_1 \quad \text{------------------------}\ (5.51)$$

From this, a general formula for C_n can be deduced

$$C_n = [(M_n/\sigma^n) - A_n]/n! - (1/2)C_{n-2} - (1/2.4)C_{n-4} - (1/2.4.6)C_{n-6} \text{-----} - [1/2.4.6...(n-3)]C_3 - [1/2.4.6....(n-3)(n-1)]C_1 \quad \text{----}(5.52)$$

for n odd

$$C_n = [(M_n / \sigma^n) - A_n]/n! - (1/2)C_{n-2} - (1/2.4)C_{n-4}$$

$$-(1/2.4.6)C_{n-6} ----- -[1/2.4.6...(n-4)]C_4 -[1/2.4.6...(n-4)(n-2)]C_2 \quad ----(5.53)$$

for n even

Using equation (5.53) and equation (5.42) for $H_n(t/\sigma)$, h(t) can be written for nth order as below

$$h(t) = A_h/[\sigma\sqrt{(2\pi)}]\, e^{-t^2/2\sigma^2} [1 + C_1H_1 + C_2H_2 + ... + C_nH_n] \quad ---- (5.54)$$

5.2.2 The Frequency Response

The frequency response can be evaluated using the moments of both the input and the output pulses $y_s(t)$ and $y_r(t)$[5.6].

$$H(\omega) = A_H \exp[-j\omega M_1 - \omega^2\sigma^2/2 + j\omega^3 M_3/6 + \omega^4(M_4 - 3\sigma^4)/24$$

$$- j\omega^5(M_5 - 10\, M_3\sigma^2)/120 - \omega^6(M_6 - 15\, M_4\sigma^2 - 10\, M_3^2 + 30\sigma^6)/720$$

$$+ \ldots\ldots\ldots] \qquad \text{----------------- (5.55)}$$

The previous equation gives the relation between moments and the frequency response. For details see Appendix G.

$$A_H = A_r/A_s = \text{area of the input } y_s(t)/\text{area of the output } y_r(t)$$

$$= M_0 \qquad \text{----- (5.56a)}$$

$$M_1 = M_{1r} - M_{1s} \qquad \text{----- (5.56b)}$$

$$\sigma^2 = \sigma_r^2 - \sigma_s^2 = M_{2r} - M_{2s} \qquad \text{----- (5.56c)}$$

$$M_3 = M_{3r} - M_{3s} \qquad \text{----- (5.56d)}$$

$$M_4 = M_{4r} - M_{4s} + 6\, M_{2s}^2 + 6\sigma_s^2\, \sigma_r^2 \qquad \text{---- (5.56e)}$$

$$M_5 = M_{5r} - M_{5s} + 20\, M_{3s}\, M_{2s} - 10(M_{3r}\, M_{2s} + M_{3s}\, M_{2r}) \qquad \text{---- (5.56f)}$$

$$M_6 = M_{6r} - M_{6s} + 35(M_4\sigma^2 - M_{4r}\sigma_r^2 + M_{4s}\sigma_s^2)$$

$$- 30(\sigma^6 - \sigma_r^6 + \sigma_s^6) + 10(M_3^2 - M_{3r}^2 + M_{3s}^2) \qquad \text{---- (5.56g)}$$

and, the absolute value of the normalized transfer function is

$$|H_n(\omega)| = \exp\Big(- \omega^2 \sigma^2/2 + (\omega^2\sigma^2/2)^2 [M_4/ 3\sigma^4 - 1]/2$$

$$- (\omega^2\sigma^2/2)^3 [M_6 / 15\sigma^6 - M_4 /\sigma^4 -2M_3^2 / 3\sigma^6$$

$$+ 2]/6+ \ldots\ldots\ldots\ldots \Big) \text{ ----------------(5.57)}$$

Using the moments of both the input and the output signals, the moments of the impulse response h(t) can be obtained with the set of equations (5.56). Then, using equation (5.54), the impulse response h(t) can be evaluated. The normalized frequency response can be computed using equation (5.57). The impulse and frequency response were programmed for a given fiber, by using the input and the output pulses. A flow chart showing the steps of programming this algorithm is shown on p.76 and p.77.

Defining the 3 dB bandwidth B as $|H_n(2\pi B)|=1/2$, it can be shown from equation (5.57) that B is approximated by,

$$B \simeq 1/5\sigma \quad \text{------------------------} \quad (5.58)$$

5.2.3 The Flowchart for The Inpulse Response Using The Moment Method

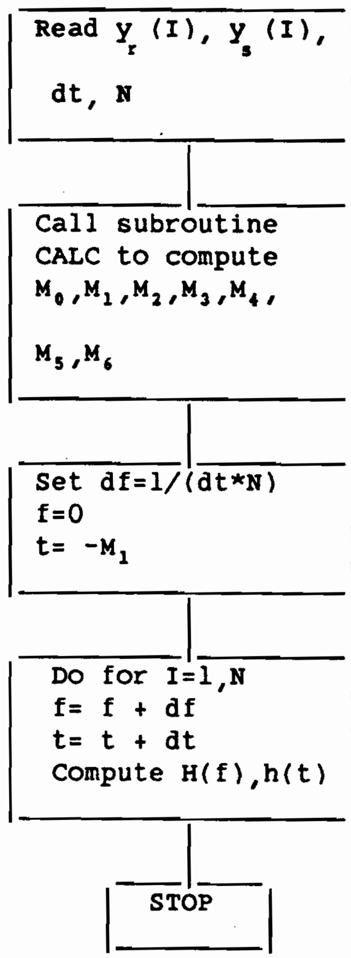

The main program.

Do For I=1,6
$M_r(I) = 0,\ M_s(I)$

Do for I=2,N
$M_r(0)=M_r(0)+y_r(I)+y_r(I-1)$
$M_s(0)=M_s(0)+y_s(I)+y_s(I-1)$
$M_r(1)=M_r(1)+(I-.5)[y_r(I)+y_r(I-1)]$
$M_s(1)=M_s(1)+(I-.5)[y_s(I)+y_s(I-1)]$

$M_r(0) = dt*M_r(0)/2$
$M_s(0) = dt*M_s(0)/2$
$M_r(1) = M_r(1)*dt*dt/[2*M_r(0)]$
$M_s(1) = M_s(1)*dt*dt/[2*M_s(0)]$

Do for J=2,6
Do for I=2,N
$M_r(J)=M_r(J)+[(I-.5)*dt$
$-M_r(1)]**J*[y_r(I)+y_r(I-1)]$
$M_s(J)=M_s(J)+[(I-.5)*dt$
$-M_s(1)]**J*[y_s(I)+y_s(I-1)]$

$M_r(J)=M_r(J)*dt/[2M_r(0)]$
$M_s(J)=M_s(J)*dt/[2M_s(0)]$

RETURN

Subroutine CALC for
calculating the moments

In order to check the validity of the algorithm, let us assume a function given as a square wave, as shown below in Fig.5.2.1

Taking the moments of the square wave we get

$$M_0 = \int_{-1}^{1} dt = 2$$

$$M_1 = 0$$

$$M_2 = \int_{-1}^{1} [t^2/M_0]\, dt = 1/3$$

$$M_3 = 0$$

$$M_4 = 1/5$$

$$M_5 = 0$$

$$M_6 = 1/7$$

$$M_7 = 0$$

$$M_8 = 1/9$$

$$M_9 = 0$$

$$M_{10} = 1/11$$

Substituting these moments in equation (5.54) for h(t), and using n = 6, 8, 10, h(t) was computed up to the tenth order as shown in Fig.5.2.1.

As it is seen from Fig.5.2.1, the amount of improvement for n = 8, 10 is not very pronounced in this case. In order to improve the accuracy of the general formula for h(t), for non-Gaussian waveforms, a scale factor T should be introduced as follows

$$\sigma = T\sigma$$

where T is a scale factor, to be determined. For more details, see Appendix F.

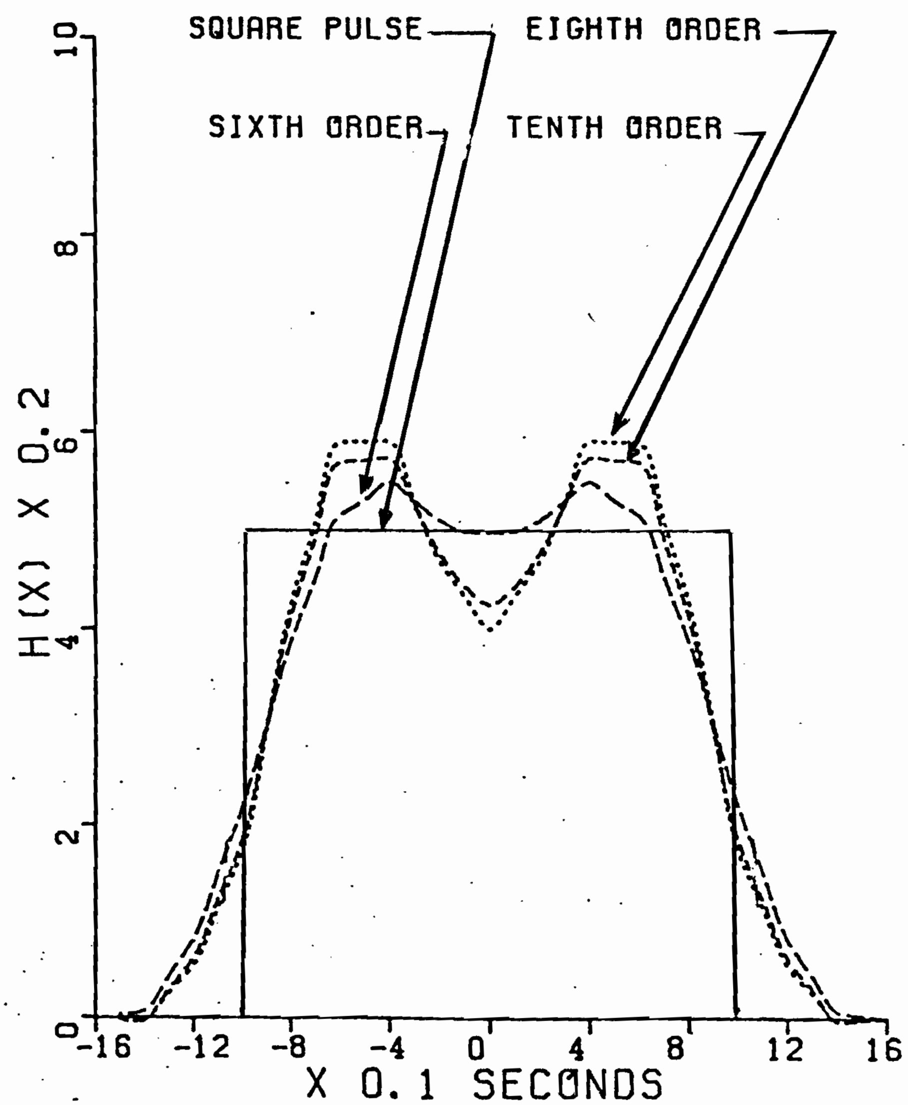

Fig. 5.2.1 The moment representation of a square wave

CHAPTER 6

IMPULSE RESPONSE MEASUREMENTS AND NUMERICAL RESULTS

Impulse response measurements were made at two wavelengths. The first was made using the Universal Fiber Optics Analyser at 904 nano meter wavelength. The second one was made using a similar set-up at 1300 nano meter designed and built at McGill university by Andrej Puc[6.1].

6.1 Impulse Response At 900 nm Wavelength

6.1.1 System Preparation

The Universal Fiber Optics Analyser as shown in Fig.6.1 was used for making the measurements at 900 nano meter wavelength[6.2]. The laser used in the Universl Analyser was LD60 GaAs laser diode operating at 904 nm wavelength. A triggering source of 400 millivolts, 20 khz signal was obtained from an HP 9013B pulse generator. A delayed pulse from the same pulse generator was used to trigger the Tektronix 7854 Sampling Oscilloscope. A beam splitter was used to reflect part of the beam in the direction of the photodetector and this part was used as the reference input signal. The other part of the beam travelled through the fiber. The output from the fiber was directed and aligned to the detector using the micro-positioners. The signal from the oscilloscope was averaged and stored using the averaging command of the 7854 Tektronix Oscilloscope[6.3]. A schematic diagram is shown in Fig.6.2.

Since only one detector was used in this method, the output and input could not be recorded at the same instant. Hence, this method would introduce an error due to the variation and jittering of the laser pulse. The beam splitter was used mainly for the alignment and viewing of the laser signal.

Averaging would be necessary in this case to minimize these errors. For long fibers, the beam splitter would further attenuate the signal so that the output signal might reach the noise level of the detector. To avoid this, the measurement for the input reference pulse was made using one-meter cut from the input side of the fiber, keeping the input end of the fiber attached to the fiber holder. The reason for cutting one meter from the input fiber side is to keep the launching conditions unchanged for both the input and the output measurements. In other words, the dispersion for one meter was considered negligible. The output was taken from the whole length of the fiber before cutting one meter of the reference fiber. After storing the input and the output pulses using the Tektronix 7854 digital oscilloscope, the input was deconvolved from the output to evaluate the impulse response of the fiber as will be shown later in this chapter.

The data from the digital oscilloscope were sent to a PDP-11/23 micro-computer system for processing.

6.1.2 List of Equipment For Measurements at 900 nm Wavelength:

The equipment and fibers used are as listed below:

(1) Tektronix 7854 digital oscilloscope.

(2) HP 8013B pulse generator.

(3) PDP-11/23 micro-computer.

(4) 7S12 Tektronix plug-in unit.

(5) 7S11 Tektronix plug-in unit.

(6) Photon Kinetic Universal Fiber Optics Analayser.

(7) LD-60 GaAs laser diode at 904 nm wavelength.

(8) PD-1000 avalanche photodiode.

(9) Deutsch fiber cutter.

(10) Northern Telecom and Corning fibers.

6.1.3 Results and Discussion

The results were based upon storing the digitized waveform and transferring it to the PDP-11/23 micro-computer. The impulse response and frequency response of the fiber under test were obtained using both the moment and the FFT method. The program for the moment method is listed in Appendix A. This program calculates the attenuation of the fiber (M_0), the pulse dispersion (σ), (or the square root of the second moment), and the bandwidth of the fiber. The attenuation is calculated from equation (5.56a) and the pulse dispersion from equation (5.56c). The bandwidth is the frequency at which equation (5.57) drops to half its maximum value. The programs listed in Appendices B and C also evaluate the impulse response of the fiber using the FFT method. A comparison between the two methods was made for each set of measurements. A combined graph for the results from the two methods was obtained using the program listed in appendix D[6.4].

In measurement set #1, the FFT impulse response has a sharper rise. The values of the attenuation and pulse dispersion are close to the manufacturer's values as shown in Table 6.2.b. In set #2, the values of the attenuation and pulse dispersion are somewhat below the values obtained by the manufacturer. In set #3 , the impulse response using the moment method has a high ripple. This is due to the fact that the output pulse of this particular fiber has a sharp fall and rise time. In set #4, the impulse response for both the moment method and FFT method are in very good agreement. The measured attenuation value is below the manufacturer's value, while the pulse dispersion is in close agreement. In set #5, a Corning fiber was used. The attenuation and the bandwidth were the only data supplied by the manufacturer. The bandwidth is in close agreement, while the attenuation is lower than the one supplied by the manufacturer. In set #6, the attenuation is in agreement with the manufacturer's value, while the bandwidth value is much lower than the one given by the manufacturer. But referring to the same kind of measurement in reference (6.1, P.124) for the same fiber, the value obtained there is even lower than the value obtained here. In set #7, the bandwidth value is higher than the manufacturer's value. In set #8, the attenuation is lower while the pulse dispersion is higher than the one given by the manufacturer. In set #9, all the values are in good agreement. In set #10, the value of the attenuation is lower than that found by the manufacturer, but the pulse dispersion is close.

As far as the comparison between the FFT and the moment method is concerned, the moment method is, in general, much faster than the FFT. The running time for the FFT was 63 seconds, while it was only 19 seconds for the moment method as shown in Table 6.1. This comparison is based upon using the PDP-11/23 computer system in the computation. The moment method showed good agreement in the cases where the impulse response followed a Gaussian pulse shape. The moment method required higher order terms to achieve sufficient accuracy in the cases where the impulse response deviated from the Gaussian shape. The problem in getting into higher order terms or more moments is that the error in calcuating these moments becomes higher as we go higher in order as shown previously in the case of the square pulse. To solve this problem, a higher number of sampling points is needed. Also, a more rigorous method of performing the numerical integration might give better results.

METhOD	COMPILATION + RUNNING TIME	RUNNING TIME
FFT	93 seconds	63 seconds
MOMENT	64 seconds	19 seconds

Table 6.1 Computation time for the two methods for all fibers used.

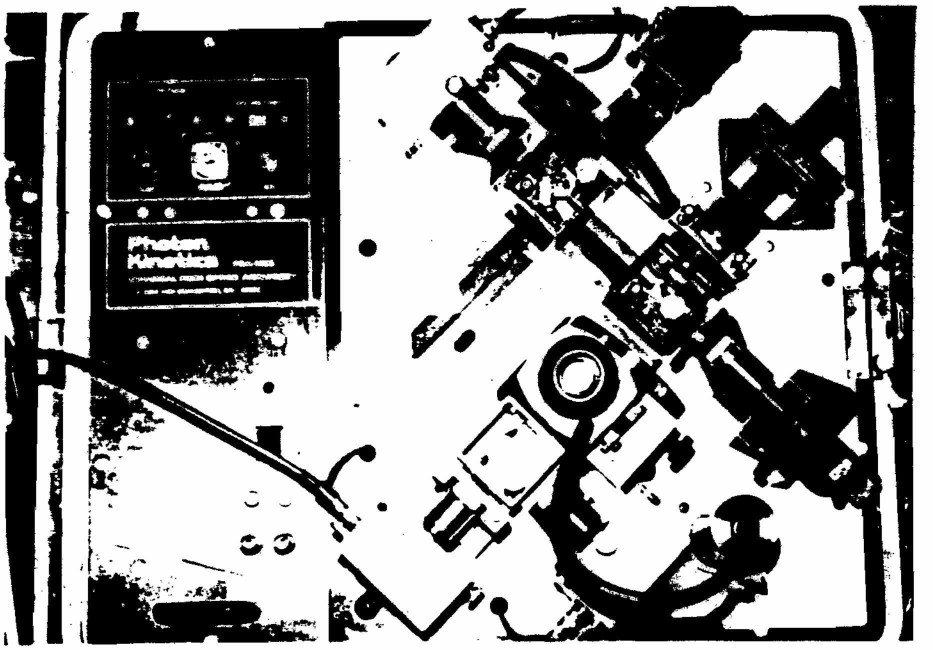

Fig.6.1 The Universal Fiber Optics Analyser

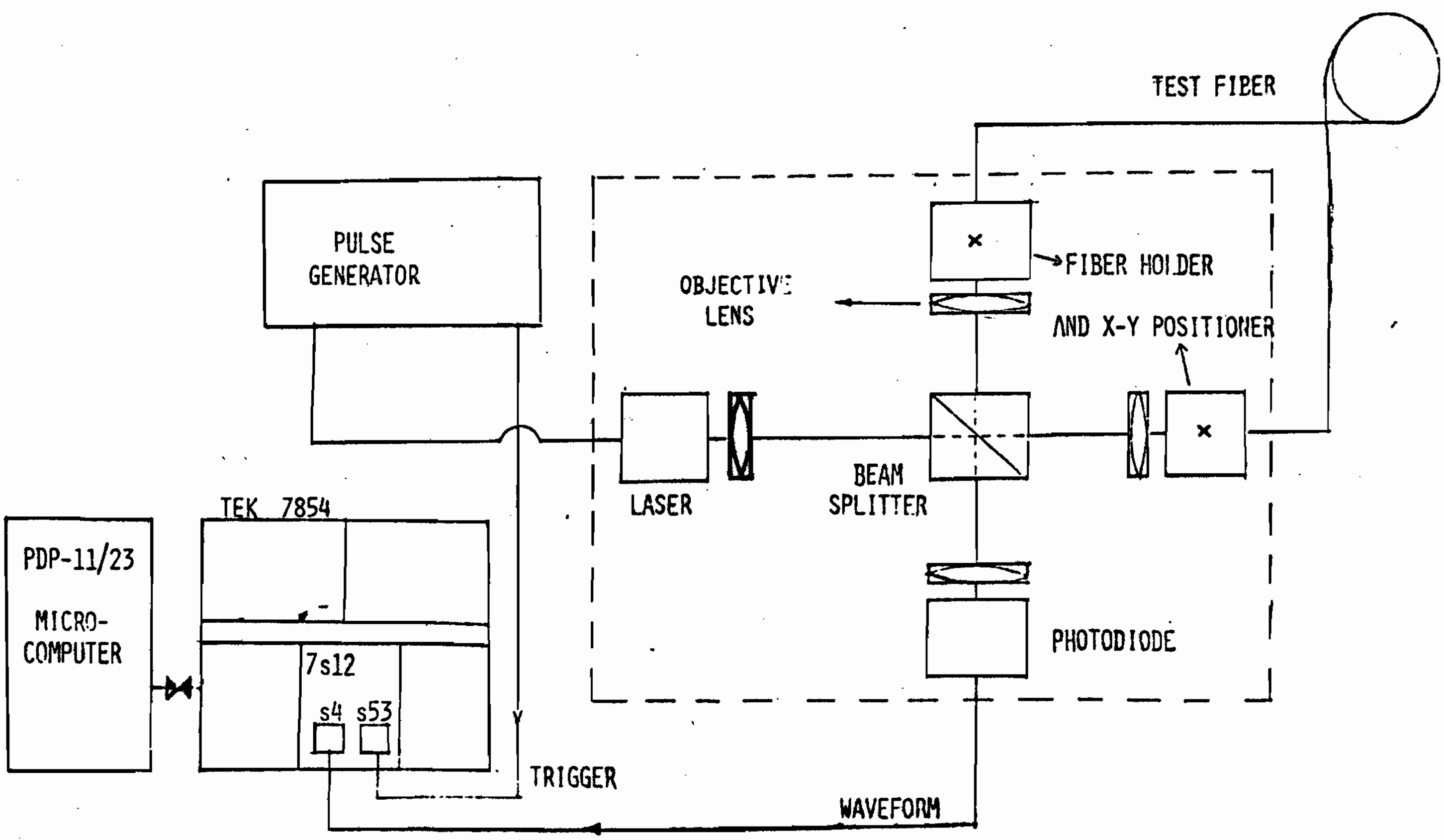

Fig.6.2 The experimental set-up for pulse dispersion measurements at 900 nm.

Measurement set	#1
Fiber code:	10/523B
Manufacturer:	Northern Telecom.
Fiber Length:	920 m. (L)
Wavelength:	900 nm.

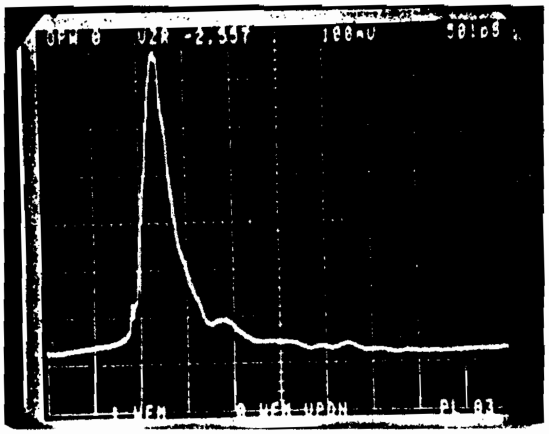

Fig.6.3.a Input waveform

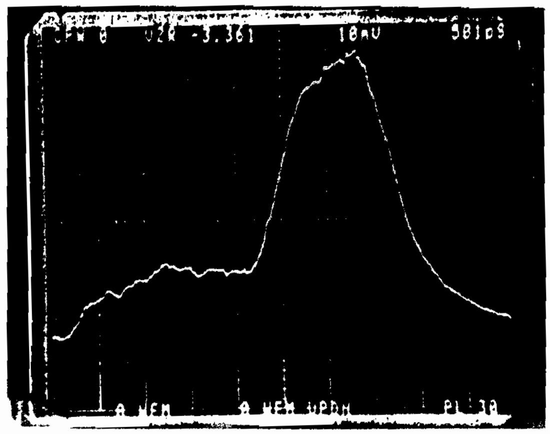

Fig.6.3.b Output waveform

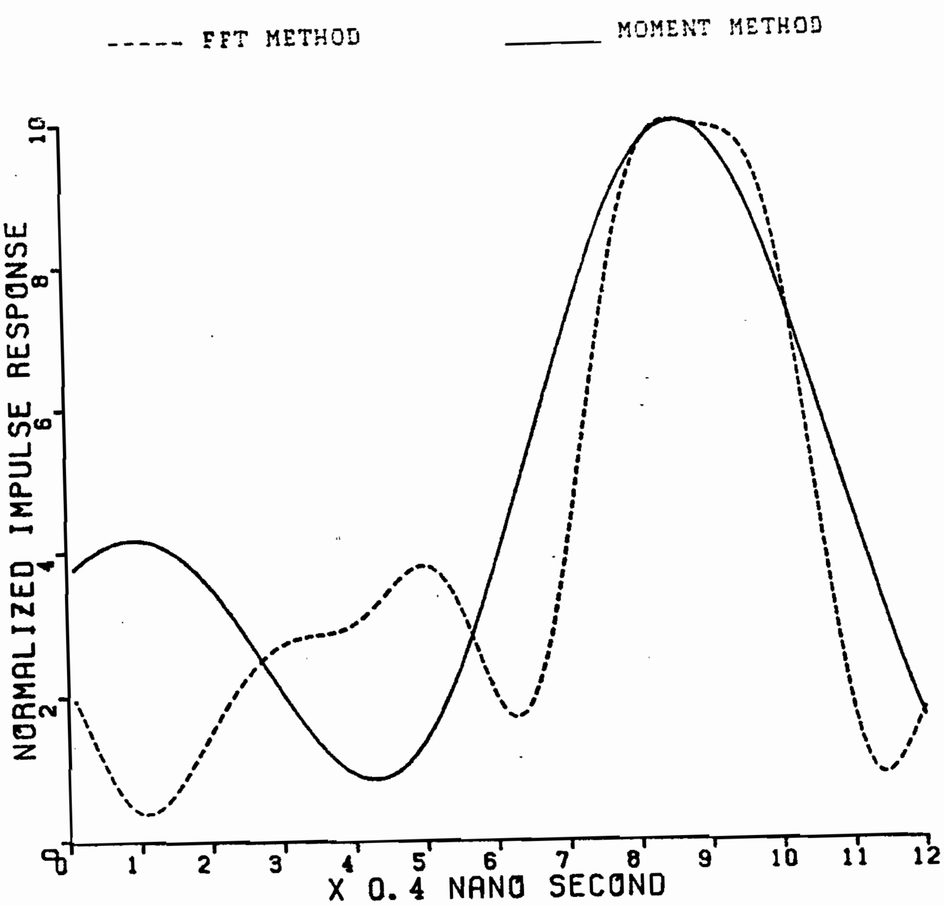

Fig.6.3.c Normalized impulse response as a function of time

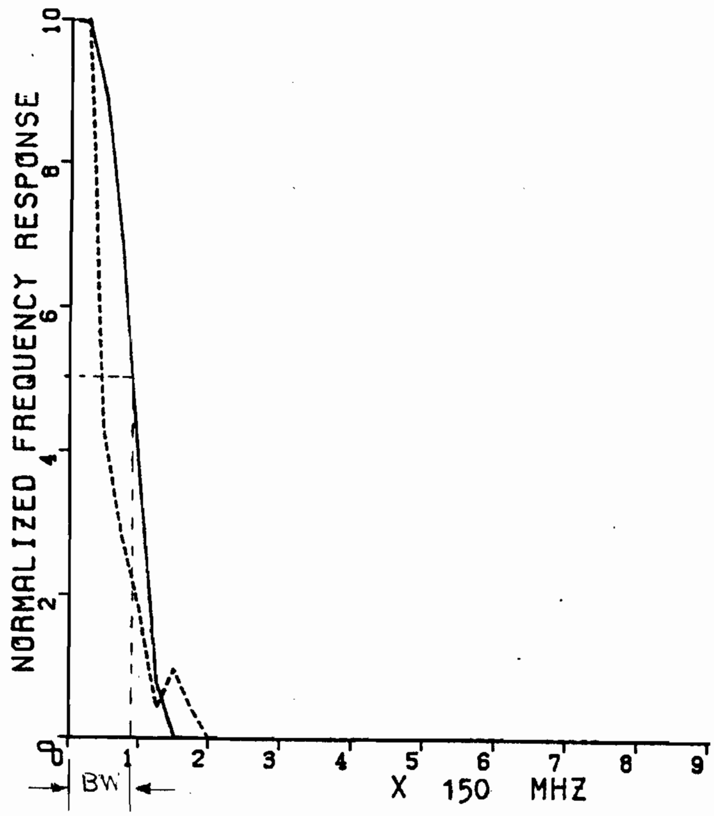

Fig.6.3.d Normalized frequency response versus frequency

MOMENT	CALCULATED VALUE
M_0	0.521
M_1	2.271 E-9 SEC.
M_2	1.694 E-18
M_3	-2.748 E-27

Table 6.2.a Calculated values of the moments

$\alpha = (10/L)\log_{10}[M_0] = 3.077$ dB/km

$\sigma = (1/L)\sqrt{M_2} = 1.415$ ns/km

The bandwidth B was calculated

from $H(2\pi B) = 1/2$ shown in Fig.6.3.d

PARAMETER	CALCULATED VALUE	MANUFACTURER'S VALUE
ATTENUATION	3.077 db/km	2.7 db/km
PULSE DISPERSION	1.415 E-9 SEC.	1.4 E-9 SEC.
BANDWIDTH	141.34 MHZ	–

Table 6.2.b Comparison between the calculated values of fiber parameters and manufacturer's data

Fig.6.3.d Normalized frequency response versus frequency

MOMENT	CALCULATED VALUE
M_0	0.521
M_1	2.271 E-9 SEC.
M_2	1.694 E-18
M_3	-2.748 E-27

Table 6.2.a Calculated values of the moments

$\alpha = (10/L)\log_{10}[M_0] = 3.077$ dB/km

$\sigma = (1/L)\sqrt{M_2} = 1.415$ ns/km

The bandwidth B was calculated

from $H(2\pi B) = 1/2$ shown in Fig.6.3.d

PARAMETER	CALCULATED VALUE	MANUFACTURER'S VALUE
ATTENUATION	3.077 db/km	2.7 db/km
PULSE DISPERSION	1.415 E-9 SEC.	1.4 E-9 SEC.
BANDWIDTH	141.34 MHZ	–

Table 6.2.b Comparison between the calculated values of fiber parameters and manufacturer's data

Measurement set #2
Fiber code: 10/497A
Manufacturer: Northern Telecom.
Fiber Length: 830 m.
Wavelength: 900 nm.

Measurement set	#2
Fiber code:	10/497A
Manufacturer:	Northern Telecom.
Fiber Length:	830 m.
Wavelength:	900 nm.

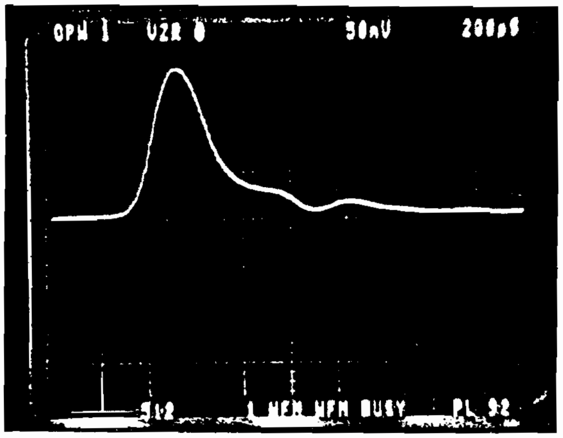

Fig.6.4.a Input waveform

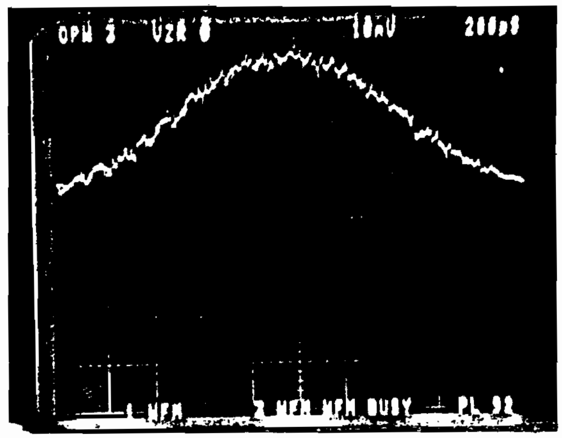

Fig.6.4.b Output waveform

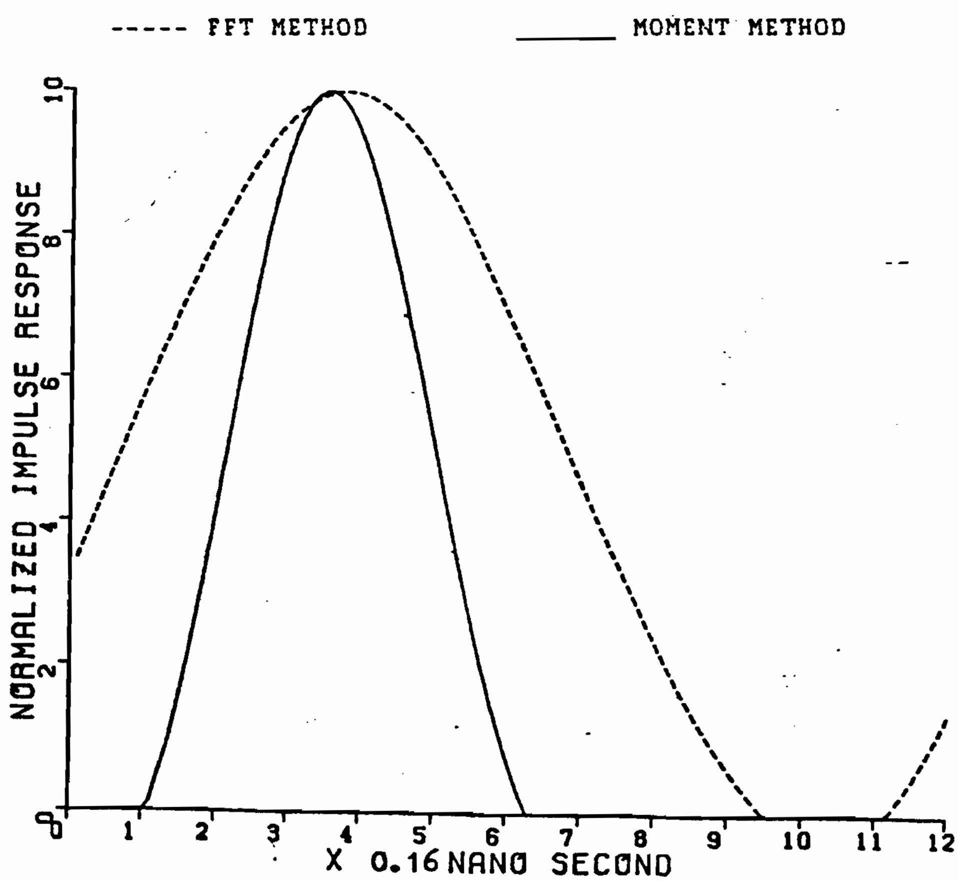

Fig.6.4.c Normalized impulse response as a function of time

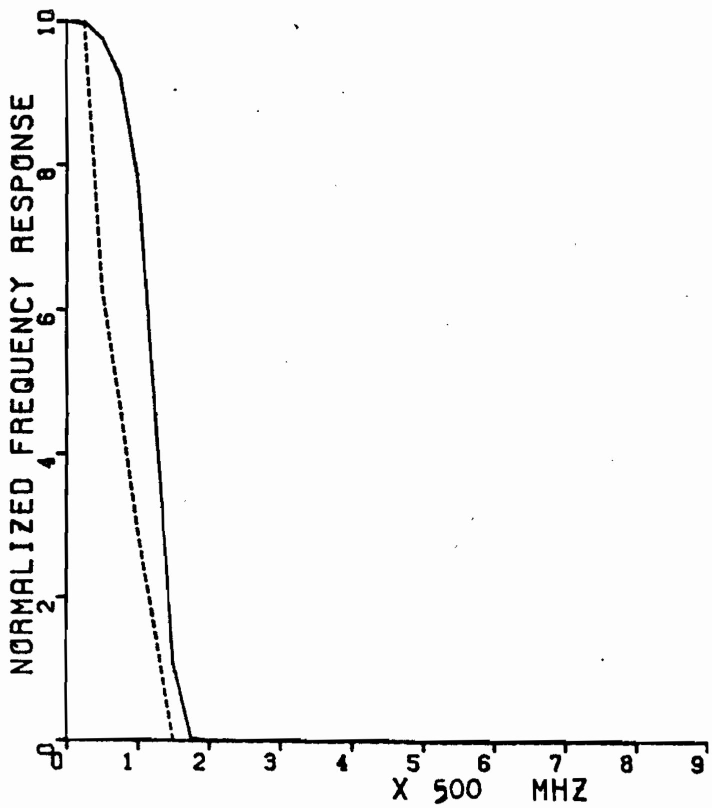

Fig.6.4.d Normalized frequency response versus frequency

MOMENT	CALCULATED VALUE
M_0	0.6477
M_1	0.360 E-9 SEC.
M_2	0.0985 E-18
M_3	-.1116 E-27

Table 6.3.a Calculated values of the moments

PARAMETER	CALCULATED VALUE	MANUFACTURER'S VALUE
ATTENUATION	2.27 db/km	2.9 db/km
PULSE DISPERSION	0.378 E-9 SEC.	0.6 E-9 SEC.
BANDWIDTH	529.1 MHZ	—

Table 6.3.b Comparison between the calculated values of fiber parameters and manufacturer's data

Measurement set #3
Fiber code: 6/1064B
Manufacturer: Northern Telecom.
Fiber Length: 1196 m.
Wavelength: 900 nm.

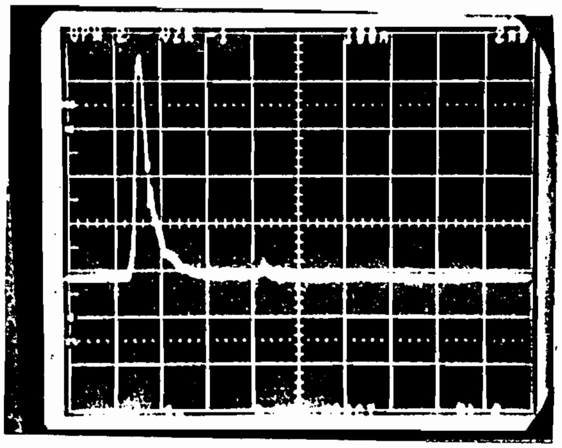

Fig.6.5.a Input waveform

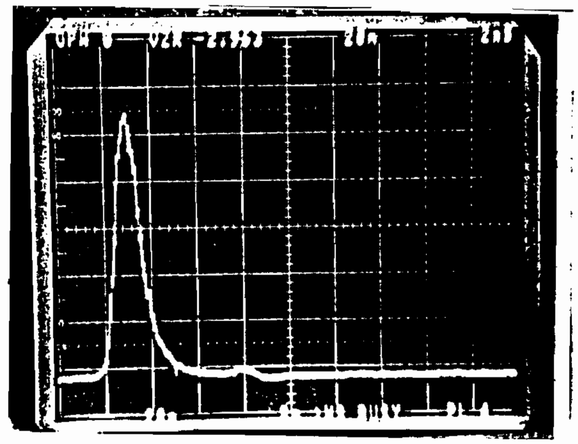

Fig.6.5.b Output waveform

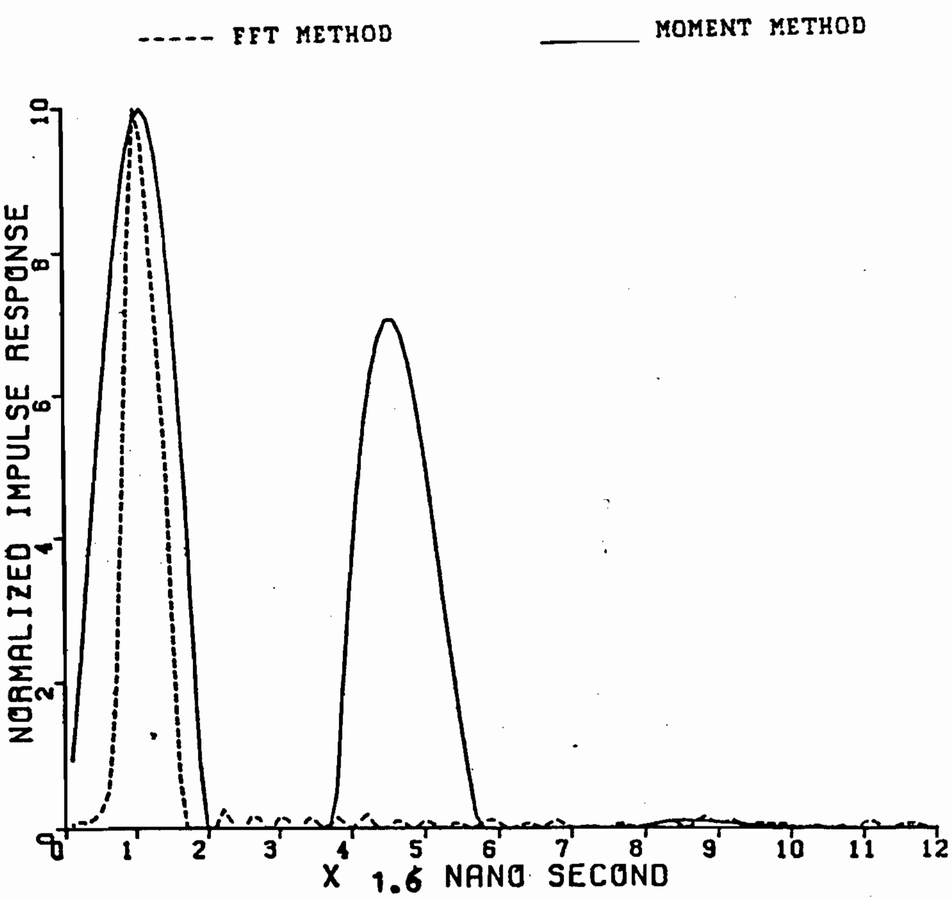

Fig.6.5.c Normalized impulse response as a function of time

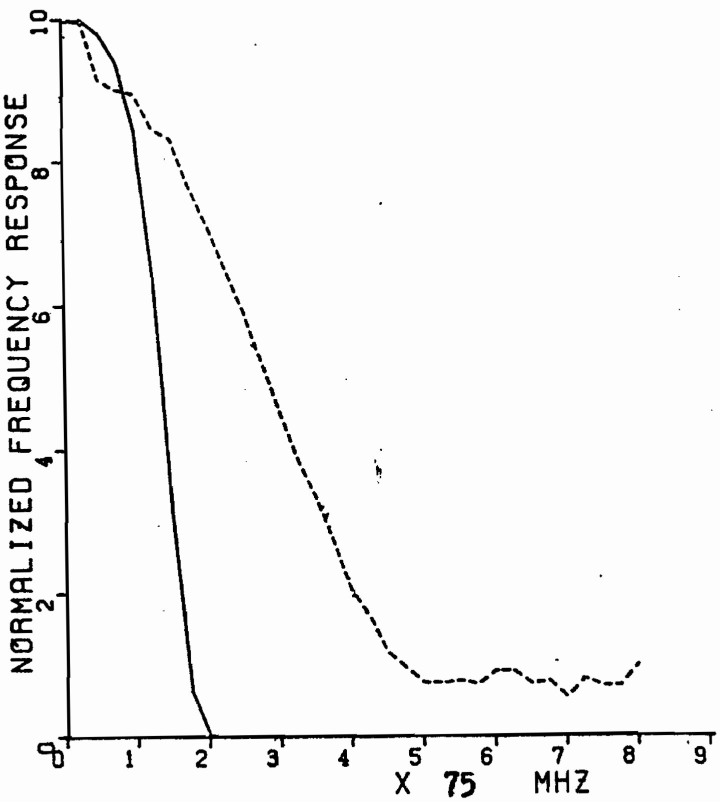

Fig.6.5.d Normalized frequency response versus frequency

MOMENT	CALCULATED VALUE
M_0	0.4618
M_1	4.308 E-9 SEC.
M_2	5.299 E-18
M_3	16.77 E-27

Table 6.4.a Calculated values of the moments

PARAMETER	CALCULATED VALUE	MANUFACTURER'S VALUE
ATTENUATION	2.8 db/km	2.9 db/km
PULSE DISPERSION	1.92 E-9 SEC.	1.3 E-9 SEC.
BANDWIDTH	104.16 MHZ	–

Table 6.4.b Comparison between the calculated values of fiber parameters and manufacturer's data

Measurement set #4
Fiber code: 8/780A
Manufacturer: Northern Telecom.
Fiber Length: 1160 m.
Wavelength: 900 nm.

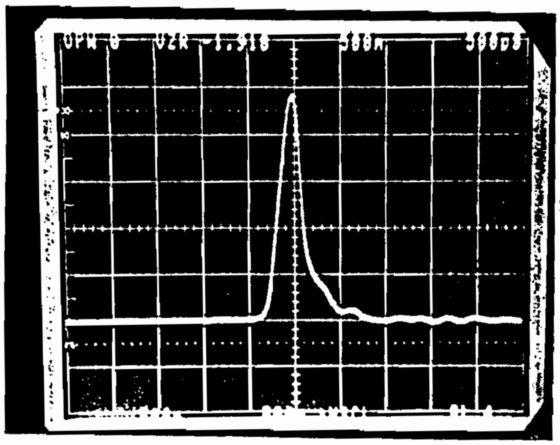

Fig.6.6.a Input waveform

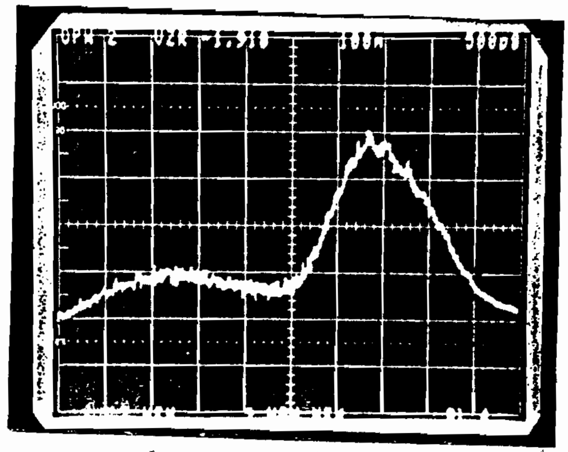

Fig.6.6.b Output waveform

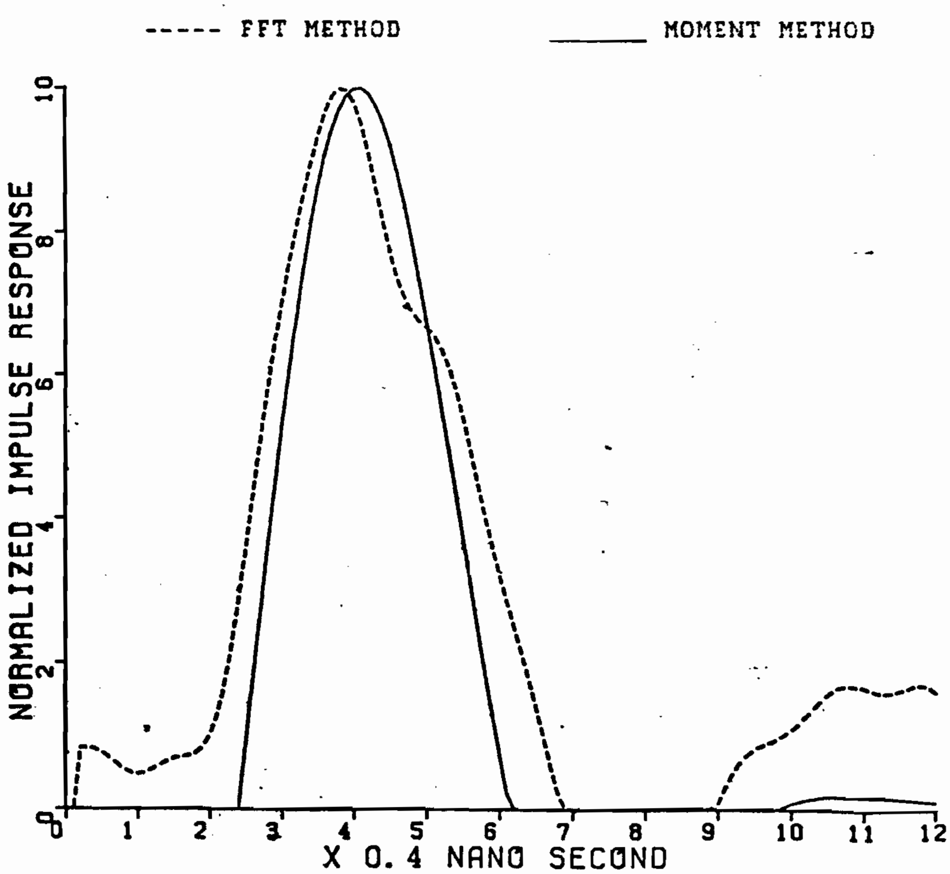

Fig.6.6.c Normalized impulse response as a function of time

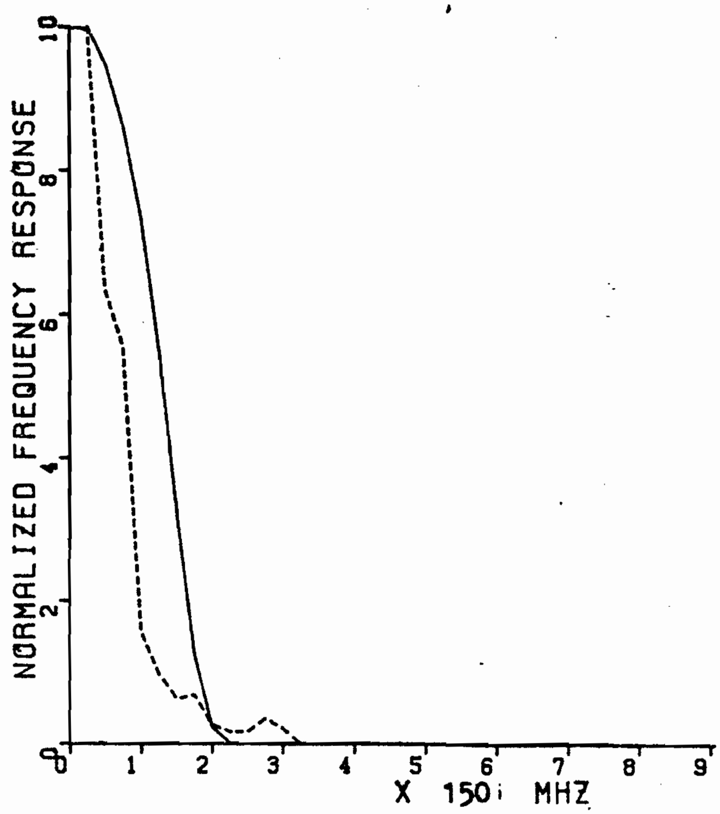

Fig.6.6.d Normalized frequency response versus frequency

MOMENT	CALCULATED VALUE
M_0	0.6131
M_1	0.6570 E-9 SEC.
M_2	0.8643 E-18
M_3	1.7208 E-27

Table 6.5.a Calculated values of the moments

PARAMETER	CALCULATED VALUE	MANUFACTURER'S VALUE
ATTENUATION	1.83 db/km	3.0 db/km
PULSE DISPERSION	0.801 E-9 SEC.	0.9 E-9 SEC.
BANDWIDTH	250 MHZ	_

Table 6.5.b Comparison between the calculated values of fiber parameters and manufacturer's data

Measurement set	#5
Fiber code:	60337107
Manufacturer:	Corning Glass
Fiber Length:	1100 m.
Wavelength:	900 nm.

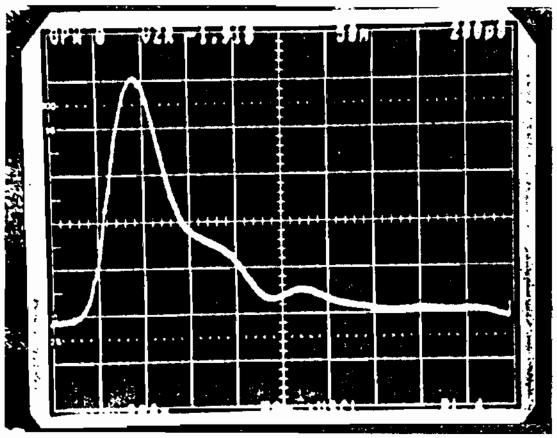

Fig.6.7.a Input waveform

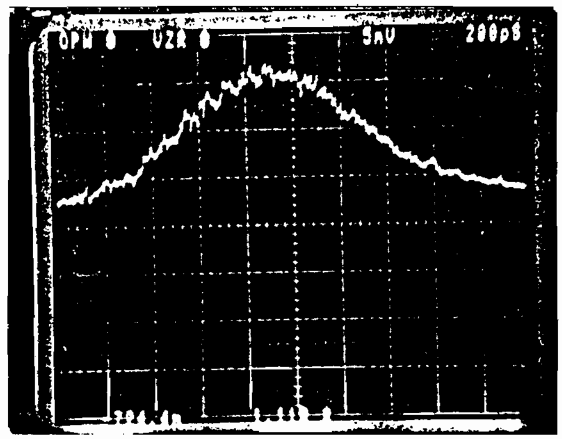

Fig.6.7.b Output waveform

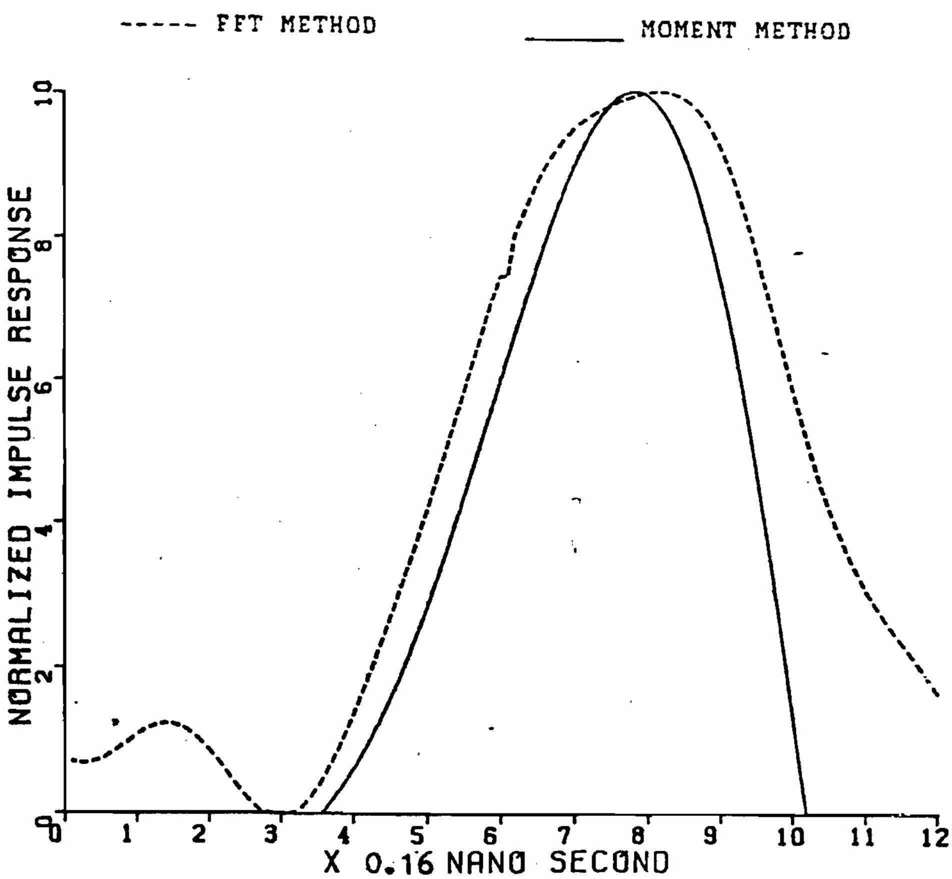

Fig.6.7.c Normalized impulse response as a function of time

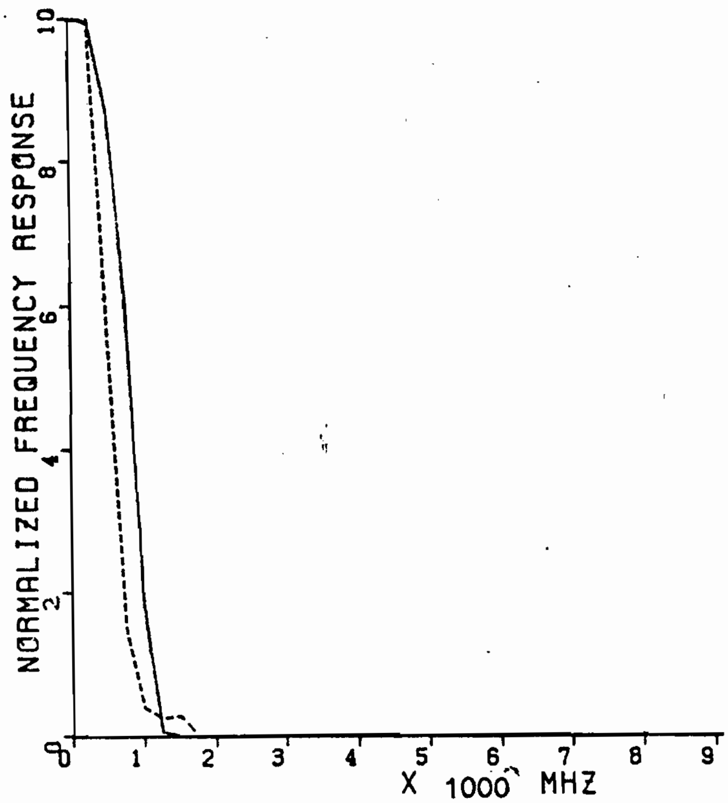

Fig.6.7.d Normalized frequency response versus frequency

MOMENT	CALCULATED VALUE
M_0	0.1606
M_1	.35067 E-9 SEC.
M_2	.0516 E-18
M_3	-7.048 E-27

Table 6.6.a Calculated values of the moments

PARAMETER	CALCULATED VALUE	MANUFACTURER'S VALUE
ATTENUATION	7.23 db/km	4.6 db/km
PULSE DISPERSION	0.206 E-9 SEC.	-
BANDWIDTH	970.87 MHZ	1170 MHZ

Table 6.6.b Comparison between the calculated values of fiber parameters and manufacturer's data

Measurement set #6
Fiber code: 133806
Manufacturer: Corning Glass
Fiber Length: 815 m.
Wavelength: 900 nm.

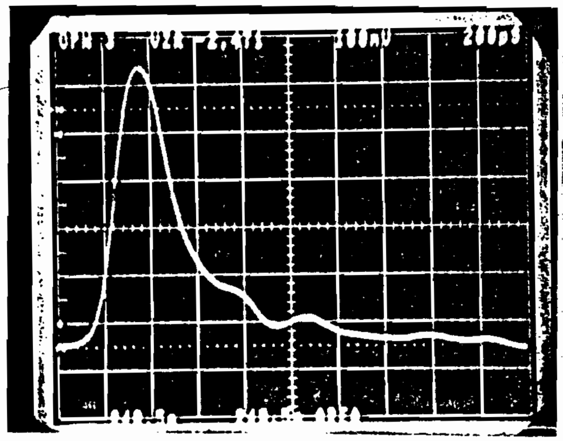

Fig.6.8.a Input waveform

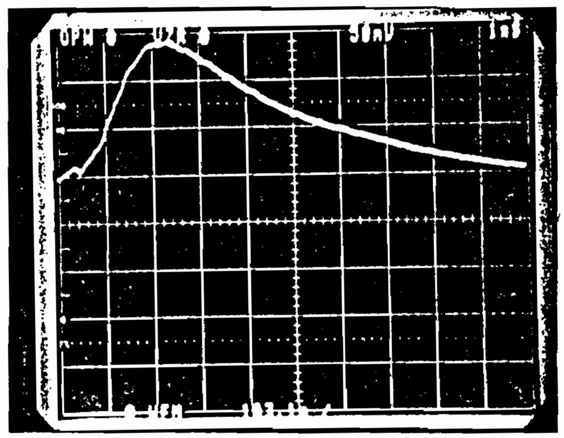

Fig.6.8.b Output waveform

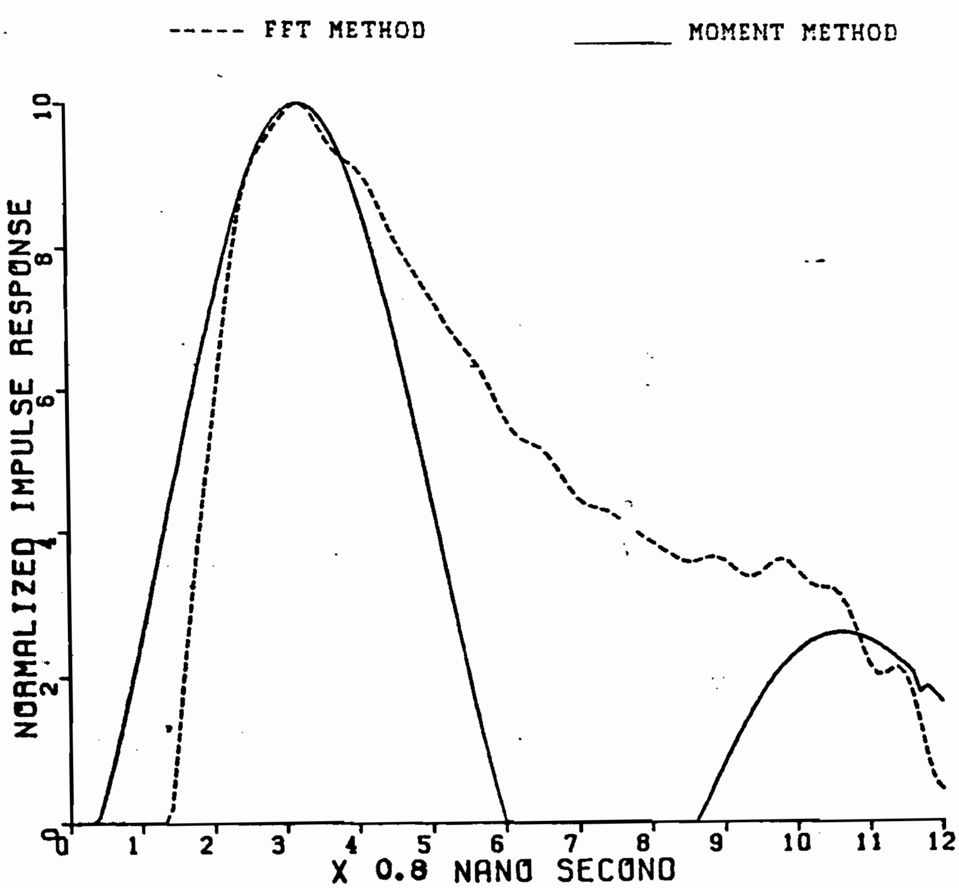

Fig.6.8.c Normalized impulse response as a function of time

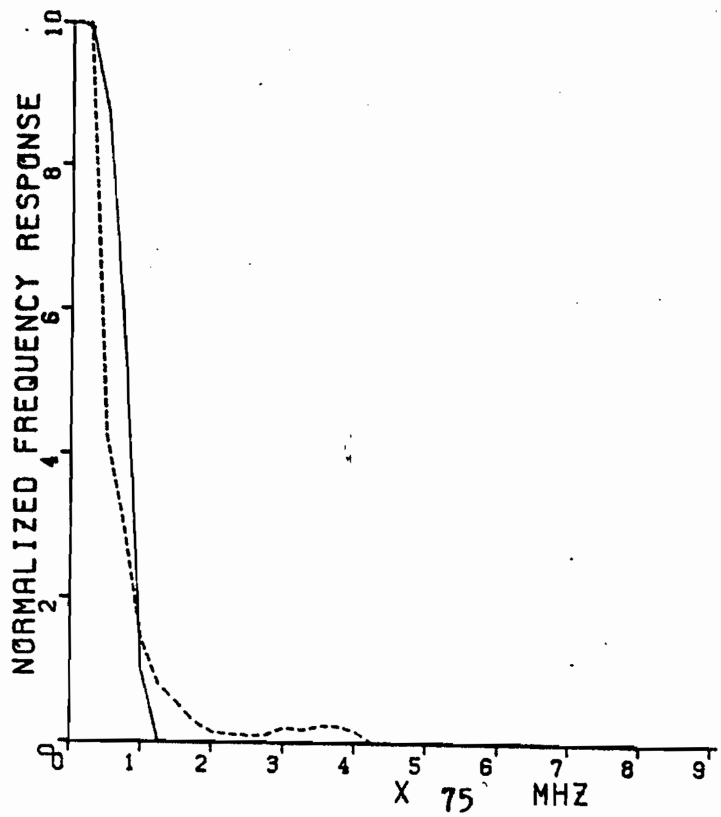

Fig.6.8.d Normalized frequency response versus frequency

MOMENT	CALCULATED VALUE
M_0	0.3642
M_1	3.556 E-9 SEC.
M_2	6.956 E-18
M_3	-3.801 E-27

Table 6.7.a Calculated values of the moments

PARAMETER	CALCULATED VALUE		MANUFACTURER'S VALUE
ATTENUATION	5.38	db/km	5.4 db/km
PULSE DISPERSION	3.236 E-9	SEC.	-
BANDWIDTH	61.8	MHZ	1500 MHZ

Table 6.7.b Comparison between the calculated values of fiber parameters and manufacturer's data

Measurement set #7
Fiber code: 31329204
Manufacturer: Corning Glass
Fiber Length: 1100 m.
Wavelength: 900 nm.

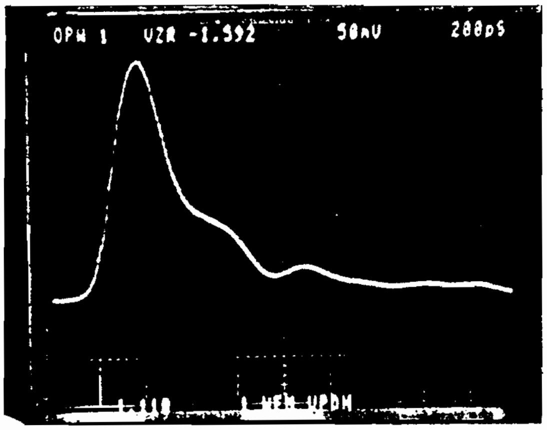

Fig.6.9.a Input waveform

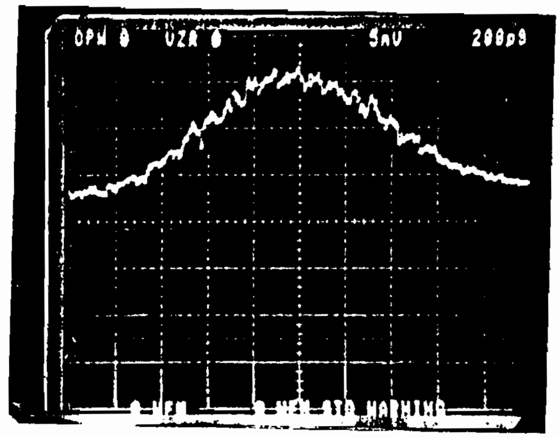

Fig.6.9.b Output waveform

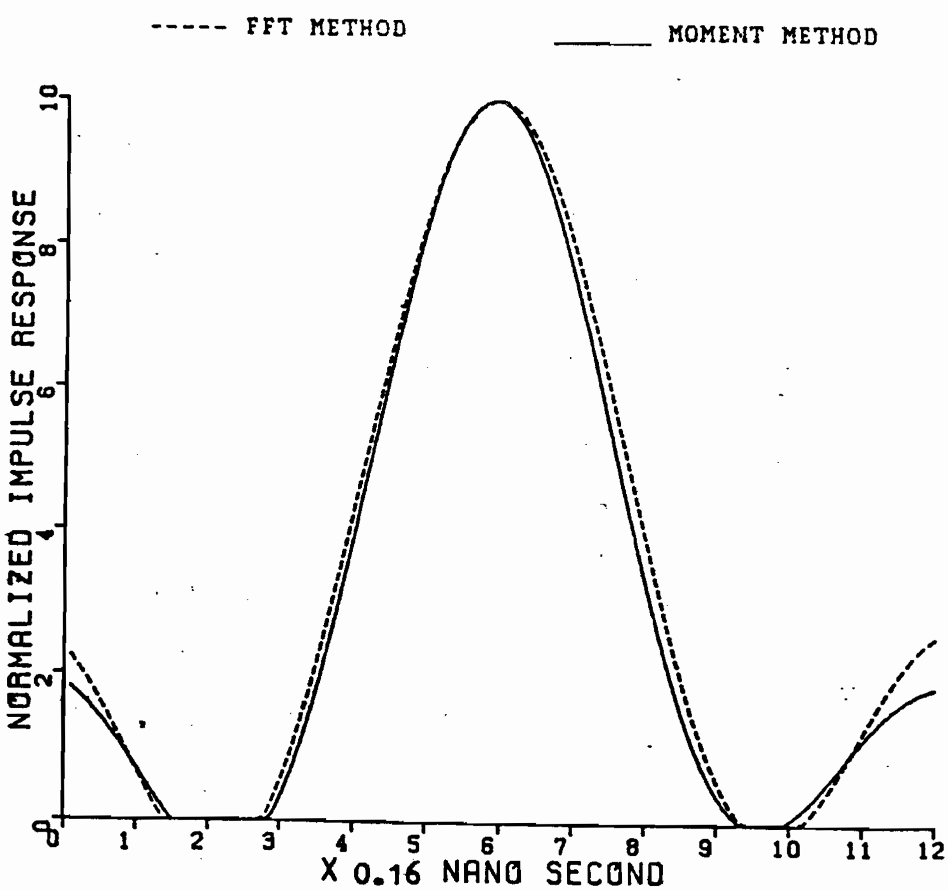

Fig.6.9.c Normalized impulse response as a function of time

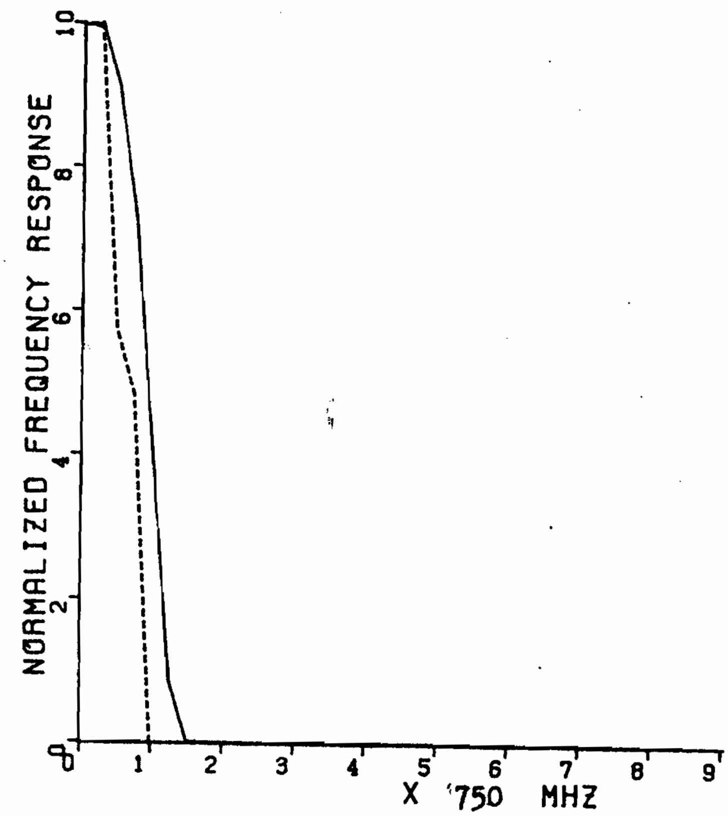

Fig.6.9.d Normalized frequency response versus frequency

MOMENT	CALCULATED VALUE
M_0	0.3387
M_1	0.3080 E-9 SEC.
M_2	0.0723 E-18
M_3	-0.099 E-27

Table 6.8.a Calculated values of the moments

PARAMETER	CALCULATED VALUE	MANUFACTURER'S VALUE
ATTENUATION	4.27 db/km	4.3 db/km
PULSE DISPERSION	0.244 E-9 SEC.	-
BANDWIDTH	819.67 MHZ	460 MHZ

Table 6.8.b Comparison between the calculated values of fiber parameters and manufacturer's data

Measurement set #8
Fiber code: 9/574BB
Manufacturer: Northern Telecom.
Fiber Length: 2270 m.
Wavelength: 900 nm.

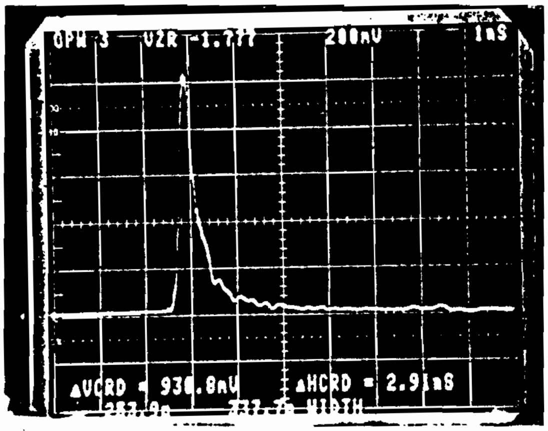

Fig.6.10.a Input waveform

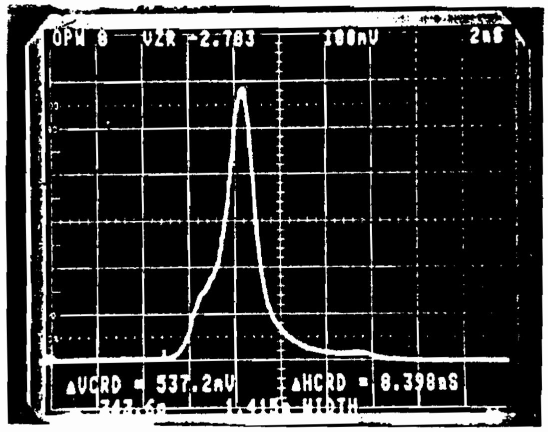

Fig.6.10.b Output waveform

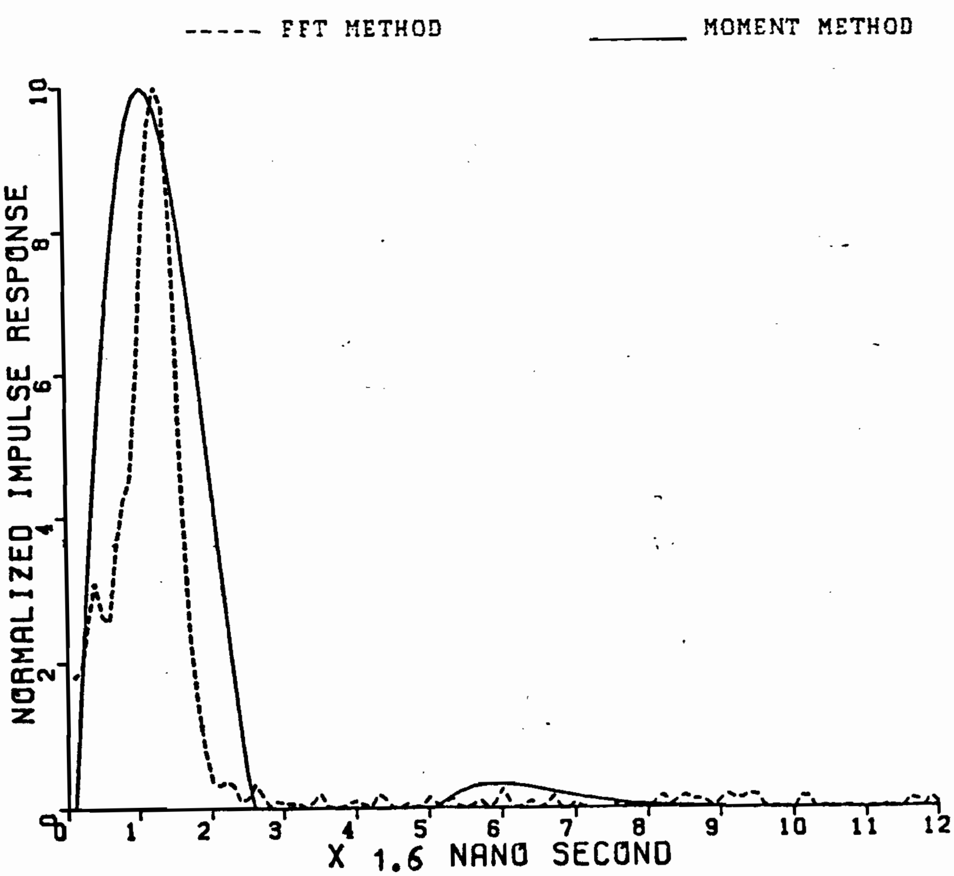

Fig.6.10.c Normalized impulse response as a function of time

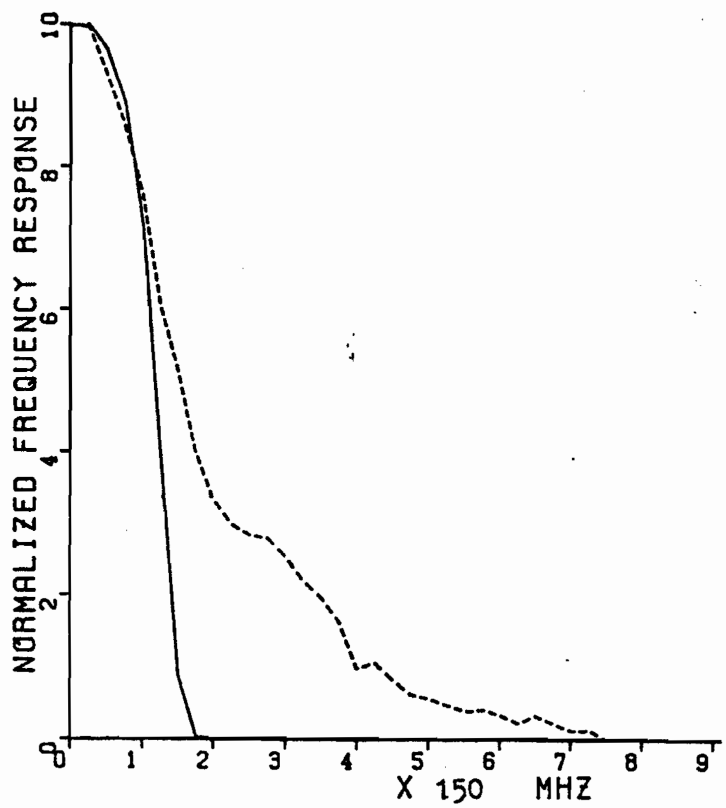

Fig.6.10.d Normalized frequency response versus frequency

MOMENT	CALCULATED VALUE
M_0	0.4595
M_1	-2.008 E-9 SEC.
M_2	8.7790 E-18
M_3	97.055 E-27

Table 6.9.a Calculated values of the moments

PARAMETER	CALCULATED VALUE	MANUFACTURER'S VALUE
ATTENUATION	1.487 db/km	3.4 db/km
PULSE DISPERSION	1.3 E-9 SEC.	0.7 E-9 SEC.
BANDWIDTH	153.85 MHZ	–

Table 6.9.b Comparison between the calculated values of fiber parameters and manufacturer's data

Measurement set #9
Fiber code: 10/477B
Manufacturer: Northern Telecom.
Fiber Length: 1200 m.
Wavelength: 900 nm.

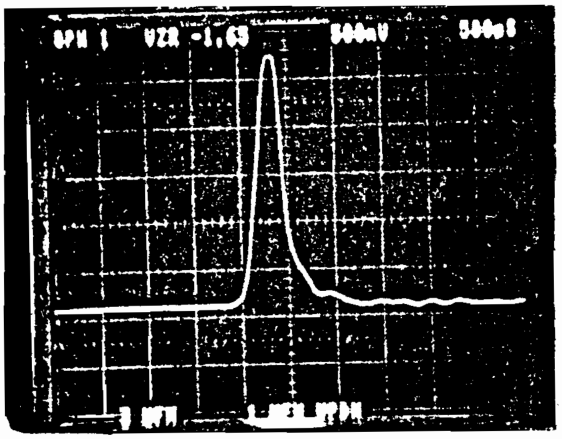

Fig.6.11.a Input waveform

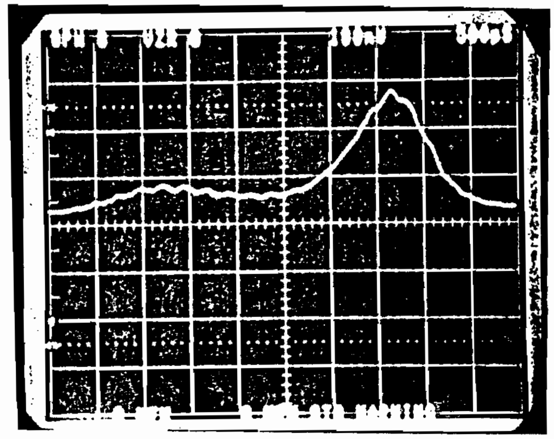

Fig.6.11.b Output waveform

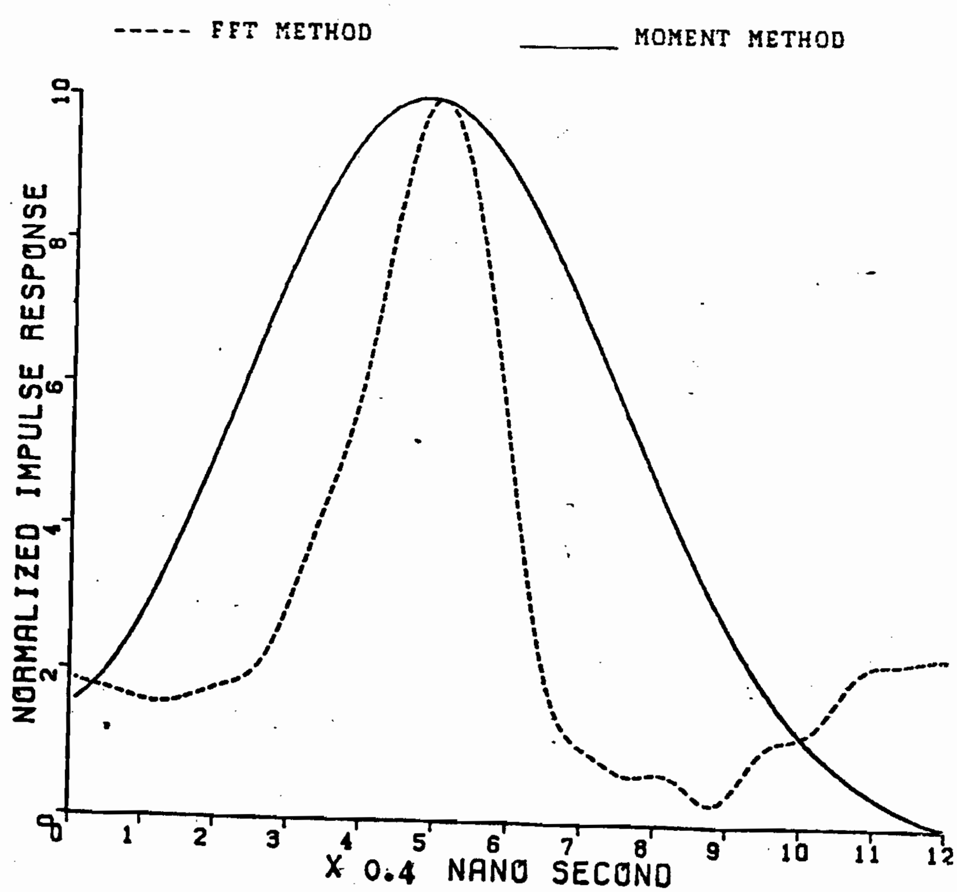

Fig.6.11.c Normalized impulse response as a function of time

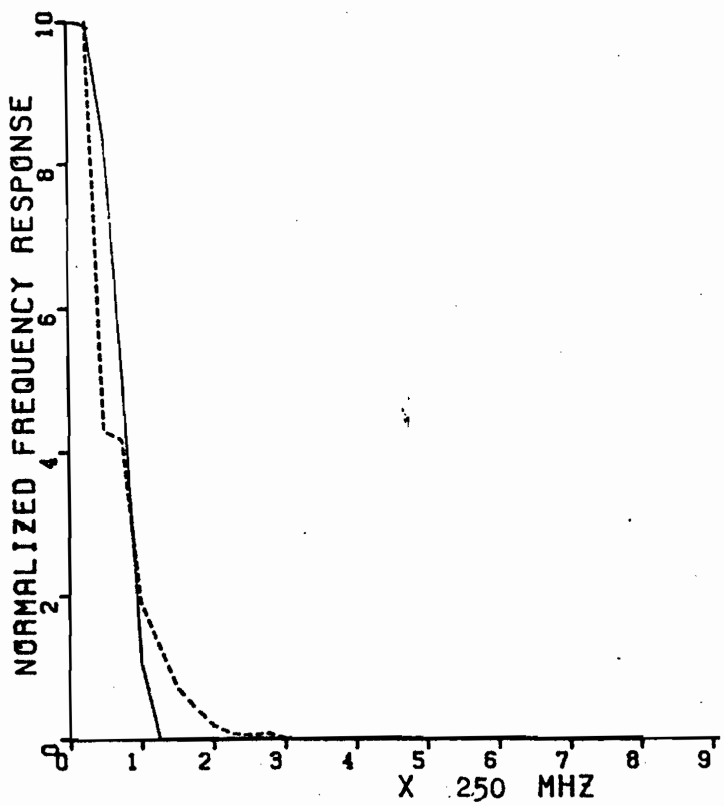

Fig.6.11.d Normalized frequency response versus frequency

MOMENT	CALCULATED VALUE
M_0	0.4365
M_1	0.4882 E-9 SEC.
M_2	1.0535 E-18
M_3	-1.307 E-27

Table 6.10.a Calculated values of the moments

PARAMETER	CALCULATED VALUE	MANUFACTURER'S VALUE
ATTENUATION	3 db/km	2.6 db/km
PULSE DISPERSION	0.855 E-9 SEC.	0.5 E-9 SEC.
BANDWIDTH	234 MHZ	_

Table 6.10.b Comparison between the calculated values of fiber parameters and manufacturer's data

Measurement set #10
Fiber code: 3/1209A
Manufacturer: Northern Telecom.
Fiber Length: 1512 m.
Wavelength: 900 nm.

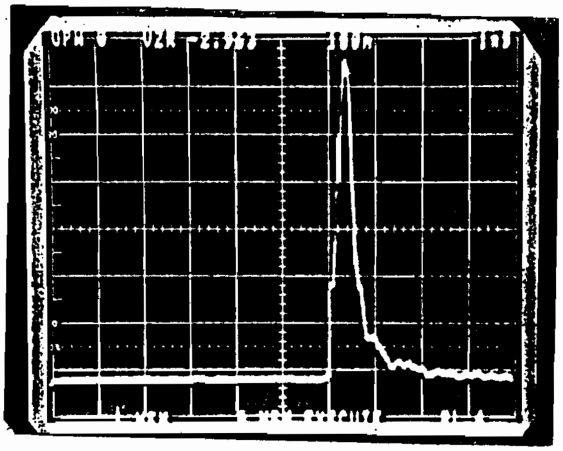

Fig.6.12.a Input waveform

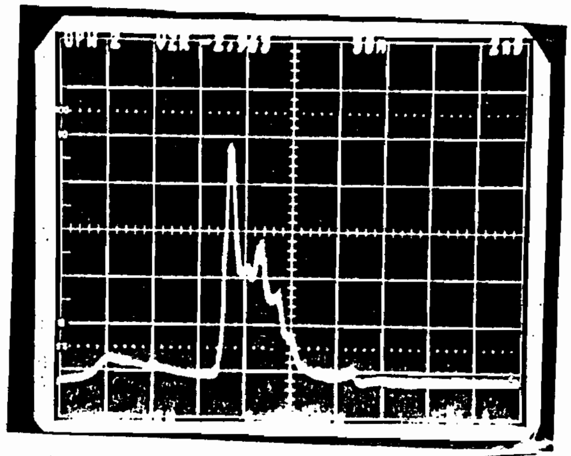

Fig.6.12.b Output waveform

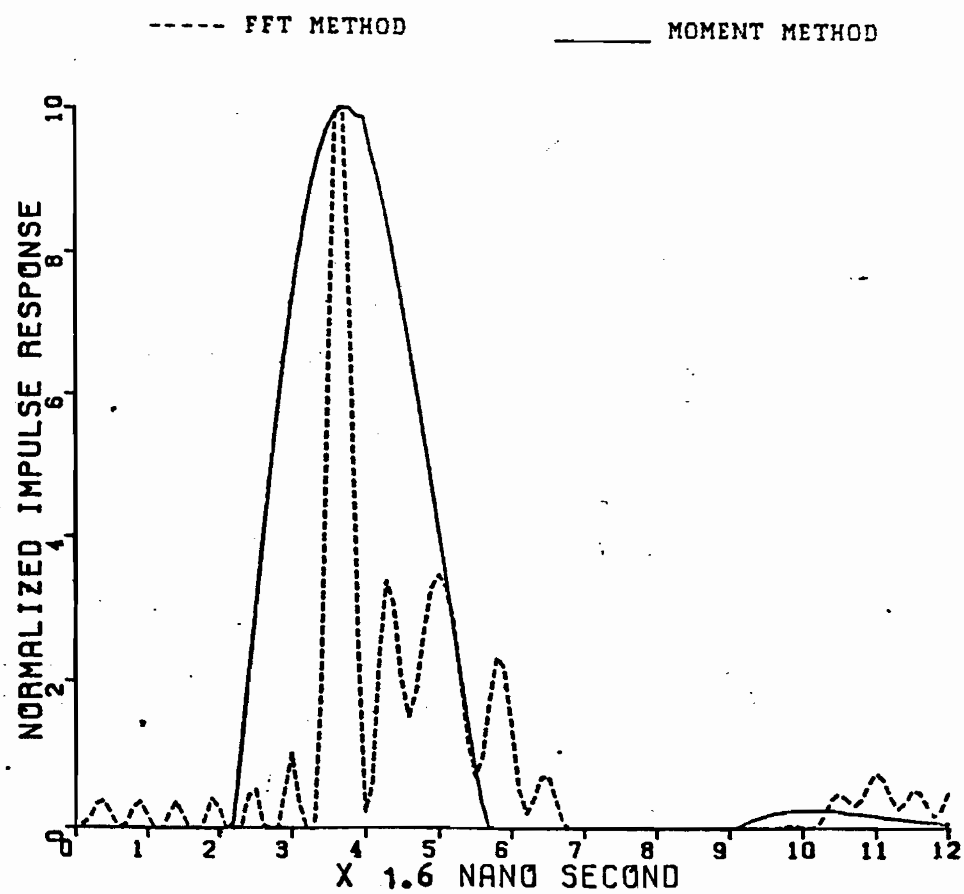

Fig.6.12.c Normalized impulse response as a function of time

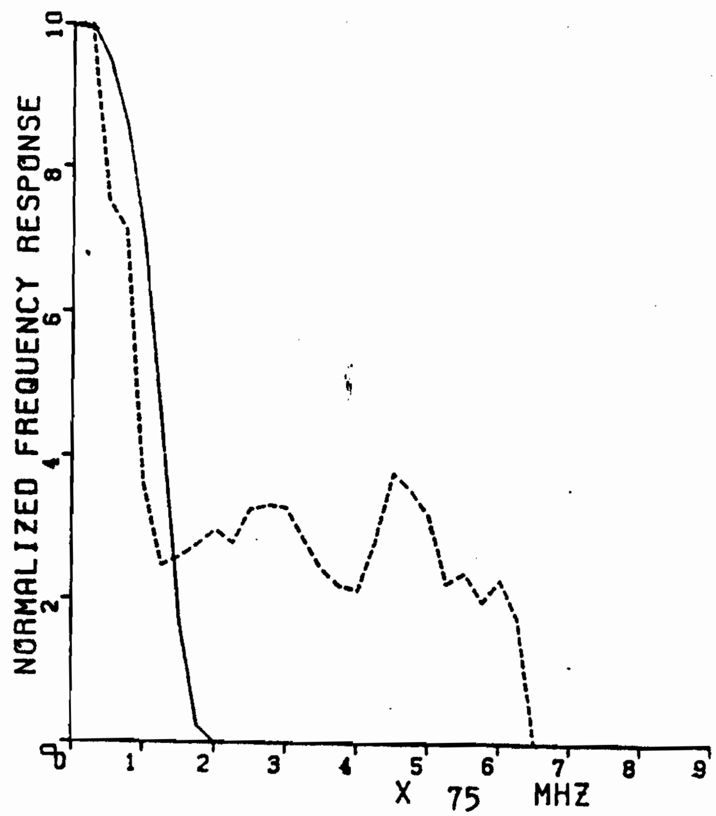

Fig.6.12.d Normalized frequency response versus frequency

MOMENT	CALCULATED VALUE
M_0	0.574
M_1	1.440 E-9 SEC.
M_2	4.458 E-18
M_3	-23.02 E-27

Table 6.11.a Calculated values of the moments

PARAMETER	CALCULATED VALUE		MANUFACTURER'S VALUE
ATTENUATION	1.74	db/km	2.9 db/km
PULSE DISPERSION	1.421 E-9	SEC.	1.4 E-9 SEC.
BANDWIDTH	93	MHZ	_

Table 6.11.b Comparison between the calculated values of fiber parameters and manufacturer's data

6.2 Impulse Response Measurements at 1300 nm Wavelength

6.2.1 System Preparation

Fig.6.13 shows the measurement set-up designed by Andrej Puc. The transmitter in this set-up consisted of a GaAl laser diode which had a full-wave-half maximum pulse width of about 400 pico second. The detector was a germanium photodiode. The triggering signal for the laser was one volt in amplitude and had a repetition rate of 100 khz.

The fiber was cut first and then was inspected for a good surface cut. It was placed in the fiber holder and was aligned using the micro-positioners. The whole length of the fiber was used to measure the output signal. The input signal was taken from one-meter length cut from the input end, keeping the input end itself fixed. A schematic diagram giving the measurement layout is shown in Fig.6.14

6.2.2 List of Equipment:

The equipment and fibers used are listed below:

1- Laser GaAl source

This laser source has a bias voltage of 60 volts, a triggering voltage of one volt and a repetition rate of 100 khz. The output power was 10 milliwatt at 1300 nano meter wavelength, and the pulse width was 400 picosecond.

2- Germanium photodiode which has a bias voltage of 50 volts.

3- Four objective lenses (BICK X10).

5- One beam splitter.

6- Lambda power supply LQD-425 (0-250V).

7- HP 8013B pulse generator.

8- Deutsch fiber cutter.

9- 7854 Tektronix digital oscilloscope.

10- PDP-11/23 micro-computor.

11- Northern Telecom fibers.

6.2.3 Results and Calculations

The results are listed in measurement sets #11-#17. These results were obtained using the same procedure as for the 900 nanometer wavelength. The programs used to obtain the impulse response and the frequency response are listed in Appendices A, B, and C.

6.2.4 Discussion of The Results

In measurement set #11, the attenuation value obtained here is lower than the one obtained by the manufacturer. The pulse dispersion is higher than the one obtained by the manufacturer. This fiber was the same fiber previously used for the 900 nanometer wavelength in set #4. The values of attenuation and pulse dispersion are somewhat higher as shown in Table 6.13. In set #12, the measured attenuation is almost the same as the manufacturer's value, but the pulse dispersion is lower. In set #13, the pulse dispersion is close to the manufacturer's value but the attenuation is lower. In set #14, the attenuation value was not reported by the manufacturer for this particular fiber. The pulse dispersion in this set is in agreement with the one reported by the maker. In set #15, the attenuation given by the manufacturer is lower than the one obtained in this set. The pulse dispersion in this set is lower than the one obtained by the manufacturer. In set #16, the pulse dispersion is close to the one reported by the manufacturer. The attenuation reported here is lower than the one given by the manufacturer. In set #17, the attenuation value obtained here is higher than the one obtained by Northern Telecom. The pulse dispersion reported here is slightly lower.

Regarding the impulse response, the sets 12, 14, 15, and 16 showed a reasonable agreement between the moment method and the FFT method.

Table 6.12 shows a comparison between the measured data at 900 and 1300 nano meter wavelengths. As shown in the table, the attenuation and the pulse dispersion at 1300 nano meter for the first and the last fiber are higher than the ones at 900 nano meter wavelength. The opposite is true for the other two fibers.

	900 nano meter wavelength		1300 nano meter wavelength	
fiber code	attenuation in db/km	pulse dispersion	attenuation in db/km	pulse dispersion
8/780A	1.83	.801 n sec	2.98	1.74 n sec
10/523B	3.077	1.367 n sec	2.435	1.12 n sec
6/1064B	2.8	1.92 n sec	1.9	0.97 n sec
3/1209A	1.74	1.42 n sec	2.67	2.2 n sec

Table 6.12 Comparison between measured data at 900 nm and 1300 nm.

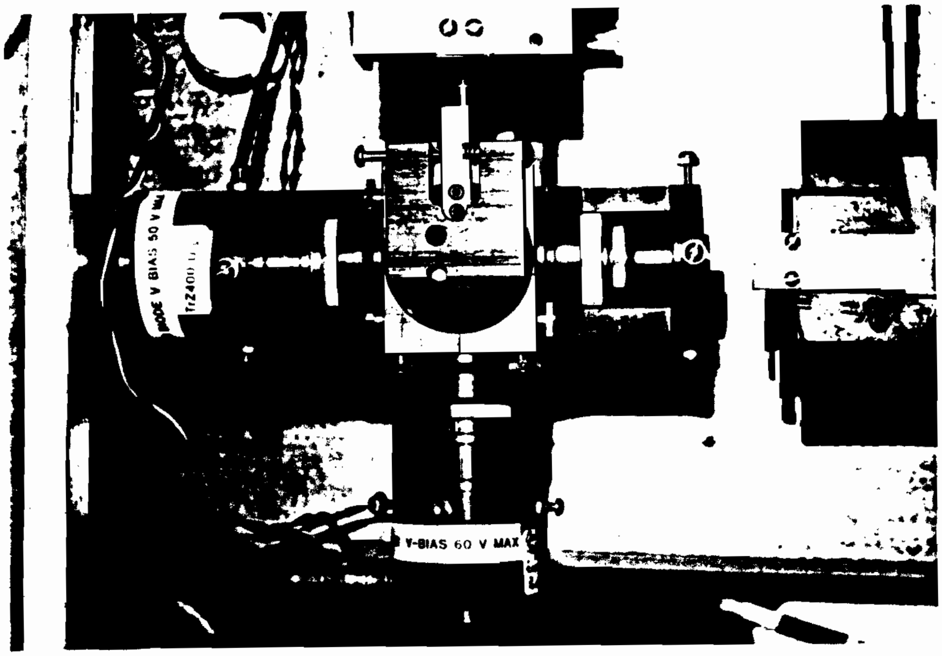

Fig.6.13 The measurement set-up at 1300 nm.

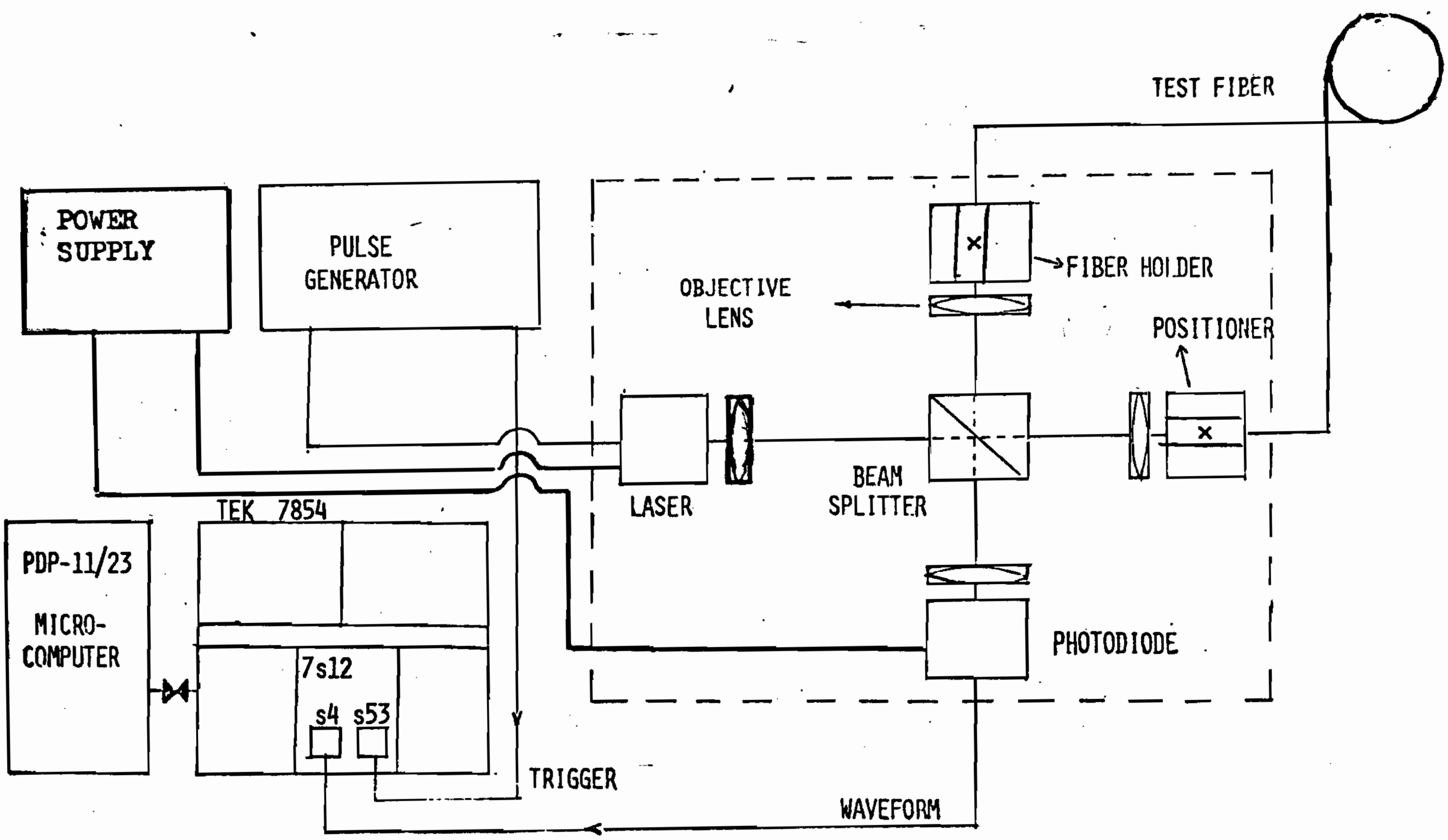

Fig.6.14 The experimental set-up for pulse dispersion measurement at 1300 nm.

Measurement set #11
Fiber code: 8/780A
Manufacturer: Northern Telecom.
Fiber Length: 1165 m.
Wavelength: 1300 nm.

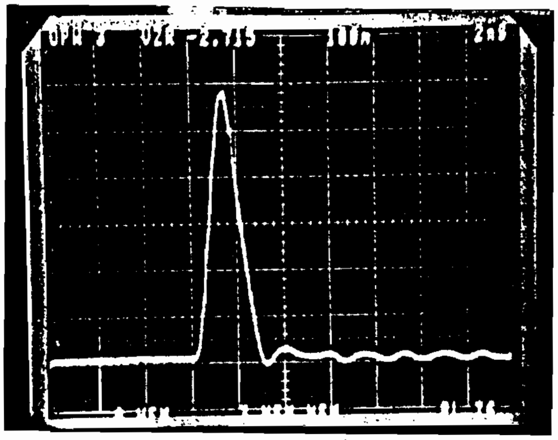

Fig.6.15.a Input waveform

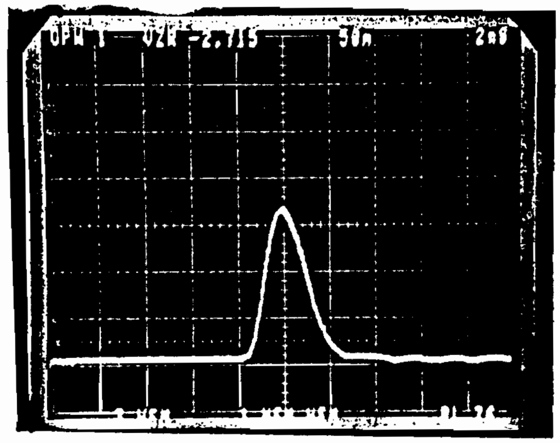

Fig.6.15.b Output waveform

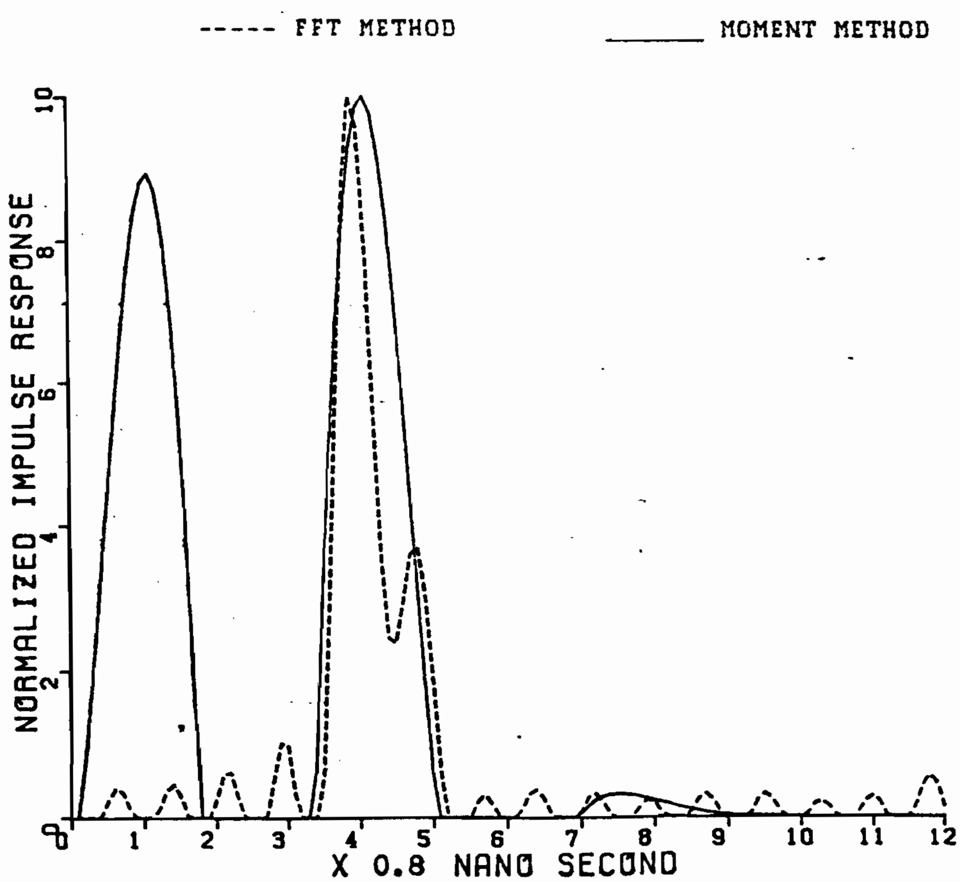

Fig.6.15.c Normalized impulse response as a function of time

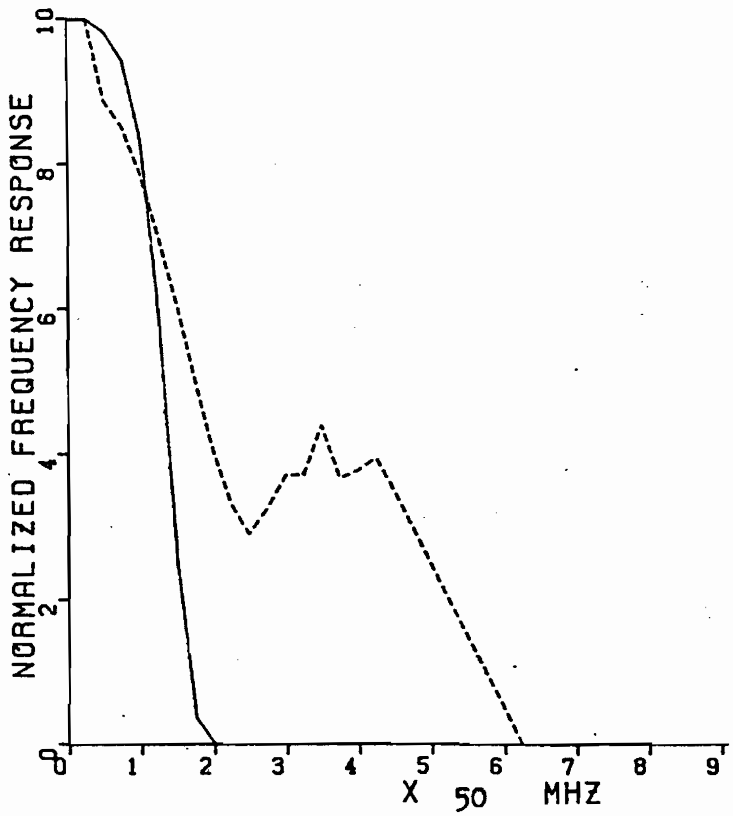

Fig.6.15.d Normalized frequency response versus frequency

MOMENT	CALCULATED VALUE
M_0	0.450
M_1	4.026 E-9 SEC.
M_2	4.112 E-18
M_3	-102.4 E-27

Table 6.13.a Calculated values of the moments

PARAMETER	CALCULATED VALUE	MANUFACTURER'S VALUE
ATTENUATION	2.98 db/km	4.4 db/km
PULSE DISPERSION	1.74 E-9 SEC.	0.3 E-9 SEC.
BANDWIDTH	98.6 MHZ	_

Table 6.13.b Comparison between the calculated values of fiber parameters and manufacturer's data

Measurement set #12
Fiber code: 3/1213B
Manufacturer: Northern Telecom.
Fiber Length: 1415 m.
Wavelength: 1300 nm.

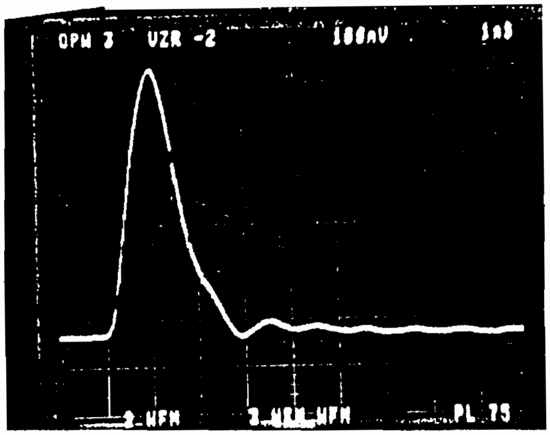

Fig.6.16.a Input waveform

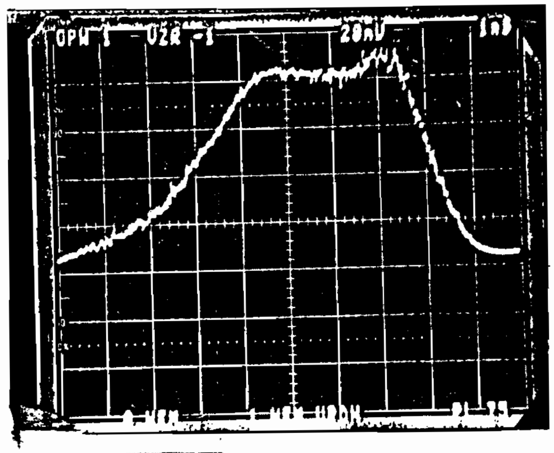

Fig.6.16.b Output waveform

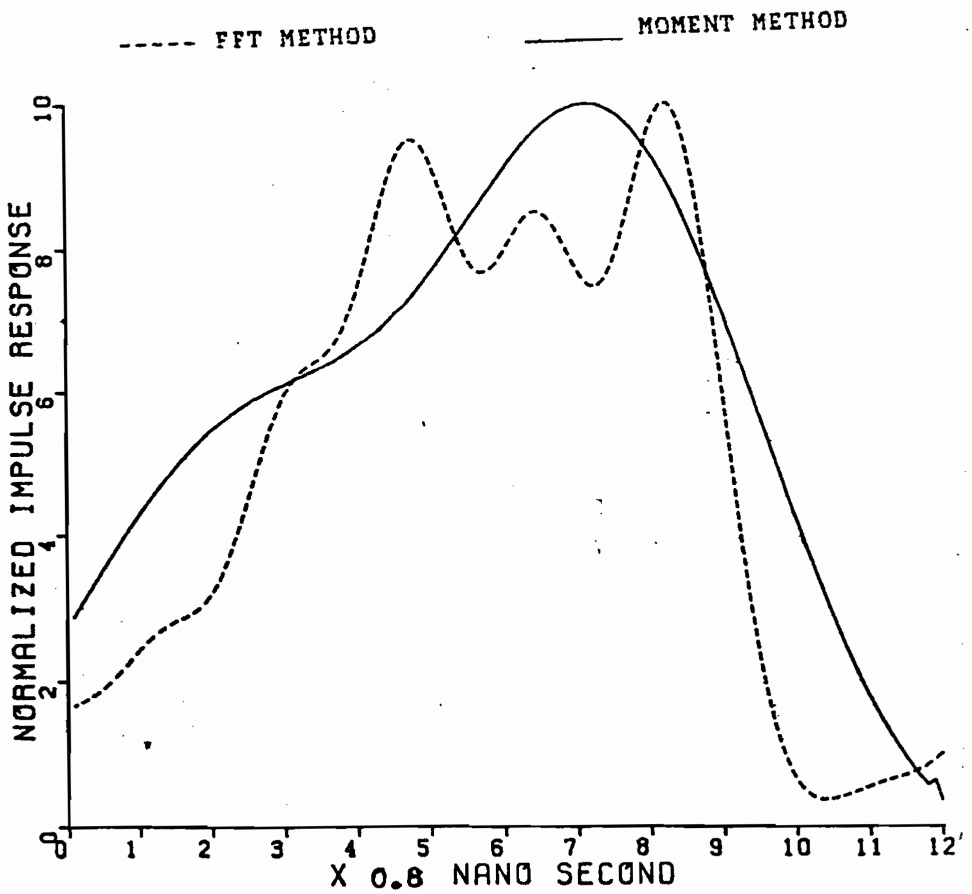

Fig.6.16.c Normalized impulse response as a function of time

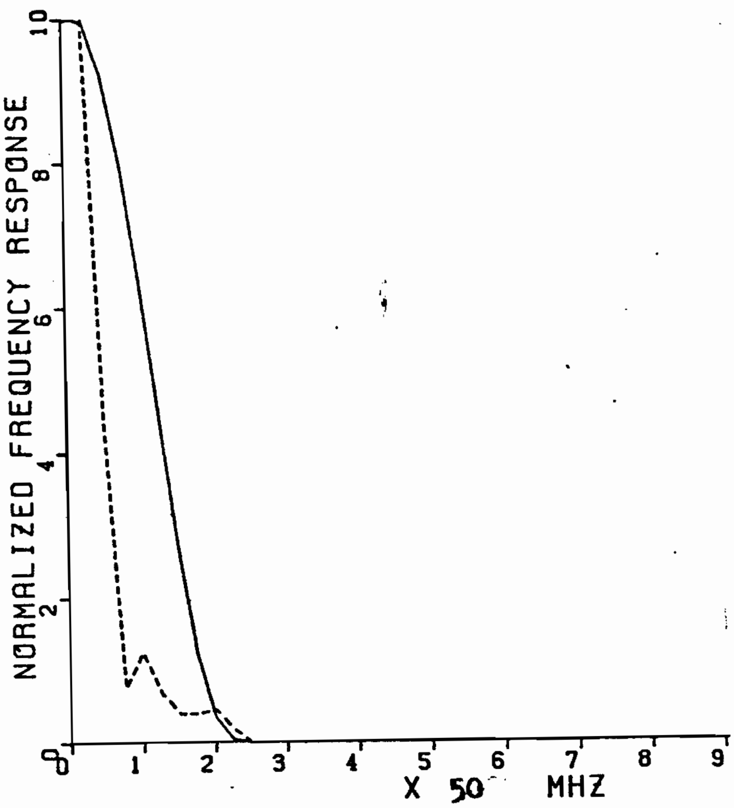

Fig.6.16.d Normalized frequency response versus frequency

MOMENT	CALCULATED VALUE
M_0	0.72160
M_1	4.289 E-9 SEC.
M_2	5.129 E-18
M_3	-4.426 E-27

Table 6.14.a Calculated values of the moments

PARAMETER	CALCULATED VALUE	MANUFACTURER'S VALUE
ATTENUATION	1.0 db/km	1.1 db/km
PULSE DISPERSION	1.6 E-9 SEC.	2.5 E-9 SEC.
BANDWIDTH	88.305 MHZ	–

Table 6.14.b Comparison between the calculated values of fiber parameters and manufacturer's data

Measurement set #13
Fiber code: 10/497A
Manufacturer: Northern Telecom.
Fiber Length: 830 m.
Wavelength: 1300 nm.

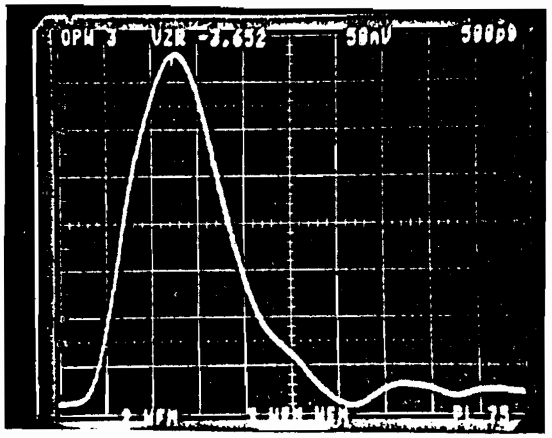

Fig.6.17.a Input waveform

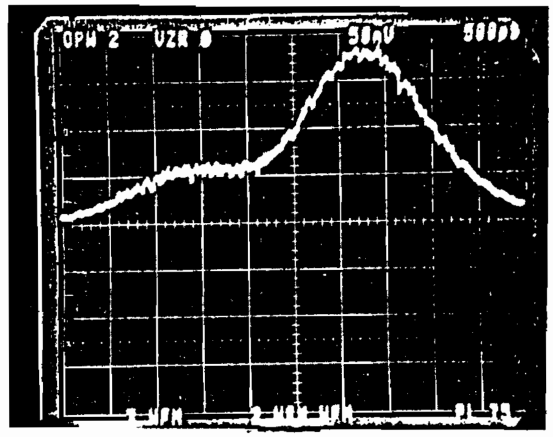

Fig.6.17.b Output waveform

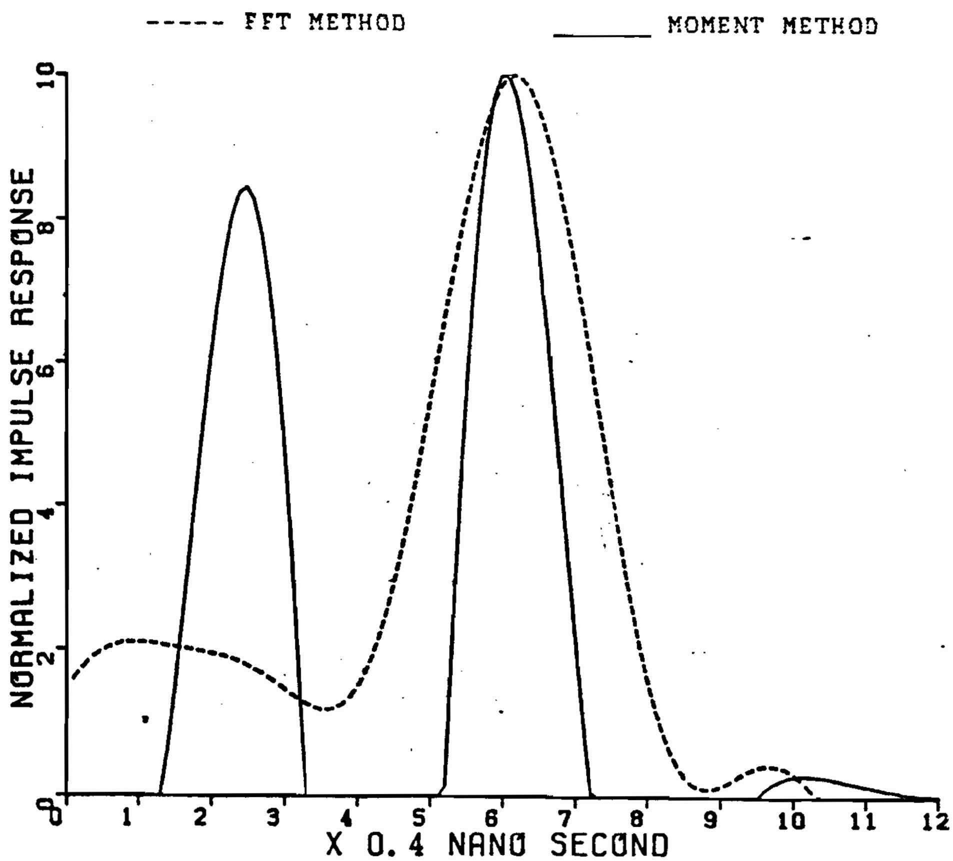

Fig.6.17.c Normalized impulse response as a function of time

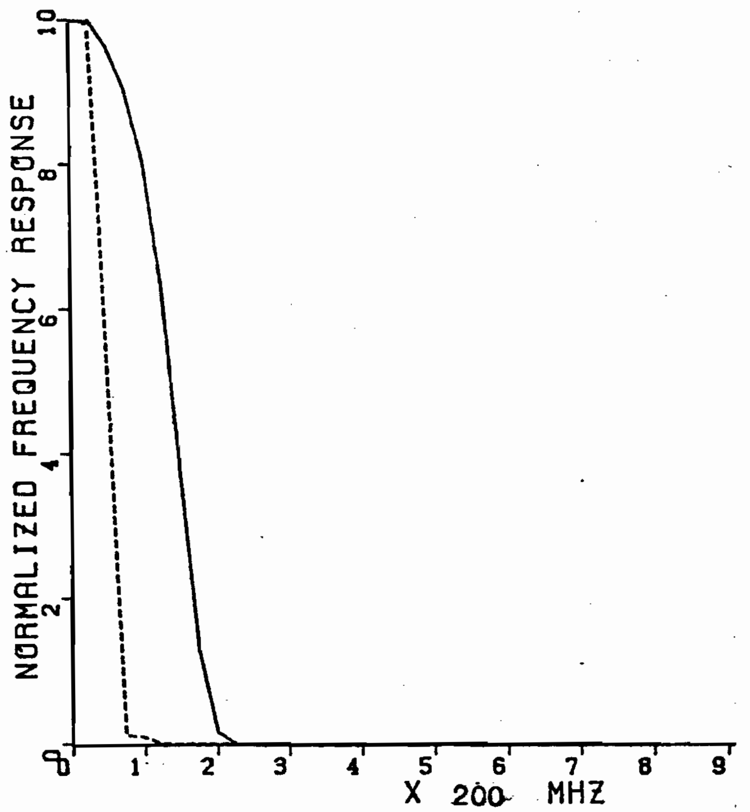

Fig.6.17.d Normalized frequency response versus frequency

MOMENT	CALCULATED VALUE
M_0	0.752
M_1	1.674 E-9 SEC.
M_2	1.360 E-18
M_3	2.567 E-27

Table 6.15.a Calculated values of the moments

PARAMETER	CALCULATED VALUE	MANUFACTURER'S VALUE
ATTENUATION	1.5 db/km	2.2 db/km
PULSE DISPERSION	0.72 E-9 SEC.	0.9 E-9 SEC.
BANDWIDTH	333 MHZ	–

Table 6.15.b Comparison between the calculated values of fiber parameters and manufacturer's data

Measurement set #14
Fiber code: 10/523B
Manufacturer: Northern Telecom.
Fiber Length: 935 m.
Wavelength: 1300 nm.

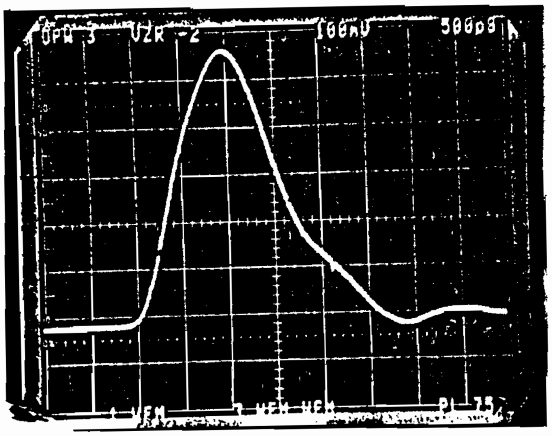

Fig.6.18.a Input waveform

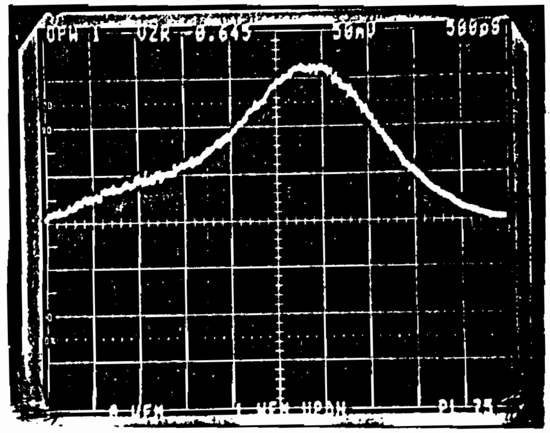

Fig.6.18.b Output waveform

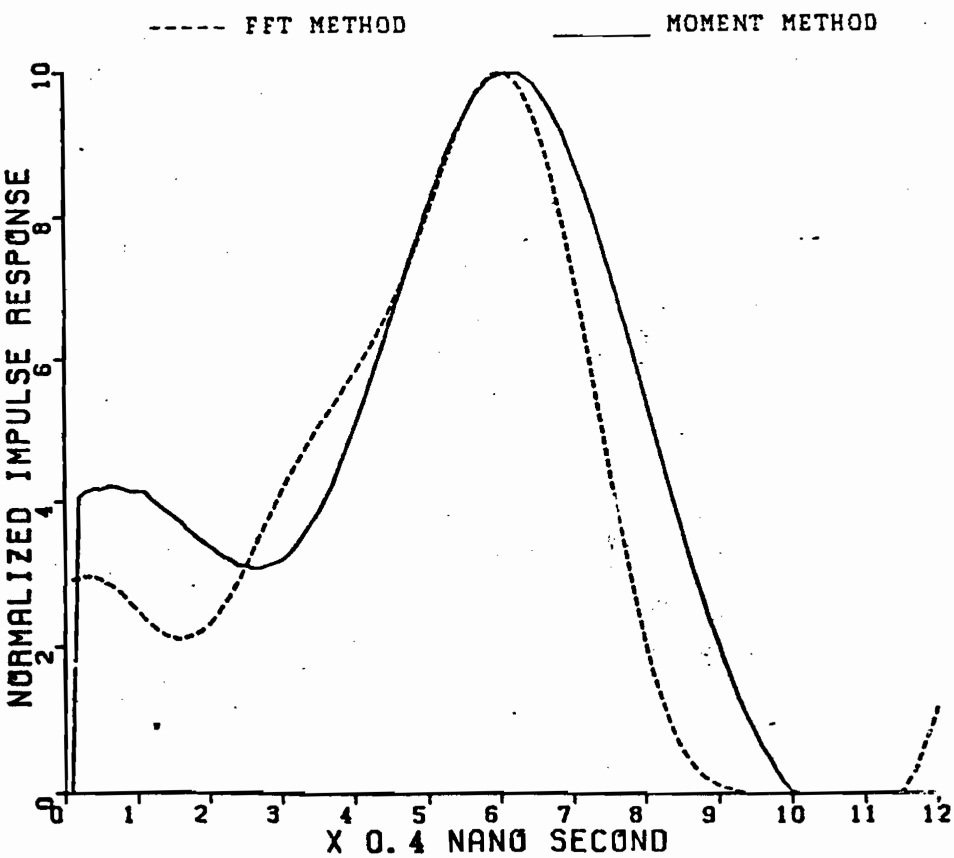

Fig.6.18.c Normalized impulse response as a function of time

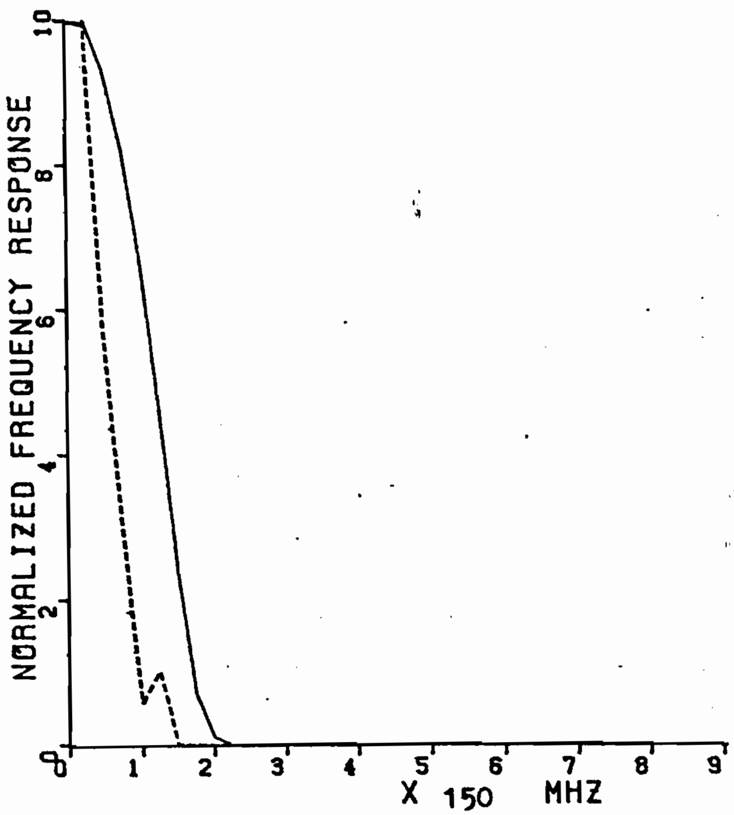

Fig.6.18.d Normalized frequency response versus frequency

MOMENT	CALCULATED VALUE
M_0	0.592
M_1	1.639 E-9 SEC.
M_2	1.102 E-18
M_3	-0.941 E-27

Table 6.16.a Calculated values of the moments

PARAMETER	CALCULATED VALUE	MANUFACTURER'S VALUE
ATTENUATION	2.435 db/km	- db/km
PULSE DISPERSION	1.123 E-9 SEC.	1.1 E-9 SEC.
BANDWIDTH	190 MHZ	_

Table 6.16.b Comparison between the calculated values of fiber parameters and manufacturer's data

Measurement set #15
Fiber code: 6/1064B
Manufacturer: Northern Telecom.
Fiber Length: 1196 m.
Wavelength: 1300 nm.

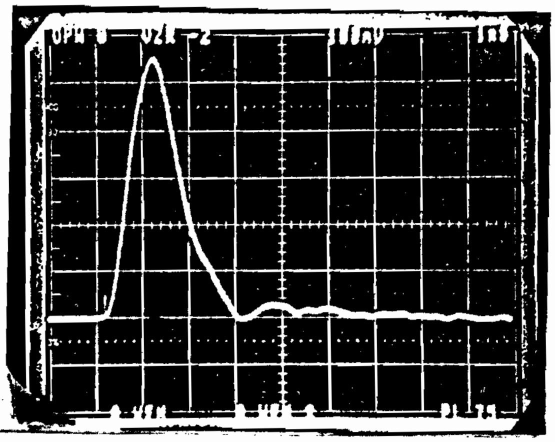

Fig.6.19.a Input waveform

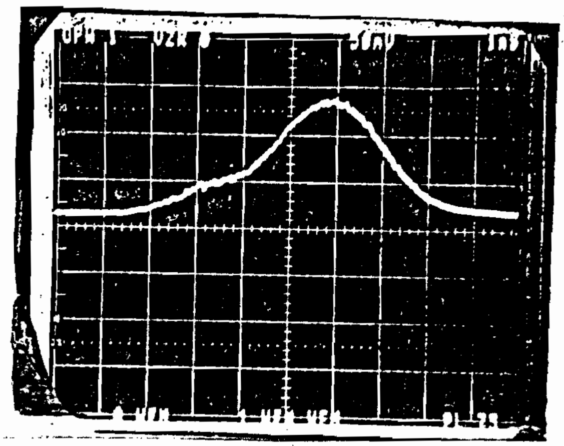

Fig.6.19.b Output waveform

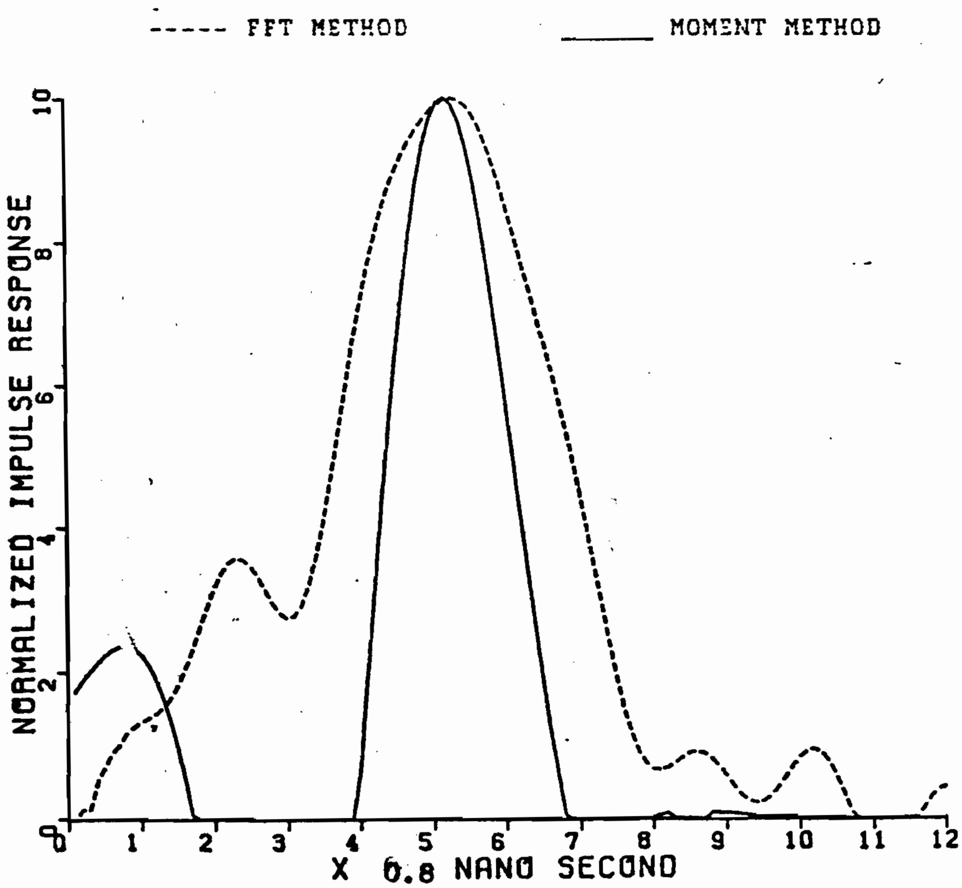

Fig.6.19.c Normalized impulse response as a function of time

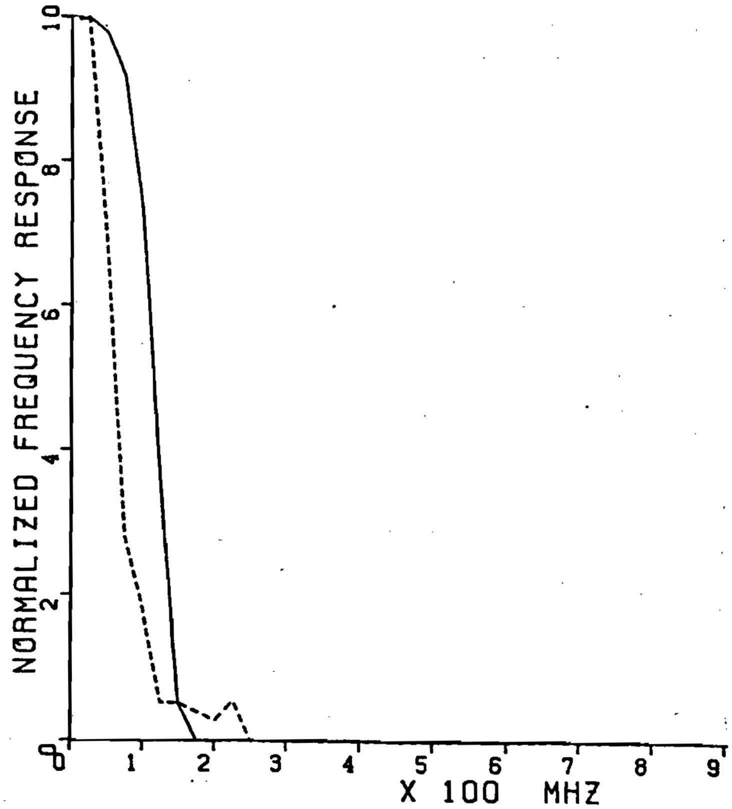

Fig.6.19.d Normalized frequency response versus frequency

MOMENT	CALCULATED VALUE
M_0	0.592
M_1	3.215 E-9 SEC.
M_2	1.328 E-18
M_3	-2.168 E-27

Table 6.17.a Calculated values of the moments

PARAMETER	CALCULATED VALUE	MANUFACTURER'S VALUE
ATTENUATION	1.9 db/km	1.5 db/km
PULSE DISPERSION	0.968 E-9 SEC.	2.6 E-9 SEC.
BANDWIDTH	173.51 MHZ	–

Table 6.17.b Comparison between the calculated values of fiber parameters and manufacturer's data

Measurement set #16
Fiber code: 6/1103B
Manufacturer: Northern Telecom.
Fiber Length: 1647 m.
Wavelength: 1300 nm.

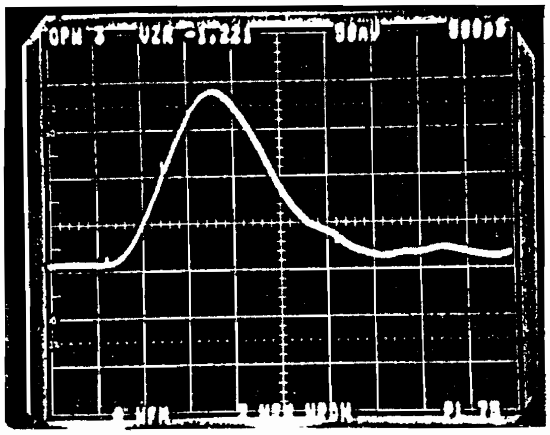

Fig.6.20.a Input waveform

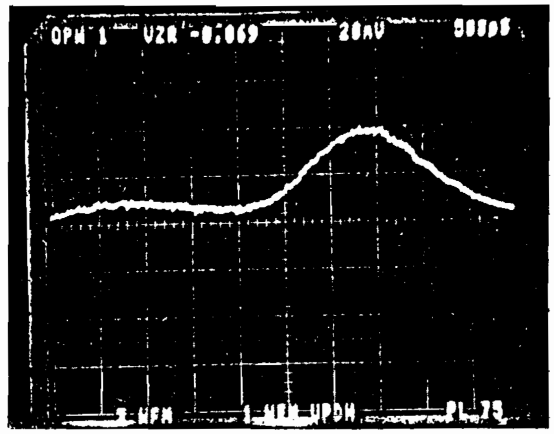

Fig.6.20.b Output waveform

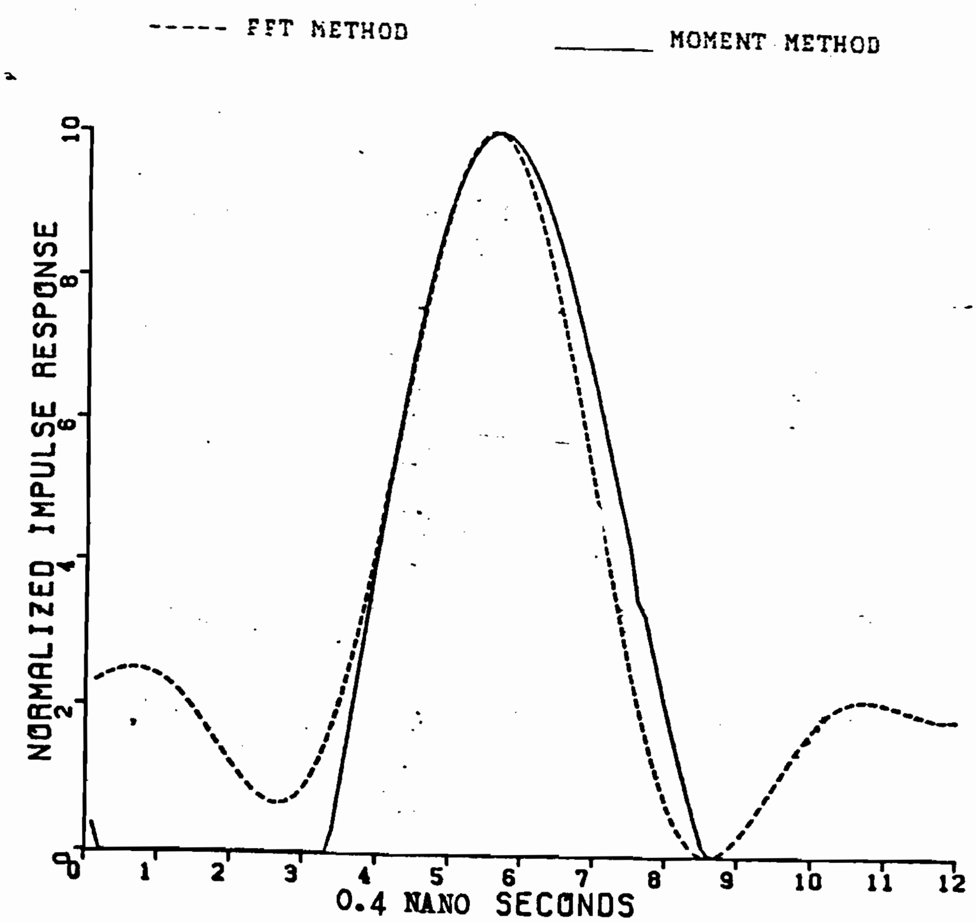

Fig.6.20.c Normalized impulse response as a function of time

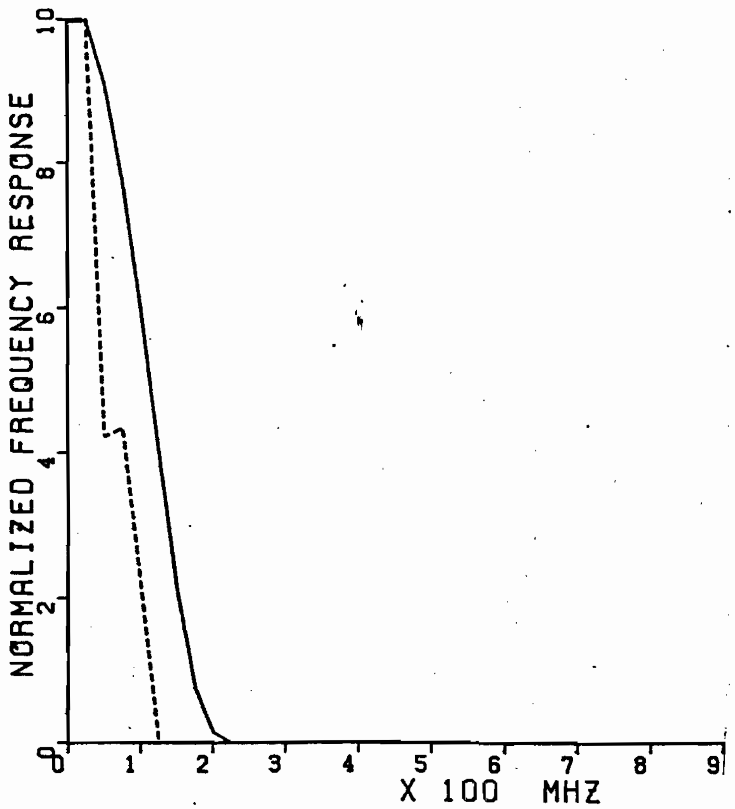

Fig.6.20.d Normalized frequency response versus frequency

MOMENT	CALCULATED VALUE
M_0	0.453
M_1	1.099 E-9 SEC.
M_2	1.475 E-18
M_3	-3.655 E-27

Table 6.18.a Calculated values of the moments

PARAMETER	CALCULATED VALUE	MANUFACTURER'S VALUE
ATTENUATION	2.09 db/km	3.7 db/km
PULSE DISPERSION	0.740 E-9 SEC.	0.9 E-9 SEC.
BANDWIDTH	164.6 MHZ	–

Table 6.18.b Comparison between the calculated values of fiber parameters and manufacturer's data

Measurement set #17
Fiber code: 3/1209A
Manufacturer: Northern Telecom.
Fiber Length: 1500 m.
Wavelength: 1300 nm.

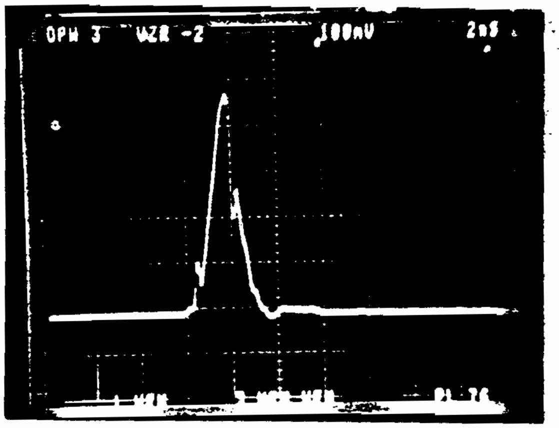

Fig.6.21.a Input waveform

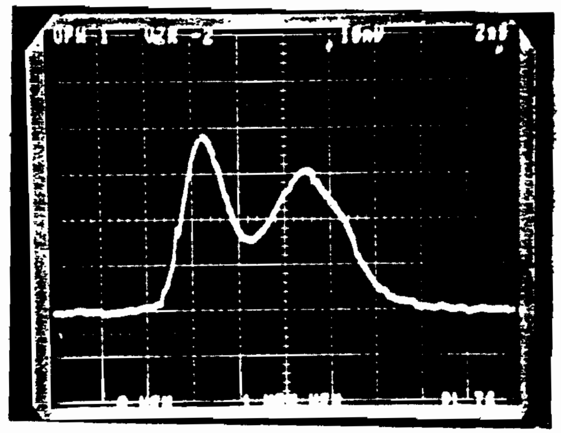

Fig.6.21.b Output waveform

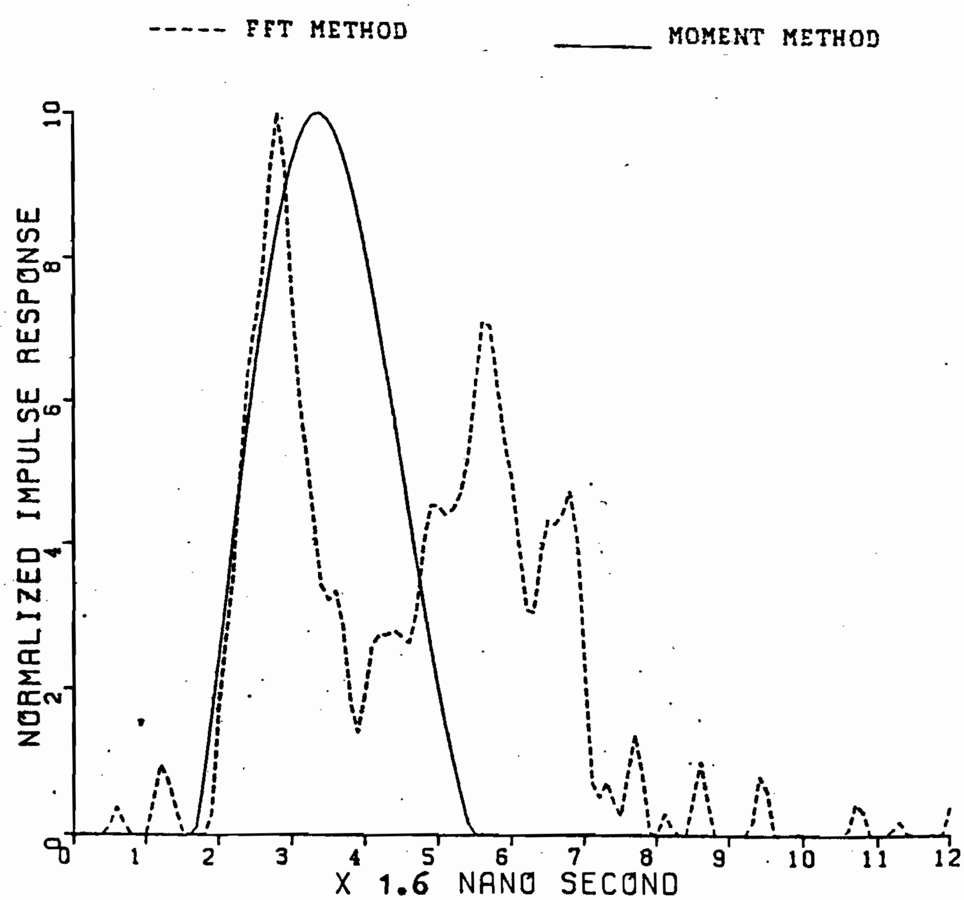

Fig.6.21.c Normalized impulse response as a function of time

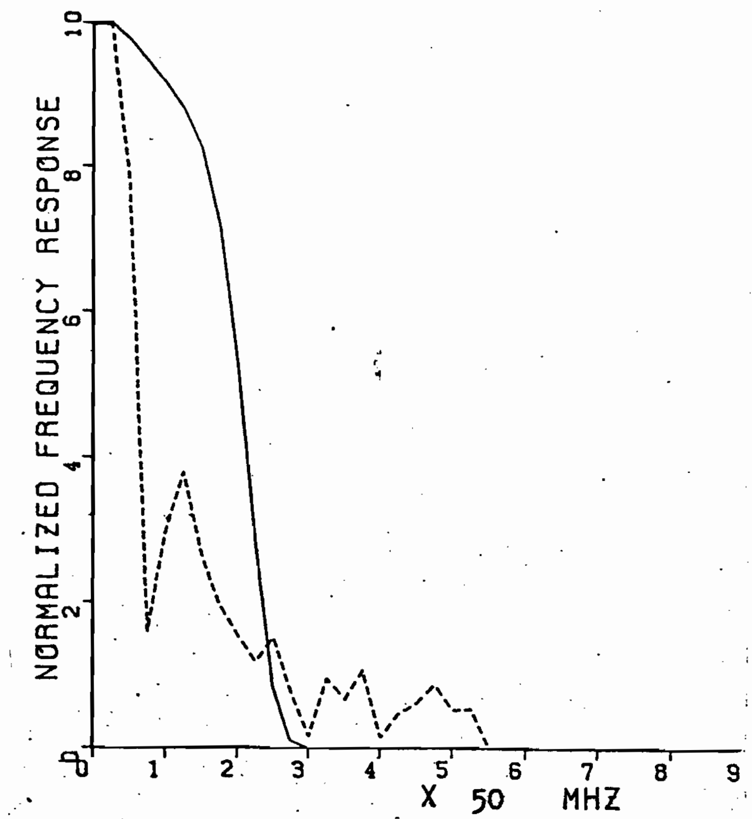

Fig.6.21.d Normalized frequency response versus frequency

MOMENT	CALCULATED VALUE
M_0	0.39730
M_1	3.0889 E-9 SEC.
M_2	10.940 E-18
M_3	-1.424 E-27

Table 6.19.a Calculated values of the moments

PARAMETER	CALCULATED VALUE		MANUFACTURER'S VALUE
ATTENUATION	2.67	db/km	1.4 db/km
PULSE DISPERSION	2.2 E-9	SEC.	2.5 E-9 SEC.
BANDWIDTH	91.51	MHZ	–

Table 6.19.b Comparison between the calculated values of fiber parameters and manufacturer's data

6.3 The Impulse Response Using The 7854 Tektronix Oscilloscope

6.3.1 Programming The Oscilloscope

The 7854 digital oscilloscope was programmed to calculate the attenuation, pulse dispersion, and the impulse response of the fiber under test.

The program written to perform and plot the impulse response of a given input and output waveform is listed in Appendix D. The input is stored in the memory of the oscilloscope, (the input is given a memory space labelled 1WFM), and the output is stored in (3WFM)[6.5]. The program generates a time function T and stores it in (2WFM). Each time a certain moment needs to be calculated, the time function stored in (2WFM) will be multiplied by one of the waveforms (1WFM) or (3WFM). The integration will be performed using the (AREA) command of the oscilloscope. A comparison between performing the integration and the moment calculation using the oscilloscope and using the PDP-11/23 computer system is listed in Tables 6.20, 6.21, and 6.22. Figure 6.22 shows the impulse response of a square pulse for three different orders, the fourth, the sixth, and the eighth, which also was done previously in Chapter 5 using the PDP-11/23 computer. Figure 6.23 shows the time function T generated by the program listed in Appendix D. This time function was used to calculate the different moments. Figure 6.24 to Figure 6.30 show the input waveforms, the output waveforms, and their impulse responses using the Tektronix 7854 digital oscilloscope. Figure 6.31 to Figure 6.39 show the impulse response for some of the fibers which were done previously in sections 6.1 and 6.2. The same input and output waveforms were used in the computation done here.

6.3.2 Results and Calculations

Figure 6.26 shows the input waveform for the fiber code 10/523B and Figure 6.27 shows the output waveform for the same fiber. The impulse response for this fiber was done using the program listed in Appendix D. The impulse response for this fiber is shown in Figure 6.28 and Figure 6.29 for the fourth and sixth order moments respectively. Figures 6.24 and 6.25 show the input, output and the impulse response for the Corning fiber with the lot# 31329204. Figures 6.30 to 6.39 show the same impulse responses, which were previously calculated using the computer, and were computed here using the oscilloscope.

The programming of the 7854 Tektronix oscilloscope to perform the calculation and to plot the impulse response of the fiber is convenient particularly when the micro-computer is not available. The disadvantage is that the oscilloscope is much slower than the PDP-11/23 micro-computer as it is shown in Table 6.23. The Tektronix oscilloscope needed 19 minutes to compute and plot the impulse response, while the PDP-11/23 computer required only 1.1 minute to compute and plot the same impulse response.

In some cases, the number of moments was not sufficient to get a reasonable accuracy. In this case, more moments and a larger number of sampling points are needed. The reason for not considering this is that the oscilloscope has a limited memory and, hence, it is not possible to add any more lines to the existing program. Also, if the sampling points are increased to the next higher number, which is 1024 points, then the waveform storage area will be sufficient for one waveform only. This makes it impossible to perform the computation because at least three waveform storage areas are needed. Considering the moment calculation, there is no significant difference in the accuracy as shown in Tables 6.20, 6.21, and 6.22.

One more point about the convenience in using the Tektronix oscilloscope is that the oscilloscope keeps track of the scaling for each computational step, unlike the PDP-11/23 computer system, where the time has to be scaled up in order not to cause underflow while the moments are being calculated. The underflow point of the PDP-11/23 computer is E-35. At the same time, if we are working in the nano second time scale, the sixth order moment will be of the order of E-54. On the other hand the underflow point of the Tektronix oscilloscope is E-99, which is much lower than the sixth order moment, for example. Hence, there is no scaling needed when working on the Tektronix oscilloscope.

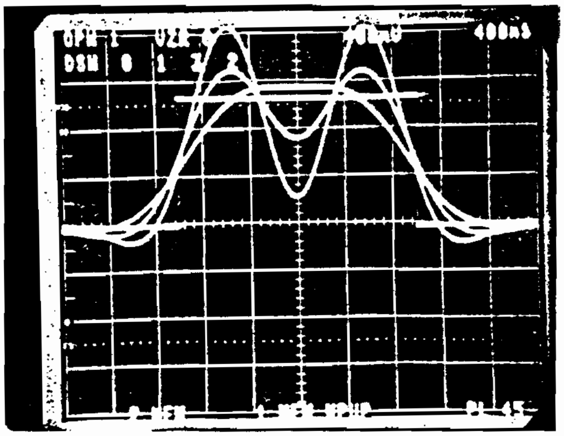

Fig.6.22 Impulse response for a square waveform (the fourth order shows no ripples, while the sixth and eight order show strong ripples)

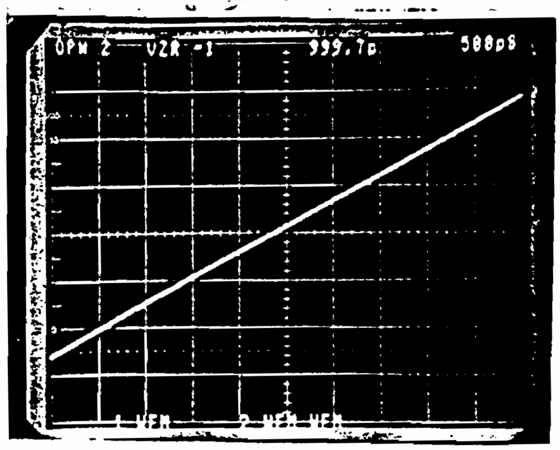

Fig.6.23 The time function T used in the calculation of the moments using the oscilloscope

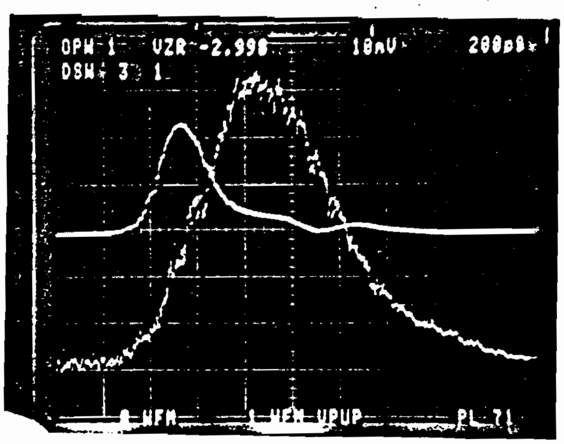

Fig.6.24 The input and output waveforms for the fiber (code 204/corning) at 900 nm.

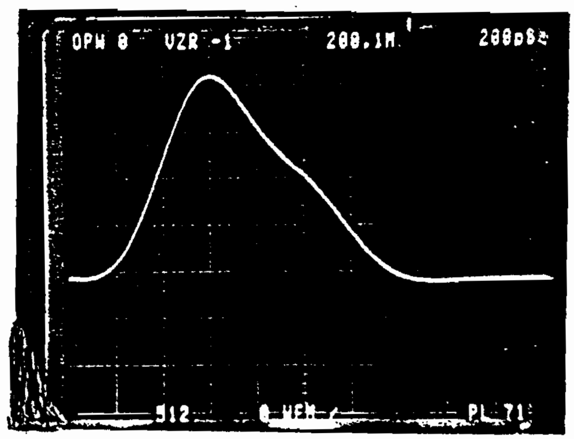

Fig.6.25 The impulse response for the fiber (code 204/ corning) at 900 nm.

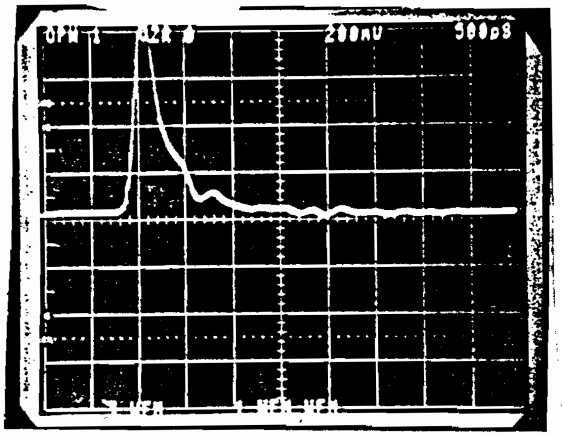

Fig.6.26 Input waveform for the fiber (code 10/523B) at 900 nm.

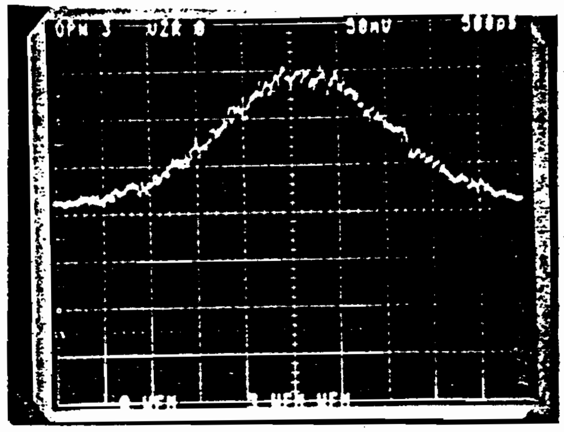

Fig.6.27 Output waveform for the fiber (code 10/523B)

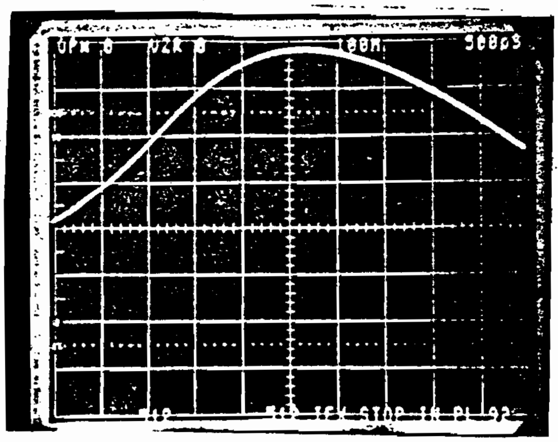

Fig.6.28 Impulse response for the fiber (code 10/523B, fourth order) at 900 nm.

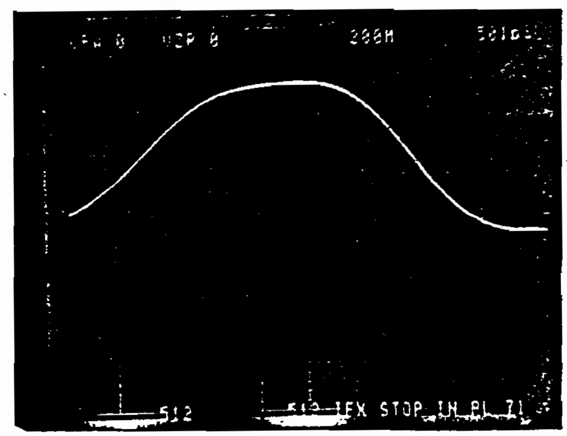

Fig.6.29 Impulse response for the fiber (code 10/523B, sixth order) at 900 nm.

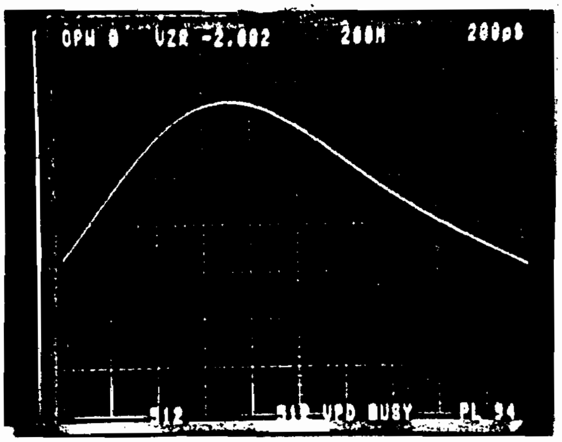

Fig.6.30 Impulse response for the fiber (code 10/497A) at 900 nm.

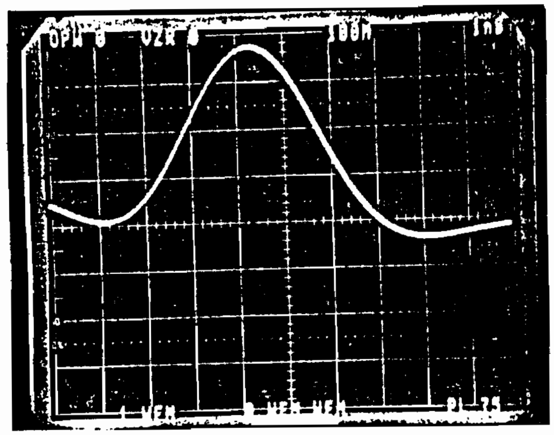

Fig.6.31 Impulse response for the the fiber (code 6/1064B at 1300 nm.

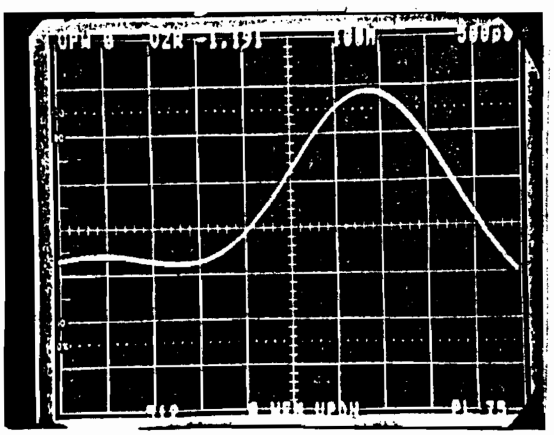

Fig.6.32 Impulse response for the fiber (code 6/1103B) at 1300 nm.

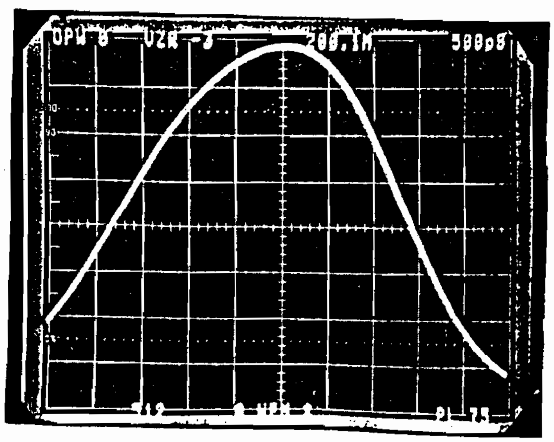

Fig.6.33 Impulse response for the fiber (code 10/523B) at 1300 nm.

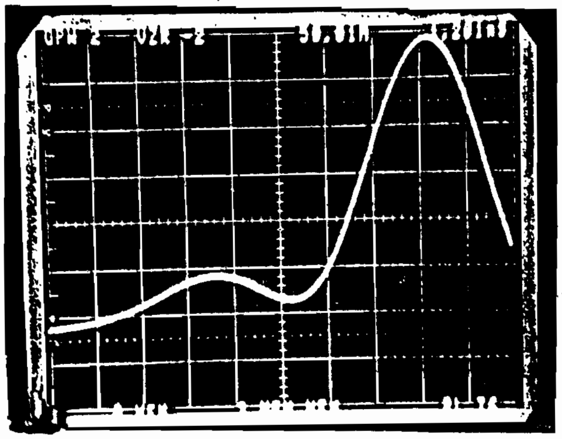

Fig.6.34 Impulse response for Fiber
(code 3/1209A) at 1300 nm

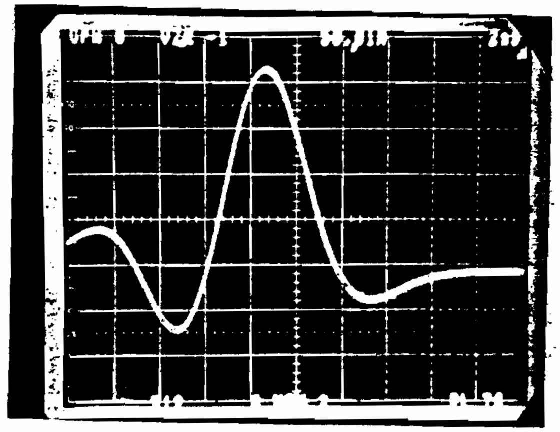

Fig.6.35 Impulse response for fiber
(code 3/1209A) at 900 nm

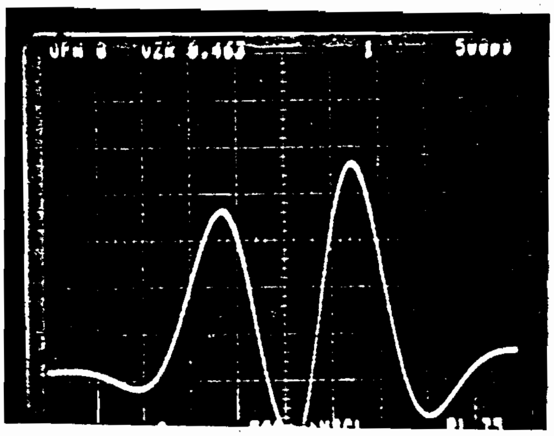

Fig.6.36 Impulse response for Fiber
(code 10/497A) at 1300 nm

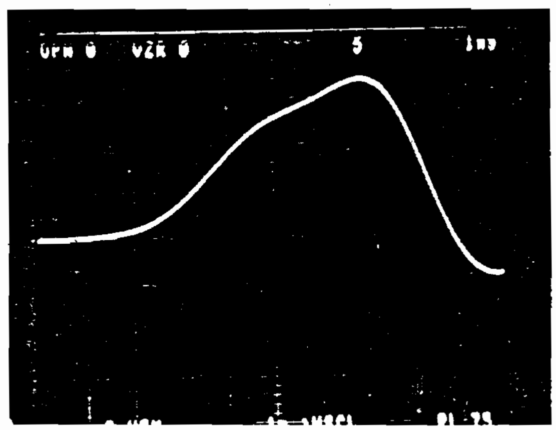

Fig.6.37 Impulse response for fiber
(code 3/1213B) at 900 nm

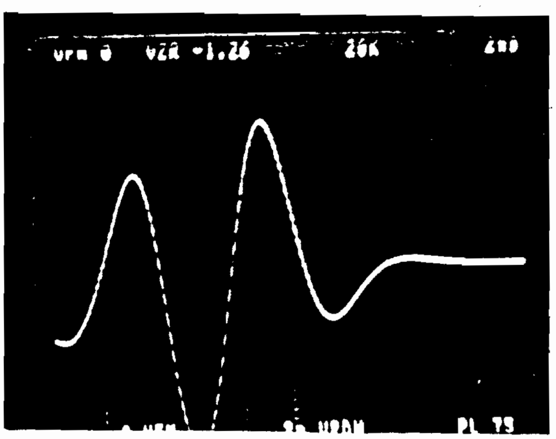

Fig.6.38 Impulse response for Fiber
(code 8/780A) at 1300 nm

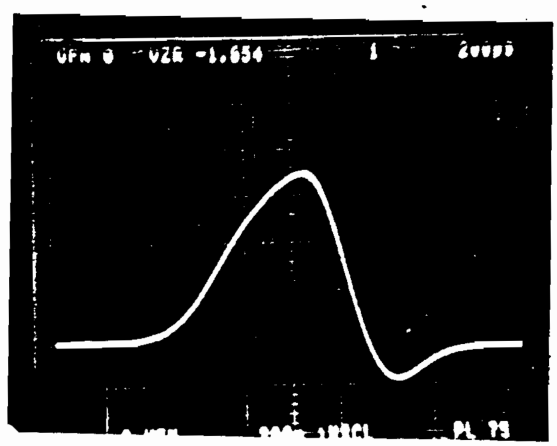

Fig.6.39 Impulse response for fiber
(code 60337107) at 900 nm

Moment	PDP-11/23	Tektronix 7854
M_0	0.3387	0.340
M_1	0.308 E-9	0.3053 E-9
M_2	0.0723 E-18	0.0729 E-18
M_3	-.0991 E-27	-.1076 E-27
M_4	-.3605 E-38	-.3972 E-38
M_5	-.2316 E-46	-.2379 E-46
M_6	-.1016 E-55	-.1608 E-55

Table 6.20 Comparison between the moments evaluation using the 7854 oscilloscope and the PDP-11/23 computer system.
Fiber Code: 31329204
Wavelength: 900 nm

Moment	PDP-11/23	Tektronix 7854
M_0	0.6477	0.6479
M_1	0.369 E-9	0.385 E-9
M_2	0.098 E-18	0.096 E-18
M_3	-.1116 E-27	-.1102 E-27
M_4	-.0689 E-36	-.0687 E-36
M_5	-.3375 E-45	-.0324 E-44
M_6	0.1451 E-54	0.1434 E-54

Table 6.21 Comparison between the moments evaluation using the 7854 Tektronix oscilloscope and the PDP-11/23 computer system.
Fiber Code : 10/497A
Wavelength : 900 nm

Moment	PDP-11/23	Tektronix 7854
M_0	0.5210	0.5209
M_1	2.3715 E-9	2.3720 E-9
M_2	1.6943 E-18	1.583 E-18
M_3	-.2743 E-26	-.2744 E-26
M_4	-.7336 E-36	-.8213 E-36
M_5	-.2084 E-43	-.2008 E-44
M_6	0.1581 E-51	0.1544 E-51

Table 6.22 Comparison between the moments evaluation using the 7854 Tektronix oscilloscope and the PDP-11/23 computer system.
Fiber Code : 10/523B
Wavelength : 900 nm

computation time for Tektronix 7854	computation time for PDP-11/23
19 minutes	1.1 minutes

Table 6.23 Comparison between the computation time for the PDP-11/23 Computer and the 7854 Tektronix oscilloscope.

CHAPTER 7

CONCLUSIONS AND SUGGESTIONS FOR FUTURE WORK

The main advantage of the moment method is that it can compute the impulse response directly from the moments of the input and the output signals in the time domain. The FFT method on the other hand, requires two Fourier transformations for both of the input and output signals. The first transformation is from the time domain to the frequency domain to perform the division and obtain the frequency response. The second transformation is from the frequency domain back into the time domain to obtain the impulse response. It is obvious that the moment method gives an explicit expression for the impulse response in terms of the moments of the input and output signal without the need for the frequency response. Unlike the moment method, the FFT method has to have the frequency response in order to get the impulse response.

We were able to fit the impulse response program using the moment method into the memory of the Tektronix 7854 oscilloscope (30 k), as was shown in Section 6.3. On the other hand, it was not possible to adapt the impulse response program using the FFT for computing in the oscilloscope, because it requires more memory space. Hence, the moment method enables us to use the oscilloscope for both recording the measurements, computing and plotting the impulse response at the same time. This makes the moment method more appropriate to be used in obtaining a fast characteriazation of the fiber, particularly in laboratories, industry, field measurements, and places where computers are not available.

Although the moment method gave a reasonable accuracy when the moments of the input and the output waveforms were computed up to the sixth order, an improvement could be introduced to the moment method, i.e., by relating the order of the moments to the accuracy of the method. This can be achieved by letting the accuracy of the method determine the number of moments required to give us enough information about the impulse response of the fiber. Once the accuracy of the moment method is established, there will be no need to compare with the FFT method.

As was shown in Chapter 6, the moment method can be programmed on the 7854 Tektronix oscilloscpe to give the impulse response of the fiber. The only noticeable disadvantage of computing the moments using the oscilloscope is the slow speed of the microprocessor in the Tektronix Digital Oscilloscope compared to the PDP-11/23 computer. This could be improved if some additional hardwares is incorporated in the oscilloscope to take the moments and plot the impulse response of the fiber. One important point regarding the accuracy of the moments method should be mentioned here. The accuracy of the moment method could be increased by increasing the number of sampling points to the highest number of sampling points offered by the Tektronix 7854 Digital Oscilloscope. The highest number of sampling points possible on the Tektronix 7854 DPO is 1024 points. The main disadvantage of doing this is that only one waveform is stored each time. In this case, the input and the output should be stored and transferred to the PDP-11/23 computer system separately. Although the accuracy will be increased, the program requires more running time. Also the program, written for the 7854 DPO to plot the impulse response, can not be used if the number of points is increased to 1024 sampling points. The reason for this is that the size of the memory, which is used to store the waveforms, will be increased in order to accommodate the extra number of sampling points. In other words, it is possible to store and perform the computation on up to three waveforms when the sampling points is 512. On the other hand, the number of waveforms is reduced to one when the number of sampling points is 1024. This makes it difficult to compute the impulse response because the minimum number of waveforms needed is three, the input, the output and the time function. Generally, the moment method was found to be reliable and reasonably accurate when the pulse was bell-shaped. In the cases where the output pulse did not have a bell shape, which could indicate also that the fiber has some defects, the FFT method was more reliable for computing the impulse reaponse. A more rigorous study should be made in future to examine and improve the accuracy of the moment method when the pulse shape is not close to that of a bell.

Working with the Tektronix 7854 DPO has been convenient for storing and sampling a waveform though there were some difficulties encountered when the oscilloscope was interfaced with the PDP-11/23 computer. One of the main problems was the difficulty in sending a waveform data from the PDP-11/23 computer to be displayed on the oscilloscope. Although this problem was solved using the program listed in APPENDIX-E, the oscilloscope failed to accept data sent back in the same format as they were previously received from the oscilloscope. This problem, therefore, should also be looked into with a view to successfully sending the data back from the PDP-11/23 computer to the oscilloscope's storage space for direct display on the screen of the oscilloscope.

REFERENCES

(1.1) M. R. Jones, "A comparison of lightwave, microwave, and coaxial transmission technologies", IEEE Journal of Quantum Electronics, vol. QE-88, PP. 1524-1535, Oct. 1982.

(1.2) M. R. Amicone, "Fiber optics present and future", Telephone Engineering and Management, Vol. 88, No. 16, PP. 83-86, August 15 1984.

(1.3) J. Midwinter, "Optical fiber communications present and future III", Telephony, Vol. 207, No. 18, PP. 56-62, Oct. 22, 1984.

(1.4) G. Keiser, "Optical Fiber Communications", McGraw Hill, New York, PP. 19-28, 1983.

(1.5) D. Marcuse, "Light Transmission Optics", second edition, PP. 286-287, 1982.

(1.6) E. Lacy, "Fiber Optics", pp. 69-100, Prentice-Hall, Englewood Cliffs, N.J., 1982.

(1.7) G. Keiser, "Optical Fiber Communications", McGraw Hill, New York, PP. 58-59, 1983.

(1.8) Y. Suematsu and K. Iga, "Introduction to Optical Fiber Communications", John Wiley and Sons, New York, PP. 141-146, 1982.

(1.9) S. Geckeler, "Pulse broadening in optical fibers with mode mixing", Applied Optics, Vol. 18, No. 13, PP.2192-2198, July 1979.

(1.10) A. Puc, "Study and measurements of pulse broadening in optical fibers", M. Eng. thesis, Dept. of Eect. Eng., McGill Univ., PP. 47-50, August 1980.

(2.1) Staff of CSELT, "Optical Fiber Communication " McGraw Hill, New York, PP. 152-207, 1981.

(2.2) G. Keiser, "Optical Fiber Communications", McGraw Hill, New York, PP. 50-58, 1983.

(2.3) Staff of CSELT, "Optical Fiber Communication " McGraw Hill, New York, PP. 745-747, 1981.

(2.4) H. F. Wolf, "Handbook of Fiber Optics: Theory and Applications", Garland, New York, PP. 85-86, 1979.

(2.5) M. K. Barnoski and S. M. Jensen," Fiber waveguides: a novel technique for investigating attenuation characteristics", App. Opt., Vol 15, No. 9, PP. 2112-2115, 1976.

(2.6) S. D. Personick," Photon probe-an optical time domain reflectometer", Bell Sys. Tech. J. Vol 50, No.3, PP. 355-366, March 1977.

(2.7) B. Costa and B. Sordo," Experimental study of optical fiber attenuation by modified backscattering technique", Third European Conference on optical fiber communication, Munich, PP. 69-71, Sept. 1977.

(2.8) R. Worthington," Acceptance angle measurement of multimode fibers a comparison of techniques", App. Opt., Vol 21, No. 19, PP. 3515-3519, Oct., 1982.

(2.9) A. S. Gerchicov, "Effective aperture of optical fibers", Sov. J. Opt. Technol., Vol 42, No. 8, PP. 434-436, August 1975.

(2.10) H. Matsumura, "Light acceptance angle in graded-index fiber", Opt. and Quant. Elect., Vol 7, No. 2, P. 81,March 1975.

(2.11) E. M. Kim, D. L. Frazen," Measurement of far-field and near-field radiation patterns from optical fibers", NBS, Boulder, Co., PP. 1-15, Feb. 1981.

(2.12) G. W. Day ," Measurement of optical fiber bandwidth in the frequency domain", NBS, Boulder, Co., PP. 1-40, Sept. 1981.

(2.13) A. Puc, "A study and measurements of pulse broadening of optical fibers", M. Eng. thesis, Dept. of Elect. Eng., McGill Univ., PP. 95-138, Aug., 1980.

(2.14) E. O. Brigham, "The Fast Fourier Transform", Prentice Hall, New York, PP.

10-74, 1974.

(2.15) N. A. Glavatskikh and et al.," Investigation of the dispersion of multimode dielectric waveguide by the optical heterodyne method", Sov. J Quant. Electron, Vol 12, No. 6, PP. 779-782, June, 1982.

(2.16) W. Freude, C. Fritzsche, and G. K. Grau, "Bandwidth estimation for multimode optical fibers using speckle pattern", App. Opt., Vol 22, No. 21, PP.3319-3320, Nov., 1983.

(2.17) M. Drajev and L. Piccari," Application of pulsed spectral method for bandwidth measurement of optical fibers", Opt. and Quant. Elect., Vo. 16, No.1, PP. 91-93, 1984.

(2.18) A. Puc, "A study and measurements of pulse broadening of optical fibers", M. Eng. thesis, Dept. of Elect. Eng., McGill Univ., PP. 102-103, Aug., 1980.

(3.1) M. Born and E. Wolf, "Principles of Optics", New York, P.121, 1959

(3.2) L. Jacomme, "A model for a ray propagation in a multimode graded-index fiber", Optics Communication, Vol.14, No.1, PP.134-138, May, 1975.

(3.3) E. G. Rawson, D. R. Herriott, and J. McKenna "Analysis of refractive index distribution in cylindrical graded-index glass rods, used in image relays", Applied Optics, Vol. 9, No. 3, PP. 753-759, March 1970.

(3.4) D. Marcuse, "Light Transmission Optics", Second Edition, P. 90, 1982.

(3.5) P. DiVita, R. Vannucci, "Loss mechanisms of leaky skew rays in optical fibers ", Optical and Quantum Electronics, PP. 177-188, Sept., 1977.

(3.6) Technical Staff of CSELT, "Optical Fiber Communication", McGraw Hill, New York, PP. 47-82, 1981.

(3.7) M. J. Adams, D. N. Payne and F. M. E. Sladen, "Length dependent effects due to leaky modes on multimode graded index fibers", Optics Communication Vol.17, No.2, PP. 204-209, May 1976.

(3.8) Colin Pask, "Generalized parameters for tunneling ray attenuation in optical fibers", J. OPt. Soc. Am., Vol. 68, No.1, PP. 110-116, January, 1978.

(3.9) A. W. Snyder and J. D. Love, "Attenuation coefficient for tunneling leaky rays in graded-index fibers", Electronics Letters Vol.12, No.13, PP. 324-326, June, 1976.

(3.10) E. Wolf (Ed.), "Progress in Optics", Vol.18, North Holland Publishing Company, PP. 3-82, 1980.

(3.11) G. Keiser, "Optical Fiber Communications", McGraw Hill, New York, pp. 54-55, 1983.

(3.12) A. H. Cherin, "An Introduction to Optical Fibers", McGraw Hill, New York, PP. 149-156, 1983.

(3.13) Photon Kinetic, "FOA-1000 Universal Fiber Optics Analyser Operation Manual", Photon Kinetic, Beaverton, Oregon, 1980.

(4.1) Franzen L. and M. Kim, "Measurement of far-field and near-field radiation patterns from optical fibers", Notes from National Bureau of Standards, Boulder, Colorado, February, 1981.

(4.2) R. Gallawa, " Notes on the definition of fiber numerical aperture", Electromagnetic Technology Division, National Bureau of Standards, Boulder, Colorado, 1980.

(4.3) H. Matsumura, "The light acceptance angle of a graded-index fiber", Optical and Quantum Electronics, Vol 7, No 2, PP. 81-86, March 1975.

(4.4) J. Versluis and Peelen, "Fiber Manufacture and Properties", Philips Telecomm., Philips Telecomm., Review, No 37, PP.215-230, 1979.

(4.5) R. Worthington, "Acceptance angle measurement of multimode fibers: a comparison of techniques", Applied Optics, Vol 21, No 18, PP. 3515-3519, October, 1982.

(4.6) Photon Kinetic," Operating Manual for the Universal Fiber Optics Analayser FOA - 1000", Photon Kinetic, Beaverton, Oregon, 1980.

(5.1) M. Jong, "Methods of Discrete Signal and System Analysis", New York, McGraw Hill, (a) PP. 231-286, (b) P. 250, 1982.

(5.2) E. O. Brigham, "The Fast Fourier Transform", New York, Printice Hall, PP. 148-165, 1974.

(5.3) R. E. Bogner and A. G. Constantinides, "Introduction to Digital Filtering", New York, Wiley, P. 119, 1975.

(5.4) D. Chulder And A. Durling, "Digital Filtering and Signal processing", St Paul, West Pub. Co., PP. 299-314, 1975.

(5.5) G. D. Bergland " A guided tour of the fast fourier transform", IEEE spectrum, Vol. 6, No. 7, PP. 41-52, July, 1969.

(5.6) A. Puc "Study and measurements of pulse broadening of optical fibers", M. Eng. thesis, Dept. of Elect. Eng., McGill University, PP. 41-46, August, 1980.

(5.7) A. Papoulis, "The Fourier Integral and its Application", New York, McGraw Hill, PP. 227-239, 1963.

(6.1) Andrej Puc, "Study and measurements of pulse broadening of optical fibers", M. Eng. thesis, Dept. of Elect. Eng., McGill Univ., PP. 51-94, August, 1980.

(6.2) Photon Kinetics,"Universal Fiber Optics Analysers Operation Manual", Photon Kinetics, Beaverton, Origon , PP. 3.15-3.16, 1980.

(6.3) Tektronix, "7854 Digital Oscilloscope Operators Manual", Manual number 070-2873-00, PP. 6.1-6.93, January 1980.

(6.4) Rainer Paduch, "Experimental techniques for impulse response measurements of optical fibers", A M. Eng. B report, Dept. of Elect. Eng., McGill University, PP. 97-100, 1980.

(6.5) Tektronix, "Tektronix 7854 Oscilloscope Operators Manual", Manual number 070-2873-00, PP. 6.94-6.137, January 1980.

APPENDIX - A

Impulse Response Program Using the Moment Method

```
c----
c     This program is used to calculate and plot the impulse
c     response using the moment method.
c----
c              FILE NAME=ALgg.sim
        OPEN (UNIT=7, NAME='PLSE.bro', TYPE='OLD')
        OPEN (UNIT=8, NAME='RESULT.sim', TYPE='NEW')
        OPEN (UNIT=9, NAME='PLOT.DAT',TYPE='NEW')
        IMPLICIT REAL (A-Z)
        REAL YR(512),YS(512),MR(6),MS(6),M(6),Y(512),HNW(512),HT(
     1,xx(128),MAXR,MAXS,hnwj
     INTEGER I,J,K,N,JJ,KK,mm,nn
         REAL*8 X1(20),YMU,YMU2,FIBC
         write(8,*)'result.fun'
         DO 29 I=1,20
         READ (7,9) X1(I)
         IF(X1(I).EQ.'XZERO:') READ(7,11)X1(I),DT
         IF(X1(I).EQ.'YZERO:') READ(7,11)X1(I),YMU
         IF(X1(I).EQ.'FIBER#') READ(7,111)FIBC
         IF(X1(I).EQ.'CURVE ')GO TO 32
 29      CONTINUE
C 32      DT=1./128.
 32       WRITE(8,111)FIBC
          write (8,*)dt
     n=512
     mm=4
         MAX=0.
        DO 10 I=1,512
        READ(7,*) Ys(I)
        IF(MAX LT.YS(I))MAXS=YS(I)
  10    CONTINUE
         DO 129 I=1,20
         READ (7,9) X1(I)
         IF(X1(I) EQ.'XZERO:') READ(7,11)X1(I),XINC
         IF(X1(I).EQ.'YZERO:') READ(7,11)X1(I),YMU2
         IF(X1(I).EQ.'CURVE ')GO TO 132
129      CONTINUE
132      q=ymu/ymu2
C         q=1.
     WRITE(8,*)'YMU1=',YMU,'YMU2=',YMU2
         write(8,*)'XINC=',xinc,'Q=',Q
         write(8,*)ys(1),ys(2)
         dt=dt/1.e-9
     MAX=0
         DO 20 I=1,512
        READ(7,*) Yr(I)
        yr(I)=Yr(I)/(q)
 20     IF(MAX.LT.YR(I))MAXR=YR(I)
```

```
cp
      MAXS=MAXS*.05
      MAXR=MAXR*.05
      DO 49 I=1,512
      IF(YS(I).LT.MAXS)YS(I)=0
      IF(YR(I).LT.MAXR)YR(I)=0
   49 CONTINUE
c         do 19 j=1,512
c         y(J)=Yr(J)                   !to be used when the input
c         yr(J)=ys(J)                  !and the output data were
c         ys(j)=y(j)                   !interchanged.
c 19      continue
C     call calc(yr,ys,ar,as,mr,ms,dt,n,ts,tr)
        DO 30 KK=2,6
        JJ=KK
c         MR(KK)=FUNCT(YR,JJ,Ar,tr,dt,n)
c         MS(KK)=FUNCT(YS,JJ,As,ts,dt,n)
        MR(KK)=FSIMP(YR,JJ,AR,TR,DT,N)
        MS(KK)=FSIMP(YS,JJ,AS,TS,DT,N)
        WRITE(8,*)' MS ( ',KK,')  =',Ms(KK),' MR ( ',KK,')  =',Mr
   30   CONTINUE
      write(8,*)'AS=',as,'AR=',ar,'TS=',ts,'TR=',tr
        AH=(AR/AS)
         V=1 /ah
        TC=V*(tr-tS)
        M2=V*(MR(2)-MS(2))
        M3=V*(MR(3)-MS(3))
        M4=V*(MR(4)-MS(4)+6.*(MS(2)**2)-6.*MS(2)*MR(2))
        M5=V*(MR(5)-MS(5)+20.*(MS(3)*MS(2))-10.*(MR(3)*MS(2)+MS(3
     1)
        M6=V*(MR(6)-MS(6)+15.*(M4*M2-MR(4)*MR(2)+MS(4)*MS(2))-30.
     1-MR(2)**3+MS(2)**3)+10.*(M3**2+MS(3)**2+mr(3)**2))
C     if(m4.lt.0)m4=0.
C     m4=abs(m4)
c       AH=AR*V
c        TC=TR*V
c        M2=MR(2)*V
c        M3=MR(3)*V
c        M4=MR(4)*V
c        M5=MR(5)*V
c        M6=MR(6)*V
C     ah=.647
C     tc=.361
C     m2=.464
C     m3=.512
C     m4=.593
C     m5=.719
C     m6=.909
      seg=sqrt(m2)
```

```
c p
       WRITE(8,100)AH,TC,M2,M3,M4,M5,M6
      write(8,*)'segma =',seg
      p=float(n)
       DW=1./(p*DT)
       W=0
       T=-TC
      hnwj=1.0
       ALFA=1.177
       TPI=6.283185
c     bw=(alfa/(tpi*m2))*(1.+(m4/m2**2-3.)*0.05776)*(1.+
c     1(m6/m2**3+30.-15.*m4/(m2**2)-5.*m3**2)*0.003851)
c        call rt(s1,yI,m2,M3,m4,M5,m6)
      bw=1./(5.*sqrt(m2))
       call root(s1,m2,m4,m6)
       WRITE(8,*)'s1=',S1
       WRITE(8,*)'BAND WIDTH',BW
C        s=1./(sqrt(2.)*S1)
         S=SQRT(M2)
         s=s*1.225
c        s=(S**.5)*.75
          WRITE(9,*)'FIBER#'
          WRITE(9,111)FIBC
      do 16 j=1,n
      w=w+dw
      t=t+dt
      x=w*w*m2/2.
c     m2=abs(m2)
      if(hnwj le.0.0)go to 14
       hnw(j)=exp(-x+x*x*(m4/(3.*m2*m2)-1.)/2.-x*x*x*(
      1-m4/m3*m2-m3*m3/(3.*m2*m2*m2)+2.)/6.)
c     +m6/(15.*m2*m2*m2))
      hnwj=hnw(j)
c     ht(j)=ah/(sqrt(m2*tpi))*exp(-t**2/(2.*m2))*(1.+(m3/(12.*m2**1.
c     1))*(12.*t**3/m2**1.5-21.*t**3/m2**1.5-t**5/
c     1m2**2.5)+(1./48.)*(m4/m2**2-3.)*(17.*t**4/
c     1m2**2-57.*t**2/m2+21.-(t/m2**0.5)**6)+(1./120.)*(m5/m2**2.5)*
c     1((t/m2**0.5)**5-10.*t**3/m2**1.5
c     1+15.*t/m2**0.5)+(1./720.)*((m6/m2**3)-15.)*((t**2/m2)**3-15.*
c     1t**4/m2**2+45.*t**2/m2-15.))
c        m2=abs(m2)
CC         s1=sqrt(m2)
CC         s=(S1**.5)*.75
c        WRITE(8,*)'s=',S,'t=',t,'z=',z
 14    z=t/s
       c1=0
       C2=((M2/S**2.)-1.)/2.
       c3=(m3/s**3.)/6.-c1/2.
       c4=(m4/s**4.)/24.-1./8.-c2/2.
       c5=(m5/s**5.)/120.-c3/2.-c1/8.
       c6=(m6/s**6.)/720.-1./48.-c4/2.-c2/8.
```

```
op
        zz=z*z
     zzz=zz*z
     zzzz=zz*zz
     zzzzz=zzzz*z
     zzzzzz=zzz*zzz
      ht(j)=(ah/(s*2.507))*exp(-(t*t)/(s*s*2.))*(1.
     1+c3*(zzz-3.*z))
C     1+c4*(zzzz-6.*zz+3.)+c2*(zz-1.)
C     1+c5*(zzzzz-10.*zzz+15.*z)+c6*(zzzzzz-15.*zzzz+45.*zz-15.)
 16  continue
c
     call plot(hnw)
     call scale(n,mm,xx,kk,ht)
     call plot(xx)
        WRITE(9,*)'FIBER#'
        WRITE(9,91)FIBC
        DO 17 I=1,128
 17     WRITE(9,*)XX(I)
        WRITE(9,*)'END'
        CLOSE (UNIT=9)
c    call plot(xx)
     delta=seconds(t1)
     write(8,*)'DELTA',delta
  100.        FORMAT(//,7(/,' M ',' =',E15.8,/))
 110    FORMAT(A6,A8)
 111    FORMAT('FIBER CODE IS :',A8)
 11     format(A6,E15.5)
 9      FORMAT(A6)
 91  FORMAT(A8)
     stop
     end
C-----------------------------------------------------------------
        REAL FUNCTION FSIMP(Y,JJ,A,tc1,dt,n)
        REAL Y(512),SSS(6),YY(512)
        DO 10 I=1,6
        SSS(I)=0
   10   CONTINUE
        S=0
        SS=S
     simp=0.0
        DO 1 I=1,n
     ti=float(i)
     that1=2*y(i)
     that2=2*ti*y(i)
     simp=simp+that1
     ss=ss+that2
     if(mod(i,2).ne.0)simp=simp+that1
     if(mod(i,2).ne.0)ss=ss+that2
    1   CONTINUE
     a=dt*(simp-that1/2.)/3.
```

```
op
      ss=(ss-that2/2.)/3.
         TC1=SS*DT*dt/(a)
         DO 2 K=1,n
         N1=JJ
      tk=float(k)
         TT=DT*(tK)-TC1
      that3=2.*y(k)*tt**n1
      sss(n1)=sss(n1)+that3
      if(mod(k,2).ne.0)sss(n1)=sss(n1)+that3
    2    CONTINUE
      sss(jj)=(sss(jj)-that3/2.)/3.
         FSIMP=(DT/a)*SSS(JJ)
         RETURN
         END
c-----------------------------------------
      Subroutine root(s,m2,m4,m6)
          implicit real(a-z)
      dimension vr(3),vi(3)
          Integer i,j,k
      vi(1)=0
          vi(2)=vi(1)
      vi(3)=vi(2)
      b=-(30./14.)*m4/m6
      c=(18./7.)*m2/m6
      d=-(6./7.)/m6
      p=(1./3.)*(3*c-b**2)
      q=(1./27.)*(27.*d-9*b*c+2.*b**3)
      r=(p/3.)**3+(q/2.)**2
      if(r.lt.0)go to 1
      go to 2
c    1          fi1=acos(sqrt((((q**2)/4.)/(-p**3)/27.))/3.)
    1 fia=(sqrt((((q**2)/4.)/(-p**3)/27.))/3.)
      fi1=atan(sqrt(1-fia**2)/fia)
      pi=4.*atan(1.)
      do 10 i=1,3
      fi=fi1+120.*(i-1)*pi/180.
      vr(i)=2.*sqrt(-p/3.)*cos(fi)-b/3.
      if(q.gt.0)vr(i)=-vr(I)-2.*b/3.
   10          continue
      go to 9
    2 aa=sqrt(r)-q/2.
      if(aa.lt.0)aa=-(-aa)**(1./3.)
      if(aa.gt.0)aa=aa**(1./3.)
      bb=-sqrt(r)+q/2.
      if(bb.lt.0)bb=-((-bb)**(1./3.0))
      if(bb.gt.0)bb=bb**(1./3.)
      vr(1)=aa+bb-b/3.
      vr(2)=-(aa+bb)/2.-b/3.
      vr(3)=vr(2)
      vi(2)=(sqrt(3.)/2.)*(aa-bb)
```

```
c p
      vi(3)=-vi(2)
    9 do 11 i=1,3
      if(vi(I).gt.0.and.vr(i).eq 0)s=vi(i)/2.
      if(vr(i).gt.0.and.vi(i).eq.0)s=vr(i)
   11            write(8,*)'vr(',i,') =',vr(i),'vi(',i,') =',vi(i)
      s=sqrt(s)
   77            format(/,'vr( ',i2,') =',3x,' vi( ',i2,') =',
     13x,f,//)
      return
      end
c-------------------------------------------------------------
       subroutine rt(s,y,m2,M3,m4,M5,m6)
       implicit real(a-z)
       integer i,j
       x=-1.0
       xx=-1.5
       j=0
 1     ef=f(x,m2,M3,m4,M5,m6)
       eff=f(xx,m2,M3,m4,M5,m6)
       i=0
 3     xn=(x*eff-xx*ef)/(eff-ef)
       efn=f(xn,m2,m4,m6)
       i=i+1
       if(abs(efn).lt.1.e-6)go to 5
       x=xx
       xx=xn
       ef=eff
       eff=efn
       go to 3
 5     j=j+1
       yn=f(xn,m2,M3,m4,M5,m6)
       go to 9
 7     write(8,200)xn,yn,efn
 9     s=sqrt(xn)
       y=yn
200    format(' divergence occured','xn=',f10.5,'yn=',
      1f10.5,'error=',f10.7)
       return
       end
       function f(x,m2,M3,m4,M5,m6)
       implicit real(a-z)
       f1=1-3*x*m2+(5/3)*x**2*m4-(7/6)*x**3*m6
C        F=3*F1/2+(70/3)*M3*M3*X**3-21*M5*M3*X**4
C      1-6*M2*X+(5*M4+15*M2*M2)*X*X-
C     1((35/2)*M2*M4+3.5*M6)*X**3+(21/2)*M2*M6*X**4
C      1-(3/8)*F1-4.5*M2*X+7.5*M4*X*X-
C     1(7/4*M6-17.5*M4*M2)*X**3+26.25*M4*M4*X**4
C      1-77/4*M4*M6*X**5
C         F=9/8-((245/16)*M4+15*M2*M2)*X*X
C      1+(36.25*M2*M2-21*M5*M3+(21/2)*M2*M6)*X**4
```

```
cp
C        F=-(70/3)*M3*X**3  -3*X*M2+(7/6)*X**3*M6
C        F=1-(5/2)*X*X*M4-21*M5*X**4
         F=F1
        return
        end
c-------------------
      subroutine calc(yr1,ys1,ar,as,mr,ms,dt,ii,ts,tr)
      real ys1(512),yr1(512),mr(6),ms(6),ys(1024),yr(1024)
         call scalup(ys,ys1)
         call scalup(yr,yr1)
         n=2*ii
         ii=n
         dt=dt/2.
      ar=yr(1)
      as=ys(1)
      ts=0.5*ys(1)
      tr=0.5*yr(1)
      do 10 i=2,ii
         ti=float(i)
         ar=ar+(yr(i)+yr(i-1))
         as=as+(ys(i)+ys(i-1))
         ts=ts+(ti-0.5)*(ys(i)+ys(i-1))
         tr=tr+(ti-0.5)*(yr(i)+yr(i-1))
 10           continue
      ar=(dt*ar)/2.
      as=(dt*as)/2.
      xr=dt/(2.*ar)
      xs=dt/(2.*as)
      tr=tr*xr*dt
      ts=ts*xs*dt
      do 30 n=2,6
         mr(n)=((0.5*dt-tr)**n)*yr(1)
         ms(n)=((0.5*dt-ts)**n)*ys(1)
         do 20 k=2,ii
            tk=float(k)
            mr(n)=mr(n)+(((tk-0.5)*dt-tr)**n)*(yr(k)+yr(k-1))
            ms(n)=ms(n)+(((tk-0.5)*dt-ts)**n)*(ys(k)+ys(k-1))
 20              continue
         mr(n)=mr(n)*xr
         ms(n)=ms(n)*xs
 30           continue
      return
      end
c-------------------------------------------------------
      subroutine scale(n,mm,xx,kk,rea)
c-------
c     subroutine to scale down the number of points to 64 pts
c     in order they can graphed. The scaling is done
c     by averaging each mm points and store the value as one point
c-------
```

```
op
      dimension rea(512),xx(128)
      kk=n/mm
      do 7 k1=1,kk
      xx(k1)=0
      n1=(k1-1)*mm
      do 9 j1=1,mm
      xx(k1)=xx(k1)+rea(n1+j1)
    9 continue
      xx(k1)=xx(k1)/mm
    7 continue
      return
      end
c-----------------------------------------------------------------------
      subroutine scalup(xx,rea)
c------
c     subroutine to scale up the number of points to 1024 pts
c     in order they can graphed. The scaling is done
c     by averaging each mm points and store the value as one point
c------
      dimension rea(512),xx(1024)
      do 7 k1=2,512
         n1=2*k1
         xx(n1)=(rea(k1)+rea(k1+1))/2.
         xx(n1-1)=rea(k1)
    7    continue
         xx(1)=rea(1)
         xx(2)=(rea(1)+rea(2))/2.
      return
      end
c-----------------------------------------------------------------------
         SUBROUTINE plot(Y)
C THIS SUBROUTINE GIVES A GRAPH OF Y.
         DIMENSION Y(128)
         REAL norm
         INTEGER PLOT(51),HORZ,VERT,PLUS,SPACE,POS,POINT
         DATA HORZ/'.'/,VERT/':'/,PLUS/'+'/,SPACE/' '/,POS/'*'/
         norm=Y(1)
         DO 1 I=1,128
         IF(norm.LT.Y(I))norm=Y(I)
         IF(Y(I).LT.0.0)Y(I)=0.0
    1    CONTINUE
         DO 3 I=1,128
         DO 2 I1=1,51
         II1=I1-1
         PLOT(I1)=SPACE
         IF(MOD(II1,10).EQ.0)PLOT(I1)=VERT
    2    CONTINUE
         II=I-1
         POINT=IFIX(51.5-50.0*Y(129-I)/norm)
         IF(MOD(II,5).NE.0)GO TO 100
```

```
C P
      DO 4 J=1,51
      PLOT(J)=HORZ
      JJ=J-1
      IF(MOD(JJ,10).EQ.0)PLOT(J)=PLUS
    4 CONTINUE
      PLOT(POINT)=POS
      IM=129-I
      WRITE(8,1000)IM,PLOT
      GO TO 101
  100 PLOT(POINT)=POS
      WRITE(8,1001)PLOT
  101 CONTINUE
    3 CONTINUE
      WRITE(8,1002)
      WRITE(8,1003)
 1000 FORMAT(10X,I2,2X,51A1)
 1001 FORMAT(14X,51A1)
 1002 FORMAT(13X,'1.0',7X,'0.8',7X,'0.6',7X,'0.4',7X,'0.2',7X,
 1003 FORMAT('1')
      RETURN
      END
```

```
cp

c        APPENDIX - E

         Impulse Response Program Using FFT (N=256)

c------
c     fft imf
c     this program is to calculate the impulse and friquency
c     response of an input and output data
c     the input data is ys ,and the output data is yr.
c------
      t1=seconds(0 )
      real rea(512),ima(512),rear(512),imar(512),ys(512),yr(512)
      1,array(512),rtf(512),iyr(512),iys(512),ryr(512),mag,t,tt
      1,rys(512),x1r(512),x1i(512)
      1,xx(512),y1(512),y2(512)
      OPEN (UNIT=7,NAME='plseco.br6',TYPE='OLD')
      OPEN (UNIT=8,NAME='res.imf',TYPE='NEW')
         REAL*8 X1(20),YMU,YMU2,FIBC
      n=512
      n1=n/2
c     m=8
c     m1=m-1
      mm=4
      dt=1.0/128.0
      fn1=float(n1)
      dtt=1./((fn1)*dt)
         DO 29 I=1,20
         READ (7,9) X1(I)
         IF(X1(I).EQ.'XZERO:') READ(7,11)X1(I),DT
         IF(X1(I).EQ.'YZERO:') READ(7,11)X1(I),YMU
         IF(X1(I).EQ.'FIBER#') READ(7,111)FIBC
         IF(X1(I).EQ.'CURVE ')GO TO 32
 29      CONTINUE
 32      DT=dt/1.e-9
         fn=float(n)
         dtt=1./((fn)*dt)
         WRITE(8,111)FIBC
      n=512
      mm=8
        DO 10 I=1,512
   10   READ(7,*) Ys(I)
         DO 129 I=1,20
         READ (7,9) X1(I)
         IF(X1(I).EQ.'XZERO:') READ(7,11)X1(I),XINC
         IF(X1(I).EQ.'YZERO:') READ(7,11)X1(I),YMU2
         IF(X1(I).EQ.'CURVE ')GO TO 132
129      CONTINUE
132      q=ymu/ymu2
c         q=1.
C         dt=xinc/1.e-9
         DO 20 I=1,512
        READ(7,*) Yr(I)
 20       yr(i)=yr(i)/(q)
```

```
c p
      do 710 i=1,n
 710  rea(i)=ys(I)
c     call scale(512,2,xx,kk,rea)
c     do 35 i=1,256
c   35        write(8,*)xx(i)
      do 720 i=1,n
 720  ima(i)=yr(i)
c     call scale(512,2,xx,kk,ima)
c     do 30 i=1,256
c   30        write(8,*)xx(i)
c     go to 99
      call fft(n,rea,ima,1.0,dt)
      do 4 j=1,n1-1
      rys(j)=(rea(j)+rea(n-j))/2.
      ryr(j)=(ima(j)+ima(n-j))/2.
      iys(j)=(ima(j)-ima(n-j))/2.
      iyr(j)=-(rea(j)-rea(n-j))/2.
      rear(j)=ryr(j)
      imar(j)=iyr(j)
   4  continue
      rear(n1)=rea(n1)
      imar(n1)=rea(1)
      ryr(n1)=ima(n1)
      iyr(n1)=ima(1)
      do 5 j=1,n1
      mag=rys(j)**2 +iys(j)**2
      t=rys(j)*rear(j)+iys(j)*imar(j)
      tt=iys(j)*rear(j)-rys(j)*imar(j)
      if (mag.eq.0.0)go to 51
      rea(j)=t/mag
      ima(j)=tt/mag
      x1r(j)=rea(j)
      x1i(j)=ima(j)
      array(j)=sqrt(rea(j)**2+ima(j)**2)
   5  continue
      call plot(array)
      call fft(n1,x1r,x1i,-1.0,dtt)
      do 15 j=1,n1
      write(8,*)j,array(j),x1r(j)
      if (x1r(j).lt.0.0)x1r(j)=0.0
   15         continue
      call scale(n1,mm,xx,kk,x1r)
      do 16 k=1,64
   16         write(8,*)(k,xx(k))
      call plot (xx)
      delta=seconds(t1)
      write(8,*)delta
   51         write(6,*)j,mag
 110      FORMAT(A6,A8)
```

```
c p
 111      FORMAT('FIBER CODE IS :',A8)
 11       format(A6,E15.5)
 9        FORMAT(A6)
      stop
      end
c-----------------------------------------
c-----
c     subroutine fft(n,xr,xi,kode,delt)
c     kode is equal 1 for fft and -1 for ifft
c     xr and xi are the input and later the output
c     delt is the incriment of time in fft and the incriment
c     of frequency in ifft.
c-----
      subroutine fft(n,xr,xi,kode,delt)
      dimension xr(512),xi(512)
      real kode,delt
      n1=n
      ir=0
  5   n2=n1/2
      ir=ir+1
      n1=n2
      if(n1.gt.1)go to 5
      pn=6.283185/n
      l=n/2
      ir1=ir-1
      k1=0
      do 120 is=1,ir
 102           do 130 i=1,l
      k=k1+1
      kpl=k+l
      am=kbitr(k1/2**ir1,ir)
      if(am.ne.0)go to 180
      xri=xr(kpl)
      xii=xi(kpl)
 180           arg=am*pn
      c=cos(arg)
      s=-kode*sin(arg)
      xri=c*xr(kpl)-s*xi(kpl)
      xii=c*xi(kpl)+s*xr(kpl)
 19   xr(kpl)=xr(k)-xri
      xi(kpl)=xi(k)-xii
      xr(k)=xr(k)+xri
      xi(k)=xi(k)+xii
 130           k1=k1+1
      k1=k1+l
      if(k1.lt.n)go to 102
      k1=0
      ir1=ir1-1
 120           l=l/2
      do 40 k=1,n
```

```
c
      k1=kbitr(k-1,ir)+1
      if (k1.le.k) go to 40
      xri=xr(k)
      xii=xi(k)
      xr(k)=xr(k1)
      xi(k)=xi(k1)
      xr(k1)=xri
      xi(k1)=xii
   40 continue
      if(delt.eq.1.0)return
      do 50 k=1,n
      xr(k)=delt*xr(k)
      xi(k)=delt*xi(k)
  50          continue
      return
      end
c-------------
      function kbitr(k,ir)
      k1=k
      kbitr=0
      do 200 i=1,ir
      k2=k1/2
      kbitr=kbitr*2+(k1-2*k2)
  200         k1=k2
      return
      end
c------------------------------------------------------------
      subroutine scale(n,mm,xx,kk,rea)
c------
c     subroutine to scale down the number of points to 64 pts
c     in order they can graphed. The scaling is done
c     by averaging each mm points and store the value as one point
c------
      dimension rea(512),xx(256)
      kk=n/mm
      do 7 k1=1,kk
      xx(k1)=0
      n1=(k1-1)*mm
      do 9 j1=1,mm
      xx(k1)=xx(k1)+rea(n1+j1)
    9 continue
      xx(k1)=xx(k1)/mm
    7 continue
      return
      end
c-----------------------------------------------------------------
      SUBROUTINE PLOT(Y)
C THIS SUBROUTINE GIVES A GRAPH OF Y.
         DIMENSION Y(128)
         REAL norm
```

```
op
      INTEGER PLOT(51),HORZ,VERT,PLUS,SPACE,POS,POINT
      DATA HORZ/'.'/,VERT/':'/,PLUS/'+'/,SPACE/' '/,POS/'*'/
      norm=Y(1)
      DO 1 I=1,128
      IF(norm.LT.Y(I))norm=Y(I)
      IF(Y(I).LT.0.0)Y(I)=0.0
    1 CONTINUE
      DO 3 I=1,128
      DO 2 I1=1,51
      II1=I1-1
      PLOT(I1)=SPACE
      IF(MOD(II1,10).EQ.0)PLOT(I1)=VERT
    2 CONTINUE
      II=I-1
      POINT=IFIX(51.5-50.0*Y(129-I)/norm)
      IF(MOD(II,5).NE.0)GO TO 100
      DO 4 J=1,51
      PLOT(J)=HORZ
      JJ=J-1
      IF(MOD(JJ,10).EQ.0)PLOT(J)=PLUS
    4 CONTINUE
      PLOT(POINT)=POS
      IM=129-I
      WRITE(8,1000)IM,PLOT
      GO TO 101
  100 PLOT(POINT)=POS
      WRITE(8,1001)PLOT
  101 CONTINUE
    3 CONTINUE
      WRITE(8,1002)
      WRITE(8,1003)
 1000 FORMAT(10X,I2,2X,51A1)
 1001 FORMAT(14X,51A1)
 1002 FORMAT(13X,'1.0',7X,'0.8',7X,'0.6',7X,'0.4',7X,'0.2',7X,
 1003 FORMAT('1')
      RETURN
      END
```

APPENDIX-C

Impulse Response Program Using FFT (N=512)

```
c-----
c     file name is fft.imr . This program to calculate the frequency
c        and the inplse response using fft.
c-----
      t1=seconds(0.)
      real rea(512),ima(512),rear(512),imar(512),ys(512),yr(512)
      1,array(512),xx(512),y1(512),y2(512)
      OPEN (UNIT=7,NAME='PLSE.BRo',TYPE='OLD')
      OPEN (UNIT=8,NAME='RES.IMr',TYPE='NEW')
         REAL*8 X1(20),YMU,YMU2,FIBC
      n=512
         n1=n/2
      mm1=4
      fn=float(n)
         DO 29 I=1,20
         READ (7,9) X1(I)
         IF(X1(I).EQ.'XZERO:') READ(7,11)X1(I),DT
         IF(X1(I).EQ.'YZERO:') READ(7,11)X1(I),YMU
         IF(X1(I).EQ.'FIBER#') READ(7,111)FIBC
         IF(X1(I).EQ.'CURVE ')GO TO 32
 29      CONTINUE
 32      DT=dt/1.e-9
         dtt=1./((fn)*dt)
         WRITE(8,111)FIBC
      n=512
      mm=8
        DO 10 I=1,512
   10   READ(7,*) Ys(I)
         DO 129 I=1,20
         READ (7,9) X1(I)
         IF(X1(I).EQ.'XZERO:') READ(7,11)X1(I),XINC
         IF(X1(I).EQ.'YZERO:') READ(7,11)X1(I),YMU2
         IF(X1(I).EQ.'CURVE ')GO TO 132
129      CONTINUE
132      g=ymu/ymu2
         DO 20 I=1,512
        READ(7,*) Yr(I)
        yr(i)=yr(i)/(g)
 20     rea(i)=ys(i)
      do 2 j=1,n
      array(j)=0.0
      ima(j)=0.0
    2 continue
c        do 19 j=1,512
c        y(J)=Yr(J)                !to be used when the input
c        yr(J)=ys(J)               !and the output data were
c        ys(j)=y(j)                !interchanged.
c 19     continue
```

```
      call fft(n,rea,ima,1.0,dt)
      do 4 j=1,n
      rear(j)=rea(j)
      imar(j)=ima(j)
    4 continue
      do 1 j=1,n
      ima(j)=0.0
      rea(j)=yr(j)
    1 continue
      call fft(n,rea,ima,1.0,dt)
         mag=(rear(1)**2 +imar(1)**2)*10
      tmag=mag/10.
         t=rea(1)*rear(1)+ima(1)*imar(1)
         tt=ima(1)*rear(1)-rea(1)*imar(1)
         rea(1)=t/tmag
         ima(1)=tt/tmag
         k=1
      do 5 j=2,n
      mag=(rear(j)**2 +imar(j)**2)*10
      tmag=mag/10.
      t=rea(j)*rear(j)+ima(j)*imar(j)
      tt=ima(j)*rear(j)-rea(j)*imar(j)
      if (mag.eq.0.0)go to 6
      rea(j)=t/tmag
      ima(j)=tt/tmag
         k=k+1
         y1(k)=rea(j)
         y2(k)=ima(j)
         go to 7
6        rea(J)=0
         ima(J)=0
7        array(J)=sqrt(rea(J)**2+ima(J)**2)
5        continue
         array(1)=sqrt(rea(1)**2+ima(1)**2)
      call plot(array,DT)
      call fft(n,rea,ima,-1.0,dtt)
      do 15 j=1,n
 15             if (rea(J).lt.0.0)rea(J)=0.0
        OPEN (UNIT=9,NAME='PLOT1.DAT',TYPE='NEW')
        OPEN (UNIT=11,NAME='PLOT.DAT',TYPE='OLD')
        READ(11,9)ST
        READ(11,9)FIBC
        DO 57 I=1,128
57      READ (11,*)Y1(I)
        READ(11,9)END
        WRITE(9,9)ST
        WRITE(9,9)FIBC
        WRITE(9,*)'ALDAT'
        DO 58 I=1,128
58      WRITE(9,*)Y1(I)
```

```
          WRITE(9,9)END
   19     WRITE(9,*)'FIBER#'
          WRITE(9,111)FIBC
      call scale(n,mm1,xx,kk,REA)
          WRITE(9,*)'FTDAT'
          DO 17 I=1,128
  17      WRITE(9,*)XX(I)
          CLOSE (UNIT=9)
      delta=seconds(t1)
      write(8,*)'DELTA=',delta
 110      FORMAT(A6,A8)
 111      FORMAT('FIBER CODE IS  ',A8)
  11      format(A6,E15.5)
   9      FORMAT(A6)
      stop
      end
c-------------------------------------------------------
c-----
c     subroutine fft(n,m,xr,xi,kode,delt)
c     kode is equal 1 for fft and -1 for ifft
c     xr and xi are the input and later the output
c     delt is the incriment of time in fft and the incriment
c     of frequency in ifft.
c-----
      subroutine fft(n,xr,xi,kode,delt)
      dimension xr(512),xi(512)
      real kode,delt
      n1=n
      ir=0
   5  n2=n1/2
      ir=ir+1
      n1=n2
      if(n1.gt.1)go to 5
      pn=6.283185/n
      l=n/2
      ir1=ir-1
      k1=0
      do 130 is=1,ir
 102          do 130 i=1,l
      k=k1+1
      kpl=k+l
      am=kbitr(k1/2**ir1,ir)
      if(am.ne.0)go to 180
      xr1=xr(kpl)
      xi1=xi(kpl)
 180          arg=am*pn
      c=cos(arg)
      s=-kode*sin(arg)
      xr1=c*xr(kpl)-s*xi(kpl)
      xi1=c*xi(kpl)+s*xr(kpl)
```

```
c p
19   xr(kpl)=xr(k)-xri
     xi(kpl)=xi(k)-xii
     xr(k)=xr(k)+xri
     xi(k)=xi(k)+xii
 100        k1=k1+1
     k1=k1+1
     if(k1.lt.n)go to 102
     k1=0
     ir1=ir1-1
 120        l=l/2
     do 40 k=1,n
     k1=kbitr(k-1,ir)+1
     if (k1.le k) go to 40
     xri=xr(k)
     xii=xi(k)
     xr(k)=xr(k1)
     xi(k)=xi(k1)
     xr(k1)=xri
     xi(k1)=xii
 40 continue
     if(delt.eq.1.0)return
     do 50 k=1,n
     xr(k)=delt*xr(k)
     xi(k)=delt*xi(k)
 50         continue
     return
     end
c-------------
     function kbitr(k,ir)
     k1=k
     kbitr=0
     do 200 i=1,ir
     k2=k1/2
     kbitr=kbitr*2+(k1-2*k2)
 200        k1=k2
     return
     end
c--------------------------------------------------------------
     subroutine scale(n,mm,xx,kk,rea)
c------
c    subroutine to scale down the number of points to 64 pts
c    in order they can graphed. The scaling is done
c    by averaging each mm points and store the value as one point
c------
     dimension rea(512),xx(128)
     kk=n/mm
     do 7 k1=1,kk
     xx(k1)=0
     n1=(k1-1)*mm
     do 9 i1=1,mm
```

```
cc
      xx(k1)=xx(k1)+rea(n1+j1)
    9 continue
      xx(k1)=xx(k1)/mm
    7 continue
      return
      end
c----------------------------------------------------------------------
      SUBROUTINE plot(ARRAY,DT)
c           THIS SUBROUTINE GIVES A GRAPH OF THE ARRAY.
          DIMENSION ARRAY(64)
          REAL MAX,MAXB,MAXC
          INTEGER PLOT(51),HORZ,VERT,PLUS,SPACE,POS,POINT,KK
          DATA HORZ/'-'/,VERT/'!'/,PLUS/'+'/,SPACE/' '/,POS/'*'/
          MAX=ARRAY(1)
      KK=0
          DO 1 I=1,64
          IF(MAX.LT.ARRAY(I))MAX=ARRAY(I)
          IF(ARRAY(I).LT.0.0)ARRAY(I)=0.0
      KK=KK+1
      MAXB=MAX/SQRT(2.)
      MAXC=MAX/2.
      V1=KK/DT
      IF(ARRAY(I).LE.MAXC)GO TO 1
      IF(ARRAY(I).LE.MAXB)WRITE(8,*)'B.W=',V1
    1     CONTINUE
          DO 3 I=1,64
          DO 2 I1=1,51
          II1=I1-1
          PLOT(I1)=SPACE
          IF(MOD(II1,10).EQ.0)PLOT(I1)=VERT
    2     CONTINUE
          II=I-1
          POINT=IFIX(51.5-50.0*ARRAY(65-I)/MAX)
          IF(MOD(II,5).NE.0)GO TO 100
          DO 4 J=1,51
          PLOT(J)=HORZ
          JJ=J-1
          IF(MOD(JJ,10).EQ.0)PLOT(J)=PLUS
    4     CONTINUE
          PLOT(POINT)=POS
          IM=65-I
          WRITE(8,1000)IM,PLOT
          GO TO 101
  100 PLOT(POINT)=POS
      WRITE(8,1001)PLOT
  101          CONTINUE
    3     CONTINUE
          WRITE(8,1002)
          WRITE(8,1003)
 1000     FORMAT(10X,I2,2X,51A1)
 1001     FORMAT(14X,51A1)
 1002     FORMAT(13X,'1.0',7X,'0.8',7X,'0.6',7X,'0.4',7X,'0.2',7X,'0.0')
 1003     FORMAT('1')
      RETURN
      END
```

```
c p
c p
c --   APPENDIX-D

       Impulse Response Program Using the 7854 Tektronix Oscilloscope
c --
c      this text is stored in the computer under file name "mome.txt".
c      this is the program to calculate the moments and the impise
c      response of the fiber under test using the 7854 tektronix
c      oscilloscope.
C      0CNS IS USED FOR THE ATTENUATION OR THE ZERO-MOMENT
C      1CNS IS USED FOR THE FIRST MOMENT OR THE CENTRAL TIME DELAY
C      12CNS IS USED FOR THE SECOND MOMENT
C      13CNS IS USED FOR THE THIRD MOMENT
C      14CNS IS USED FOR THE FOURTH MOMENT
C      15CNS IS USED FOR THE FIFTH MOMENT
C      AND 16CNS IS USED FOR THE SIXTH MOMENT.
c      s(t) is the input and stored in 3 WFM
c      r(t) is the output and stored in 1 WFM
c      T is the time function and stored in 2 WFM
c-------------
c              0 CNS ---> AH  20 CNS ---> AS  27 CNS ---> M3R
c      1 CNS ---> TC  21 CNS ---> AR  28 CNS ---> M4S
c      2 CNS ---> M2  22 CNS ---> TS  29 CNS ---> M4R
c      3 CNS ---> M3  23 CNS ---> TR  30 CNS ---> M5S
c      4 CNS ---> M4  24 CNS ---> M2S 31 CNS ---> M5R
c      5 CNS ---> M5  25 CNS ---> M2R 32 CNS ---> M6S
c      6 CNS ---> M6  26 CNS ---> M3S 33 CNS ---> M6R
c-----------------------
c --   30 cns is the third order, 31 cns is the fourth
c --   order, 29 cns is the fifth order, and the sixth
c --   order impulse response is stored in 32 cns
C------------------------------------
       1 WFM AREA 2 0 >CNS 3 WFM AREA NEXT
       2 1 >CNS 2 0 CNS / 0 >CNS NEXT
       0 WFM 0 * 1 + INTG 2 >WFM NEXT
       1 WFM * AREA 2 0 CNS / 2 2 >CNS NEXT
       2 WFM 3 WFM * AREA 2 1 CNS / NEXT
       2 3 >CNS 2 2 CNS - NEXT
       2 CNS / 1 >CNS NEXT
       2 2 CNS 1 0 >CNS 4 LBL GSB NEXT
       2 0 CNS 4 5 >CNS 2 4 ENTER 4 6 >CNS NEXT
       5 LBL GSB 3 WFM 0 >WFM 1 WFM 3 NEXT
       >WFM 0 WFM 1 >WFM 2 3 CNS 1 0 >CNS NEXT
       4 LBL GSB NEXT
       2 1 CNS 4 5 >CNS 2 5 ENTER 4 6 >CNS NEXT
       7 LBL GSB 2 5 CNS 2 4 CNS - 1 2 >CNS NEXT
       0 CNS / 1 2 >CNS NEXT
       2 7 CNS 2 6 CNS - NEXT
       0 CNS / 1 3 >CNS NEXT
       2 9 CNS 2 8 NEXT
       CNS - 2 4 CNS ENTER * 6 * + 2 4 CNS NEXT
       3 5 CNS * 6 * - NEXT
       0 CNS / 1 4 >CNS NEXT
```

```
3 1 CNS 3 0 CNS - 2 6 CNS 2 4 CNS * 2 6 NEXT
* + 2 7 CNS 2 4 CNS * 1 0 * - 2 6 CNS NEXT
2 5 CNS * 1 0 * - NEXT
0 CNS / 1 5 >CNS NEXT
3 3 CNS 3 2 NEXT
CNS - 1 4 CNS 1 2 CNS * 1 5 * + 2 9 NEXT
CNS 2 5 CNS * 1 5 * - 2 8 CNS 2 4 CNS NEXT
* 1 5 * + 1 2 CNS NEXT
ENTER * 1 2 CNS * 3 0 * - 2 5 NEXT
CNS ENTER * 2 5 CNS * 3 0 * + NEXT
2 4 CNS ENTER * 2 4 CNS * 3 0 * - NEXT
1 3 CNS ENTER * 1 0 * + 2 7 CNS ENTER NEXT
* 1 0 * - 2 6 CNS ENTER * 1 0 * + NEXT
0 CNS / 1 6 >CNS NEXT
STOP NEXT
0 WFM STORED NEXT
0 ENTER 4 0 >CNS 4 1 >CNS NEXT
0 CNS 9 >CNS NEXT
1 CNS CHS 0 >CNS NEXT
1 2 CNS SQRT 1 >CNS NEXT
LNK 0 0 NEXT
0 CNS HSCL 1 0 * P/W / + 0 >CNS NEXT
0 CNS 1 CNS / ENTER * 2 >CNS NEXT
0 CNS 1 CNS / * NEXT
2 >CNS 2 CNS NEXT
2 CNS * 4 >CNS NEXT
2 CNS 2 CNS * 5 >CNS 4 CNS NEXT
2 CNS * 6 >CNS NEXT
2 CNS CHS 2 / EXP 9 CNS * NEXT
7   5 0 6 / 1 CNS / 1 1 >CNS NEXT
1 3 CNS 1 CNS / 1 CNS / 1 CNS / NEXT
6 / 3 3 >CNS NEXT
1 4 CNS 1 CNS / 1 CNS / 1 CNS / NEXT
1 CNS / 3 - 2 4 / 2 4 >CNS NEXT
1 5 CNS 1 CNS / 1 CNS / 1 CNS / NEXT
1 CNS / 1 CNS / 1 2 0 / 2 3 CNS NEXT
2 / - 2 5 >CNS NEXT
1 6 CNS 1 CNS / 1 CNS / 1 CNS / NEXT
1 CNS / 1 CNS / 1 CNS / 1 5 - 7 2 0 / NEXT
2 4 CNS 2 / - 2 6 >CNS NEXT
3 CNS NEXT
3 CNS 2 CNS / 3 * - 2 3 CNS * 1 + 1 1 NEXT
CNS * 2 0 >CNS NEXT
4 CNS NEXT
2 CNS 6 * - 3 + 2 4 CNS * 1 + NEXT
1 1 CNS * 3 0 CNS + 3 1 >CNS NEXT
5 CNS 3 CNS 1 0 * - 1 CNS 1 5 * + NEXT
2 5 CNS * 1 + 1 1 CNS * 3 1 CNS + NEXT
2 9 >CNS NEXT
6 CNS 4 CNS 1 5 * - 2 CNS 4 5 * NEXT
```

```
+ 1 5 - 2 6 CNS * 1 1 CNS * 2 9 CNS + NEXT
? 2 >CNS NEXT
? 2 CNS NEXT
4 1 >CNS 4 0 CNS >PNT NEXT
1 0 CNS 1 + 4 0 >CNS NEXT
F/W IFX=Y STOP NEXT
0 LBL GOTO NEXT
LNN 0 4 NEXT
0 WFM 0 * 1 + INTG 2 >WFM NEXT
1 0 CNS HPRGT CRS1 NEXT
HSCL 1 0 * 1 0 CNS >HCRD - NEXT
1 0 HSCL * >HCRD VCRD X<>Y CLX NEXT
X<>Y / CHS ENTER 1 0 CNS * 0 >PNT NEXT
0 >HCRD 0 ENTER 1 0 CNS ITRP 0 WFM NEXT
2 >WFM RTN NEXT
LNN 0 5 NEXT
0 WFM ENTER * 1 WFM * AREA 4 5 CNS NEXT
/ 4 6 CNS >CNS 2 WFM 0 WFM * NEXT
AREA 4 5 CNS / 4 6 CNS 2 + >CNS NEXT
0 WFM 2 WFM * AREA 4 5 CNS / 4 6 CNS NEXT
4 + >CNS 0 WFM 2 WFM * AREA 4 5 CNS NEXT
/ 4 6 CNS 6 + >CNS 0 WFM 2 WFM * NEXT
AREA 4 5 CNS / 4 6 CNS 8 + >CNS NEXT
RTN NEXT
```

For saving the waveforms on the computer disc the following procedure have to be followed:

(1) The waveform has to be stored on the Tektronix 7854 Oscilloscope on 0WFM memory space.
(2) The Oscilloscope should be connected with the computer (through the IEEE-Data Bus on the back of the oscilloscope).
(3) The RT11/23 computer should be running on RT11 operating system (make sure it is not running on TSX).
(4) Run a program called "GPUTIL " on the computer (this program will communicate, arrange and store data received from the oscilloscope.
(5) If the oscilloscope is jammed and fails to respond to the computer use another program called "GUSC" this program is used to clear the IEEE Bus of the oscilloscope.
(6) The data files, used for storing a wavefrom in the computer, were given the following names: plse.br1, plse.br2, plse.br3,...... etc. It was not possible to use either "GPUTIL", or "GUSC" to send a waveform from the RT11/23 computer to the Tektronix 7854 Oscilloscope
(7) In order to send and plot a waveform data on the oscilloscope, the waveform file should be copied and renamed "plse.bro".
(8) A program called "DAPLOT" is used to arrange the data points in a format readable by the Tektronix oscilloscope. For details check Appendix E.
(9) Each of the following files, "SCOP1.DAT", "SCOP2.DAT", "SCOP3.DAT "SCOP4.DAT" and "SCOP5.DAT" (created by the "DAPLOT" program) is transfered from the computer to the oscilloscope seperately (Use the program called "GPUTIL" to send a program to the oscilloscope).
(10) Each of the previous five programs is run on the oscilloscope to plot 100 data points. The last file will plot 112 data points.

APPENDIX - E

Program to Plot the Data Using the 7854 Tektronix Oscilloscope

```
c
c----
c This file is called daplot.scp it can be used to arrnge
c a 512 points so that it can be used to plot a waveform
c on the 7854 tektronix oscilloscope.
c 5 files are created by the following program.
c the first four each to plot 100 points and
c the last one is to plot 112 points.
c These files should be transfered and run on the
c oscilloscope in the same order.
c----
      OPEN (UNIT=7, NAME='FLSE.BRO',TYPE='OLD')
      OPEN (UNIT=8, NAME='SCOP1.DAT',TYPE='NEW')
      OPEN (UNIT=9, NAME='SCOP2.DAT',TYPE='NEW')
      OPEN (UNIT=10, NAME='SCOP3.DAT',TYPE='NEW')
      OPEN (UNIT=11, NAME='SCOP4.DAT',TYPE='NEW')
      OPEN (UNIT=12, NAME='SCOP5.DAT',TYPE='NEW')
      implicit real (a-z)
      real plot1(512),plot2(512)
      REAL*8 X1(20),a1,a2,a3,a4,a5,a6,a7
c      write(8,*)'result.fun'
      integer i,j,k,n
      n=100
      write(8,21)
      DO 29 I=1,20
      READ (7,9) X1(I)
      IF(X1(I).EQ.' CURVE')GO TO 32
29    CONTINUE
32    do 1 i=1,n
      read(7,19)a1,a2,a3,a4,a5
1     write(8,20)a1,a2,a3,a4,a5
      write(9,22)
      do 2 i=1,n
      read(7,19)a1,a2,a3,a4,a5
2     write(9,20)a1,a2,a3,a4,a5
      write(10,22)
      do 3 i=1,n
      read(7,19)a1,a2,a3,a4,a5
3     write(10,20)a1,a2,a3,a4,a5
      write(11,22)
      do 4 i=1,n
      read(7,19)a1,a2,a3,a4,a5
4     write(11,20)a1,a2,a3,a4,a5
      write(12,22)
      do 5 i=1,112
      read(7,19)a1,a2,a3,a4,a5
5     write(12,20)a1,a2,a3,a4,a5
19    format(a1,a1,a1,a1,a1,a1,a1)
```

```
 20     format(a1,' ',a1,' ',a1,' ',a1,' ',a1,
       1' rt  next ')
 21     format('
       10',/,'WFM ',/,'vscl 4 1 >ons next',/,
       1'1 . >vscl >hscl next',/,
       1'0 ent 4 0 >ons 0 ent 4 1 >ons next',/,
       1'lnn 0 0 next',/,
       1'4 1 ons ent 4 0 ons >pnt next',/,
       1'4 0 ons 1 + 4 0 >ons next',/,
       1'p/w ifx=y stop next' ,/,
       1'4 0 ons 9 + gsb next',/,
       1'ent 4 1 >ons next',/,
       1'0 lbl goto next',/)
 9      FORMAT(A7)
 22     format(
       1'0 ent 4 3 >ons next',/,
       1'lnn 0 0 next',/,
       1'4 1 ons ent 4 0 ons >pnt next',/,
       1'4 0 ons 1 + 4 0 >ons next',/,
       1'p/w ifx=y stop next' ,/,
       1'4 3 ons 1 + 4 3 >ons next',/,
       1'1 0 0 ifx=y stop next' ,/,
       1'4 3 ons 7 + gsb ent 4 1 >ons next',/,
       1'0 lbl goto next',/)
        stop
        end
```

APPENDIX F

Improvement of Accuracy of the Formula for h(t)

In order to improve the accuracy of the general formula for h(t), a scale factor T should be introduced as follows

$\sigma = T\sigma$

where T is a scale factor, to be determined later on.

The general equation for h(t) can be rewritten as

$$h(t) = A_h/(T\sigma\sqrt{2\pi})\ e^{-t^2/2T^2\sigma^2}\ [1 + \sum_{1}^{6} C_n\ H_n\ (t/T\sigma)] \quad \text{------}\ (F.1)$$

Now let $1/(T\sigma\sqrt{2}\ ) = \alpha$

The scale factor T can be found by maximizing the first term of the series with respect to α

Let

$$X_0 = \int_{-\infty}^{\infty} A_h\ \alpha\ e^{-\alpha^2 t^2}\ h(t)dt \quad \text{-------------}\ (F.2)$$

and set $dX_0/d\alpha = 0$

$$\int_{-\infty}^{\infty} (-1)^n[(2n + 1)/n!]\alpha^{2n}t^{2n}h(t)\ dt \ = 0$$

or

$$\sum_{n=0}^{\infty} (-1)^n\ [(2n + 1)/n!]\ \alpha^{2n}\ M_{2n} \ = 0 \quad \text{---------------}\ (F.3)$$

By putting n = 0, 1, 2, 3 in the previous equation, α and hence T can be evaluated. Equation (F.3) gives

$$1\ -\ 3\ \alpha^2\ M_2 + (5/2)\ \alpha^4\ M_4\ -\ (7/6)\ \alpha^6\ M_6 = 0 \quad \text{-------}\ (F.4)$$

α can be found by solving the above cubic equation.

As an example, let us take the previous case of the square pulse. Substituting the values M_2, M_4, and M_6 for the square pulse in (F.4) we get α = 1.178 and T = 1.039

In Table F.1 a comparison between T=1 and T=1.039 and their least square errors was made.

t	T=1 $\epsilon(t)$	T=1.039 $\epsilon(t)$
0	0.000517	0.00078
0.2	0.01165	0.0032
0.4	0.145	0.0068
0.6	0.322	0.00005
0.8	0.2897	0.062
1.0	0.123	0.312
1.2	0.0212	0.032
1.4	0.000328	0.0012

Table F.1 Comparison of the error function with and without scaling

Another example can be considered as an impulse response is the $\cos^4 t$, which can be written as

$$\cos^4 t = (1/8)(3 + 4\cos 2t + \cos 4t)$$

and, taking its moments, we get

$$M_0 = 1.178$$

$$M_2 = (2\pi^3 - 15\pi)/(64 M_0)$$

$$M_4 = (0.009932)/M_0$$

$$M_6 = 0.2537$$

Using the same procedure the scale factor T can be evaluated and it was found to be 1.503. As it is shown in Fig.F.2 the approximation is good enough when T = 1.503 and it is much better than the square pulse case. Table F.2 shows two different values for the least square error for T=1 and T = 1.503

t radians	T=1 $\epsilon(t)$	T=1.503 $\epsilon(t)$
0	3.296	0.000001
0.2	0.3736	0.00004
0.4	1.57	0.00038
0.6	2.11	0.00088
0.8	0.152	0.00074
1.0	0.111	0.00009
1.2	0.103	0.00022
1.4	0.00852	0.0009

Table F.2 Comparison of the error function with and without scaling

The approximate function for h(t) is plotted in Fig.F.1 for different values of T. The optimum value of T was found at T=1.5. The exact function and its approximation using T=1.503 is plotted in Fig.F.2.

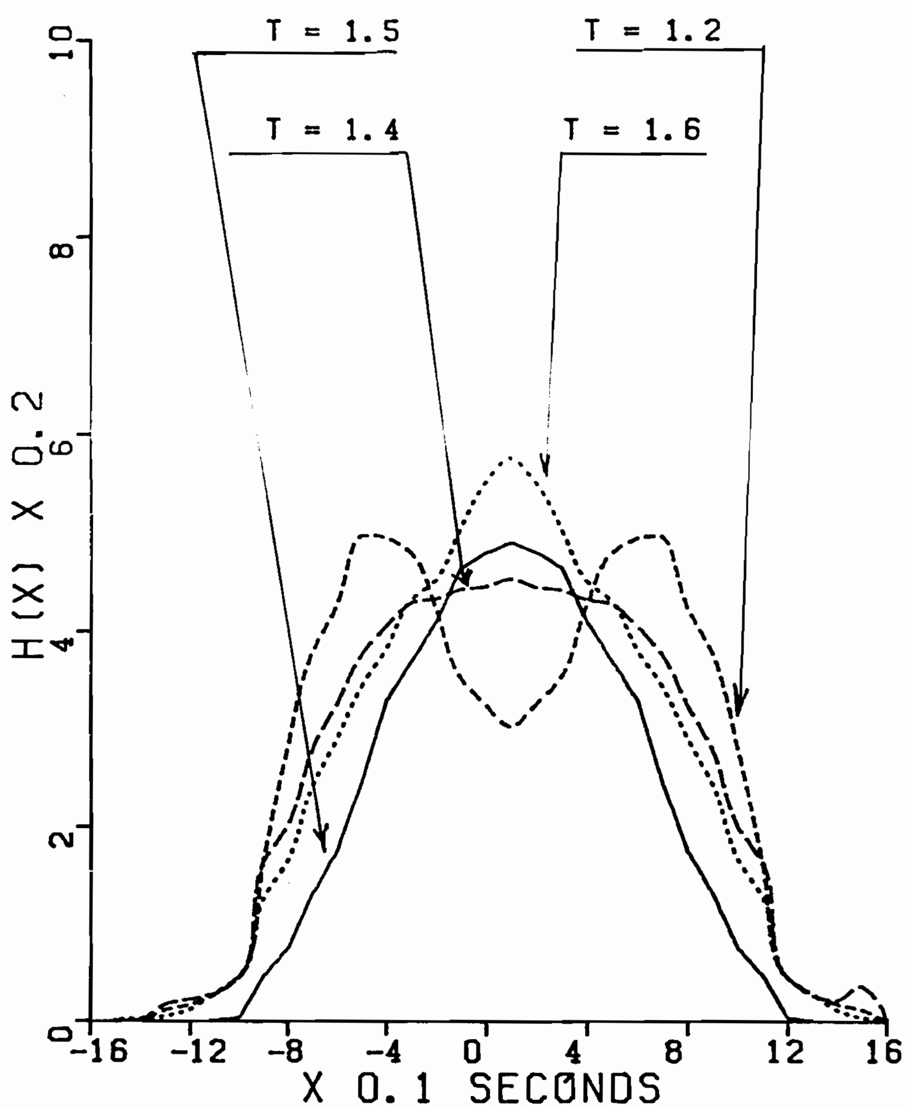

Fig.F.1 Representation of $\cos^4 t$ *by its moments for different values of T*

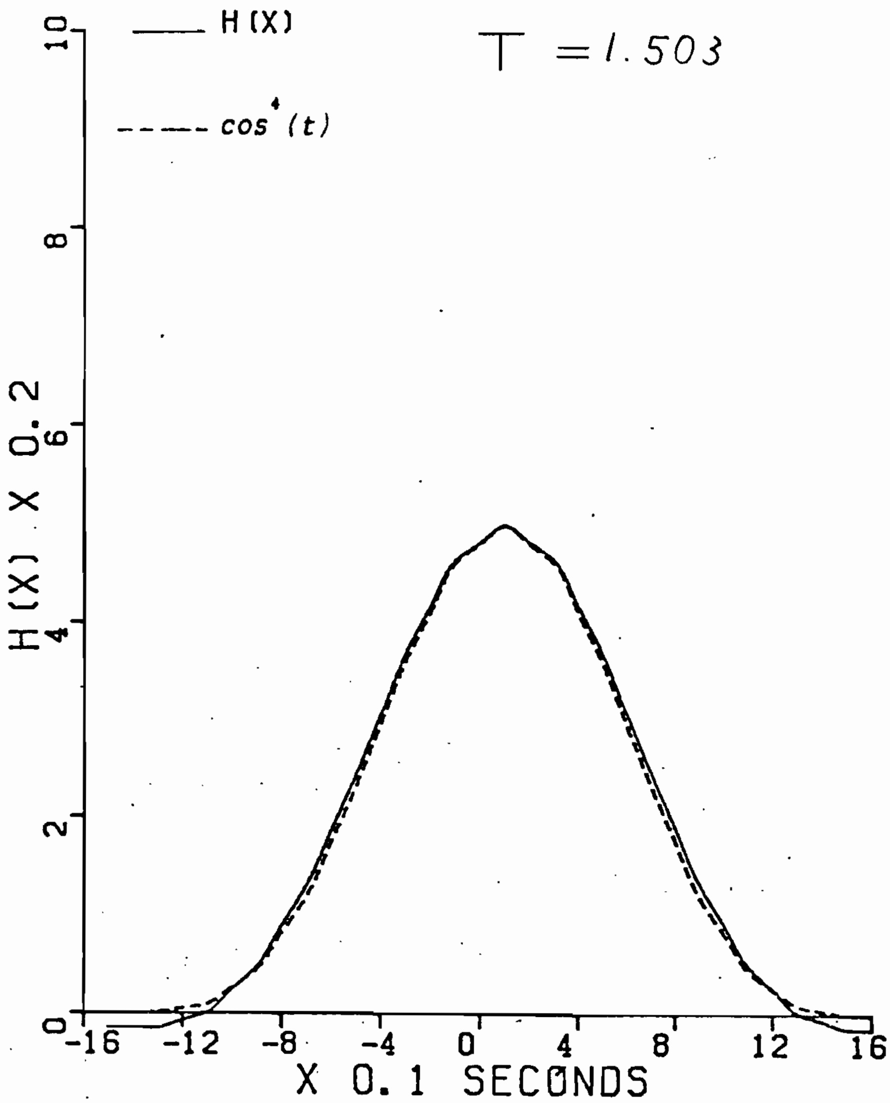

Fig.F.2 Representation of $\cos^4 t$ *and its approximation using the moments*

APPENDIX G

The Relation Between the Moments and the Frequency Response

$$H(\omega) = \int_{-\infty}^{+\infty} h(t)\ \exp(-j\omega t)dt \quad \text{--------------------} \quad (G-1)$$

$$= \exp(-j\omega\tau) \int_{-\infty}^{+\infty} h(t)\ \exp[-j\omega(t-\tau)]dt \quad \text{---------} \quad (G-2)$$

where $\tau = M_1$ the central delay time

$$\exp[-j\omega(t-\tau)] = [\ 1-j\omega(t-\tau) - \omega^2(t-\tau)^2/2! + j\omega^3(t-\tau)^3/3! +$$

$$+ \ldots\ldots\ldots\ldots + (-j)^n \omega^n (t-\tau)^n/n!] \quad \text{-----} \quad (G-3)$$

From equations (G-3) and (G-2) we get

$$H(\omega) = \exp(-j\omega\tau)A_H[1 - \omega M_2/2! + j\omega M_3/3! + \ldots + (j) M_n/n!] \quad \text{---} \quad (G-4)$$

Let

$$U = [- \omega^2 M_2/2! + j\omega^3 M_3/3! + \ldots\ldots + (j)^n \omega^n M_n/n!] \quad \text{--------} \quad (G-5)$$

Subatituting equation (G-5) into equation (G-4) we get

$$H(\omega) = \exp(-j\omega\tau)A_H[1 + U] \quad \text{------------------------} \quad (G-6)$$

Provided that $H(\omega)$ is maximum at $\omega=0$, therefore $|U| < 1$, hence the following expression is valid

$$Ln(1 + U) = [U - U^2/2 + U^3/3 + U^4/4 + \ldots\ldots\ldots\ ] \quad \text{--------} \quad (G-7)$$

or

$$(1 + U) = \exp[\ U - U^2/2 + U^3/3 + U^4/4 + \ldots\ldots] \quad \text{----------} \quad (G-8)$$

From equations (G-5), (G-6) and (G-8) we get

$$H(\omega) = A_H \exp[-j\omega M_1 - \omega^2 \sigma^2/2 + j\omega^3 M_3/6 + \omega^4 (M_4 - 3\sigma^4)/24$$

$$- j\omega^5 (M_5 - 10 M_3\sigma^2)/120 - \omega^6 (M_6 - 15 M_4\sigma^2 - 10 M_3^2 + 30\sigma^6)/720$$

$$+ \ldots\ldots] \quad \text{----------------} \quad (G-9)$$

Equation (G-9) can be written in terms of the input and output moments to give

$$H_s(\omega) = A_s \exp[-j\omega M_{1s} - \omega^2\sigma_s^2/2 + j\omega^3 M_{3s}/6 + \omega^4(M_{4s} - 3\sigma_s^4)/24$$

$$- j\omega^5(M_{5s} - 10\, M_{3s}\sigma_s^2)/120 - \omega^6(M_{6s} - 15\, M_{4s}\sigma_s^2 - 10\, M_{3s}^2 + 30\sigma_s^6)/720$$

$$+ \ldots\ldots\ldots] \qquad \text{----------------} \quad (G\text{-}10)$$

and

$$H_r(\omega) = A_r \exp[-j\omega M_{1r} - \omega^2\sigma_r^2/2 + j\omega^3 M_{3r}/6 + \omega^4(M_{4r} - 3\sigma_r^4)/24$$

$$- j\omega^5(M_{5r} - 10\, M_{3r}\sigma_r^2)/120 - \omega^6(M_{6r} - 15\, M_{4r}\sigma_r^2 - 10\, M_{3r}^2 + 30\sigma_r^6)/720$$

$$+ \ldots\ldots\ldots] \qquad \text{----------------} \quad (G\text{-}11)$$

Using $H(\omega) = H_r(\omega)/H_s(\omega)$ and equate terms we get

$A_H = A_r/A_s$ = area of the input $y_s(t)$/area of the output $y_r(t)$

$$M_1 = M_{1r} - M_{1s}$$

$$\sigma^2 = \sigma_r^2 - \sigma_s^2 = M_{2r} - M_{2s}$$

$$M_3 = M_{3r} - M_{3s}$$

$$M_4 = M_{4r} - M_{4s} + 6\, M_{2s}^2 + 6\sigma_s^2\sigma_r^2$$

$$M_5 = M_{5r} - M_{5s} + 20\, M_{3s}M_{2s} - 10(M_{3r}M_{2s} + M_{3s}M_{2r}) \qquad \text{----} \quad (5.56)$$

$$M_6 = M_{6r} - M_{6s} + 35(M_4\sigma^2 - M_{4r}\sigma_r^2 + M_{4s}\sigma_s^2)$$

$$- 30(\sigma^6 - \sigma_r^6 + \sigma_s^6) + 10(M_3^2 - M_{3r}^2 + M_{3s}^2)$$

q.e.d